Spring 2022

Innovative approach to use guayule resin as a bio-based asphalt alternative

Ahmed Hemida

Follow this and additional works at: https://scholarsmine.mst.edu/doctoral_dissertations

Part of the Structural Engineering Commons

Department: Civil, Architectural and Environmental Engineering

Recommended Citation

INNOVATIVE APPROACH TO USE GUAYULE RESIN AS A BIO-BASED

ASPHALT ALTERNATIVE

by

AHMED MAHER ABDELDAIM HEMIDA

A DISSERTATION

Presented to the Graduate Faculty of the

MISSOURI UNIVERSITY OF SCIENCE AND TECHNOLOGY

In Partial Fulfillment of the Requirements for the Degree

DOCTOR OF PHILOSOPHY

in

CIVIL ENGINEERING

2022

Approved by:

Magdy Abdelrahman, Advisor
Dimitri Feys
Cesar Mendoza
Steven Lusher
Fatih Dogan

ABSTRACT

Asphalt cement will not last long as the world encounters a diminishment in crude oil. Novel resources can contribute to replacing asphalt with the sustainable, flexible pavement. This study presented guayule resin (guayule) as an innovative bio-based asphalt alternative. Ground tire rubber was used as an asphalt enhancer. To judge the guayule's contribution, guayule-based binders were investigated and compared to control asphalt and asphalt-rubber binders. Binders were assessed according to comprehensive Superpave criteria and advanced rheological tests. Component analysis was performed to link the microscale level with the macroscale level. To validate the novel binder, satisfying mix performance tests were conducted. The outcomes revealed a lower viscosity for guayule than asphalt, indicating savings in plant energy consumption. Guayule had similarities with asphalt in component composition and rheological behavior with temperature susceptibility. Asphalt-guayule interaction yielded a physical blending with no chemical reaction. Rubber enhanced guayule at high temperatures, but not as much as asphalt, as proven by polymeric component migration through liquid binder due to depolymerization occurred. However, because of strong oxidation bonding chains attributed to guayule, the oxidative aging negatively affected the guayule-based binder's long-term distresses. Validation by mix performance assessment revealed that guayule supported mix stability against moisture (particularly at lower air contents), rutting, and fatigue cracking, but had low thermal fracture resistance. In a nutshell, guayule had potential to replace conventional asphalt to compensate or surpass the asphalt performance required partially or even entirely at specific grades.

ACKNOWLEDGMENTS

This dissertation would not have been accomplished without the support of individuals who helped me during my Ph.D. studies.

I would like to present my sincere and heartfelt gratitude to my advisor, Dr. Magdy Abdelrahman. Dr. Abdelrahman was an inspiring mentor, who provided me with research guidance and academic support. I also wish to thank my committee members:

Dr. Dimitri Feys and Dr. Cesar Mendoza, who provided me with academic support, particularly in learning the principles of rheology that made me understand the concept behind the asphalt-like rheology.

Dr. Steven Lusher, who offered me his knowledge, experience, and technical support. Dr. Lusher inspired me to think about my research point. He also trained me on most equipment needed for my research. He provided me with material samples and information based on his experience with guayule.

Dr. Fatih Dogan, who kindly offered me his knowledge and experience, particularly in understating the advanced molecular level and nanomaterials that helped me go deeper with material characterization.

I am also very grateful to the Missouri University of Science and Technology Civil, Architectural and Environmental Engineering department for providing a comfortable environment for my research development.

Finally, special thanks to my big family (mom, dad, brother, and sister) and my small family (wife, daughter, and two sons) for their love, patience, and encouragement.

TABLE OF CONTENTS

Page

LIST OF ILLUSTRATIONS

LIST OF TABLES

NOMENCLATURE

Symbol	Description
A	Control Asphalt
AASHTO	American Association of State Highway and Transportation Officials
AG	Asphalt Guayule
AGR	Asphalt Guayule Rubber
APA	Asphalt Pavement Analyzer
AR	Asphalt Rubber
ASTM	American Society for Testing and Materials
BBR	Bending Beam Rheometer
CMOD	Crack Mouth Opening Displacement
DCT	Disk-Shaped Compact Tension Test
DSR	Dynamic Shear Rheometer
DTG	Derivative Thermo-Gravimetric Curve
FTIR	Fourier Transform Infrared Spectroscopy
G'	Storage (Elastic) Modulus
G''	Loss (Viscous) Modulus
G^*	Complex Shear Modulus
$\|G^*\|/\sin\delta$	Superpave Rutting Parameter
G_f	Fracture Energy
GR	Guayule Rubber
HWT	Hamburg Wheel Tracking Test

J_c	Critical Strain Energy Release Rate
LP	Liquid Phase
PAV	Pressure Aging Vessel
P_b	Mixture's Binder Content
PG	Performance Grade
PG-HT	Performance Grade High Temperature
PG-IT	Performance Grade Intermediate Temperature
PG-LT	Performance Grade Low Temperature
RTFO	Rolling Thin Film Oven
RV	Rotational Viscometer
SCB	Semi-Circular Bend Test
SI	Separation Index
SITG	Stepwise Isothermal Thermo-Gravimetric Analysis
TGA	Thermogravimetric Analysis/Analyzer
TSR	Tensile Strength Ratio
V_a	Mixture's Air Content
WCO	Waste Cooking Oil
WM	Whole Matrix
$\Delta\rho$	Density Difference between Newtonian Liquid Medium and Dispersed Particles
δ	Phase Angle
ΔT_c	Difference of $T_{s(60s)}$ and $T_{m\text{-value}(60s)}$
η	Liquid-Medium Viscosity

1. INTRODUCTION

1.1. BACKGROUND

Asphalt sustainability was investigated by researchers due to crude oil depletion [1-3]. The sustainable development of flexible pavement was sought using approaches such as asphalt recycling by reclaimed asphalt pavement (RAP) [2, 4-6], asphalt binder modification by rubber and plastic wastes [2, 7], and asphalt replacement by biomaterials [2, 8-17]. These approaches posed challenges, and the researchers attempted to overcome such challenges to embrace competitive performances such as rheological properties and compatibility [2, 7], economics [2, 6], and environmental benefits [2, 6].

Renewable materials became attractive for asphalt binder (nonrenewable) replacement [18]. Such attraction is based on several advantages that renewable materials could provide for the pavement industry [18]. One of the most important benefits is reducing the carbon footprint associated with emissions due to the consumption of petroleum resources [18]. Many researchers thought about the potential utilization of such renewable resources in asphalt replacement, particularly the bio-based byproducts [12-14, 16] since they could solve the depletion of petroleum [18]. In other words, renewable materials could be very promising sources for sustainable pavement development [18]. Literature reported that renewable materials could provide remarkable benefits in terms of environment and economics such as reducing petroleum dependency, minimizing carbon footprint, and exploiting bio-based byproducts as landfills [18]. Despite all these benefits, biomaterials still encounter challenges in this field based on the desired performance and

resisting potential distresses [18, 19]. This research adopts one of such biomaterials that has the potential to be used as an asphalt alternative, which is guayule resin [18].

Guayule resin is a bio-based byproduct extracted during major guayule shrub product extraction, guayule natural rubber [2, 20]. Guayule shrub is cultivated in the arid zones from southwestern U.S. to northern Mexico [2, 21-23]. Many factors have limited guayule utilization since the 1900s [23], including the commercialization challenges due to high production costs associated with guayule cultivation [2, 20]. This and other difficulties made guayule less used than Hevea, the dominant worldwide natural rubber source [2, 23]. Researchers proposed co-products utilization such as guayule resin and bagasse, to reduce the overall guayule production costs, thereby overcoming such challenges [2]. Guayule commercialization deserves future research investigations since it may enhance the guayule shrub sustainability in terms of economic and environmental concerns [18, 23]. Guayule byproduct commercialization could reduce gross production costs by 26–49% [2, 24]. Literature showed that guayule rubber is significantly competitive to the current global natural rubber source (Hevea) [18, 23]. Guayule rubber may be more desirable than Hevea rubber for the following reasons: (1) it is a domestic source of natural rubber [25], (2) it is not a food crop, (3) it is not labor-intensive, (4) it is easily mechanized [23], and (5) it is safe for people with Type I latex allergy because there are no allergenic proteins [2, 23]. The major restriction that most likely stands against guayule rubber production is the economic factors, which could be balanced by exploiting other derivatives (bio-based byproducts) [18, 23].

Research showed that guayule resin has a high potential for asphalt cement replacement [18, 26]. It is a leftover and renewable biomaterial (plant extractable), unlike

conventional asphalt (nonrenewable) [9, 27]. Guayule resin seems an asphalt-like material [26]: thermo-plastic viscoelastic [26-29]. It is susceptible to temperature change: viscoelastic at room temperature, viscous at high temperatures, and solid at low temperatures [26]. Likewise, the virgin guayule resin provided rheological properties comparable to the conventional asphalt at specific grades [26, 28]. Nevertheless, since the flexible pavement binder must have specific grades to accomplish the desired performance, guayule resin may not be desired alone [30] [18]. Guayule could provide a benefit as a bio-based byproduct, and is renewable and environmentally friendly, unlike asphalt cement [26-29]. Additionally, it would support balancing guayule economics. Therefore, guayule resin could benefit both guayule commercial value and the massive, flexible pavement industry [26].

According to the Superpave grading system, asphalt cement could be classified as regular asphalt (e.g., PG52-16, PG52-28, PG64-22, and PG70-16), high-quality asphalt (e.g., PG52-34, PG70-22, and PG76-16), and modified asphalt (e.g., PG76-40) [2, 31]. Guayule resin could be categorized by a small Superpave grade range based on temperature tolerance, unlike asphalt grades discovered through extended research [2, 28]. Virgin guayule resins (used after heat-treatment) presented a 58℃ performance grade high temperature (PG-HT) [26], a 25℃ performance grade intermediate temperature (PG-IT), and a -16℃ performance grade low temperature (PG-LT) [2]. The literature reported difficulty using bio-binders at low temperatures because of low resistance to thermal cracking [2, 11, 14]. Nevertheless, modifying guayule resin could increase the high- and low-temperature tolerances [2].

1.2. PROBLEM STATEMENT

Crude oil (nonrenewable source) stands against the sustainable development of the flexible pavement industry. Additionally, literature reported that the asphalt price sharply increases and offers a severe impact on the environment as well as pavement workers [32]. As a result, seeking bioresources as innovative bio-binders to replace asphalt cement is a critical research topic at this time for the sustainable development of the flexible (asphalt) pavement [9, 28, 32, 33]. Briefly, this research approach deserves investigation [9] due to petroleum limitations, asphalt price increase, and severe adverse impact on the environment and living beings [3, 26, 32, 34]. The expectations offered no petroleum sources in the near future [9, 28, 35]. Seeking innovative binders could replace conventional asphalt to face this problem. Guayule resin is a waste material that could be a potential asphalt alternative to minimize asphalt drawbacks: natural petroleum source depletion, environmental pollution reflected on the hazards on living beings, in addition to its sharp cost increase. Utilization of guayule resin and crumb rubber modifier (CRM, extracted from scrap tire) consolidate the waste management concept in the massive flexible pavement industry.

1.3. OBJECTIVES

This study seeks to find a novel asphalt alternative in partial and full asphalt cement replacement with guayule resin. Guayule resin was investigated as an asphalt extender (high level of asphalt replacement: 20–75% replacement). Likewise, guayule resin was considered for full replacement (i.e., zero percent asphalt). To judge the guayule resin's contribution, several guayule-based binders were investigated and compared to asphalt and

asphalt-rubber binders. To judge the contribution of CRM (also named rubber in this study), binders' whole matrices (CRM particle residue involved in the blend) and liquid binders (CRM particle residue extracted from the blend) were investigated since CRM was partially dissolved in the binder blend. To validate the novel binder, mix performance tests were conducted.

1.4. SCOPE

This study investigated guayule resin's utilization to compensate for conventional asphalt cement performance at specific grades based on variant traditional and advanced-level tests. It was noticed that when used alone as a binder, guayule resin has limitations to accomplish the desired performance (i.e., provides limited performance grades). Guayule resin alone would not provide better performance than conventional asphalt cement. The CRM was used as an enhancer to boost the novel binder performance in both partial and full replacements. Future investigations will be required to expand its applicability and increase the temperature range of continuous performance grade.

2. LITERATURE REVIEW

This section aims to provide previous writings that serve for a comprehensive understanding of the guayule plant, rubber, and resin utilization in research and industry. First, a review on bio-oils/bio-binders is presented to demonstrate the potential of biomaterials to provide potential asphalt cement alternatives for sustainable, flexible pavement [9]. This review is followed by a background of guayule plant establishment and the bases of its need. Guayule resin has a potential to be utilized in the massive flexible pavement industry as offered in [2] and presented in this study. Likewise, a review on CRM was provided here since it was used for a long time as an asphalt modifier/enhancer and could be beneficial in enhancing the guayule-based binders as presented in this study. One of the most significant aspects of the asphalt industry is the energy consumption in production, followed by environmental emissions, which could be minimized by guayule resin as an asphalt alternative.

2.1. REVIEW ON BIO-OILS

This subsection implies argumentation discussed in [9]. In the past few years, the literature revealed several applications of bio-oils in the asphalt pavement industry such as waste cooking oil (WCO), waste wood, and switchgrass. By experiment, it was proven that bio-oils could substitute asphalt cement in part or in full since they provide a high compatibility with asphalt. Bio-oils provided similar trends of rheological (viscoelastic) behavior to asphalt, which are also temperature susceptible. Bio-oils have pros and cons regarding their applicability in the asphalt industry as discussed hereafter in this subsection.

However, one of their known advantages is their low viscosity compared to the conventional asphalt, indicating energy savings in the overall construction process, as well as environmental benefits.

   2.1.1. Overview.   Due to the domination of the crude oil as the main source of energy and asphalt during the 20th century, no crisis impacted the flexible pavement industry [9]. However, in the recent decades, asphalt prices sharply increased because of worldwide crude oil diminishment [3, 32]. In the asphalt industry, researchers became interested in finding novel substitutes to asphalt cement for a sustainable, flexible pavement [28, 32, 33]. Bio-oils attracted the attention of several researchers to replace asphalt in part and in full due to their similarities with the asphalt performance [14]. Nevertheless, the challenges against bio-oils' usage in asphalt industry exist due to several reasons such as rheological enhancements to achieve competitive performance levels to wide-ranged asphalt grades developed for several years by research and industry [9].

   As an asphalt alternatives, bio-oils were categorized into three divisions, which were full replacement (no asphalt), partial replacement (high portion), and modification (not exceeding 10%) [36]. Peralta et al. (2014) investigated a partial asphalt cement replacement by 20% bio-oil reporting that such a partial replacement could yield a great economic savings [15]. Using bio-oils as asphalt modifiers in 5–10% could not influence the binder performance greatly, but reduce the overall costs, reported by Yang et al. (2014) [37]. Furthermore, other researchers investigated bio-oils for full asphalt replacement and revealed a positive point in this regard [14].

   Fast pyrolysis technique is the common method employed to extract bio-oil from biomass [36, 38]. The feedstock material is the key role in the percentage of the bio-oil in

a specific biomass [9]. For example, oakwood biomass included about 69% bio-oil, corn fiber biomass included about 56% bio-oil, and cornstover biomass included about 37% bio-oil [39]. The literature reported that these kinds of bio-oils could be recognized as a produced dark-brown liquid from a rapid heating biomass in vacuum circumstances [9, 11]. Other bio-oil sources are bio-waste like WCO, which has potential to be used in partial asphalt replacement [40]. The WCO mostly contains saturates, resins, and aromatics [41]. Generally, resins and saturates in bio-oils' compositions are higher than their inclusion in asphalt [41].

The distinction of waste wood bio-oils such as oakwood, cornstover, and switchgrass, is their inclusion of lignin and little moisture [11, 39]. The literature reported that bio-oil could be used original, dewatered (pretreated), or modified [37, 42]. Bio-oils were dramatically influenced by the high temperatures that could severely change their properties [11]. Therefore, Metwally (2010) proposed a temperature up to 120°C for the heat treatment process of the designated bio-oil [11]. Peralta et al. (2014) pretreated the designated bio-oil using a shear mixer with a 50 Hz revolution speed up to a 110°C-blending temperature [15]. This process was proceeded until no foaming (bubbling) was visually noticed in the bio-oil [15], indicating little-to-no moisture.

2.1.2. Bio-Oil Viscosity. Regardless of the bio-oil source, studies reported that a common advantage in fast-pyrolysis bio-oils was their low viscosity measurements compared to conventional asphalt [9]. This pattern is desirable in the flexible pavement's process since it accomplishes savings in plant energy consumption and environmental emissions, hence minimizing the construction expenses [9]. On the other hand, since WCO

represented a pure liquid at ambient temperature, it provided significantly low viscosity measurements [41].

2.1.3. Applicability of Bio-Oils in Paving Industry. Bio-oil in the asphalt industry could be employed as binder's rejuvenator or a binder's alternative in part or in full [9]. The aim of the rejuvenators is to make either virgin asphalt or recycled asphalt softer, which is a worthwhile behavior to resist the low-temperature (thermal) cracking, meaning that rejuvenators raise the soft fractions (aromatics) concentration in the asphalt binder to rejuvenate its performance. Such rejuvenators, however, could negatively affect the high temperature performance of the binder. Therefore, the composite proportions need to be balanced to optimize the overall required performance. Bio-oils could be applicable asphalt substitutes with or without modifications according to the required grades [29]. Such categories of bio-oils are asphalt-like materials, which are thermo-plastic viscoelastic and temperature-susceptible [15]. Due to the low stiffness of bio-oils compared to the conventional asphalt, researchers used modifiers such as polymers and CRM in attempts to use bio-oils in full asphalt replacement for comparable performances [14].

Even though the bio-oils mentioned above could be a promising research approach to challenge the diminishment of asphalt sources and the paving industry's sustainable development, these approaches need further development to be valid for binder modification or being a partial or full binder. Guayule resin is a byproduct with no current commercialization. It is an asphalt-like material and has potential to be directly used as an asphalt substitute [30].

2.2. GUAYULE PLANT HISTORY

Guayule is an evergreen shrub that originated in the arid zones from southwestern U.S. to northern Mexico [21, 43]. The guayule plant is a renewable source to obtain beneficial extractions such as high-quality natural rubber [43]. Para rubber trees, the worldwide dominant source of natural rubber (Hevea), grow in a different environment compared to the environment needed for guayule plant growth [21]. World War (II) was the second spark in the 1940s to use rubber extracted from guayule shrub when rubber supplies were cut off by Japan [44]. This second spark came after the origin of guayule plant utilization in the 1900s [20]. Meanwhile, Hevea rubber was cheaper in the production process, unlike the guayule rubber, which had more overall production expenditures. The problem over the past years was that the guayule-based products were economically unattractive, as rubber was the only beneficial extracted product, and the residue was disposed of (byproducts). However, the economic problem could be solved by exploiting the residual extractables such as the extracted resin. In other words, the key to solving this problem was how to utilize the other extracted residue (byproducts) to trade off the optimum benefit of guayule extracted materials [20]. Three major products extracted from the guayule shrub are (1) natural rubber, (2) bagasse (post-rubber-extraction fibrous residue), and (3) resin [45]. The guayule plant has a historical background of more than100 years [43]. However, use of the guayule plant for a few hundred tons of rubber extracted as a natural rubber source for World War (II), World War (II) did not last, and the project stopped [44]. One of the factors that encouraged resurgence of the guayule plant research was the 1990 discovery that guayule natural rubber is not allergic, unlike Hevea rubber that represented a rubber-based source for medical products [20].

The dominant worldwide natural rubber source (Hevea) grows in Asia [23]. However, guayule could be a domestic alternative source of natural rubber [23, 28]. Guayule resin is not worthwhile by the manufacturer during the guayule natural rubber production. Therefore, researchers have focused on methods to minimize resin in the extracted rubber [28, 46]. The quality of guayule rubber decreases when rubber and resin gather with each other because resin components in rubber work as plasticizers. In other words, physical properties are degraded by the resin components [28]. Bridgestone Americas is one of the big companies doing research and succeeded in separating resin from rubber to a great extent. This could be a chance for asphalt researchers to take over the guayule resin extracted as a byproduct.

2.3. GUAYULE RUBBER IN INDUSTRY

Known corporations such as Yulex, Bridgestone, and Cooper Tire got interested in guayule rubber research as a new revolution in a natural rubber source [44]. Yulex Corporation primarily used guayule for hypo-allergic latex manufactures such as catheters and gloves as medical products [43]. Bridgestone and Cooper Tire companies followed Yulex to use the guayule rubber in the tire industry. As posted on the company's website "The Bridgestone Group's proprietary technologies were applied to every process in the production of this tire from guayule cultivation, natural rubber extraction, purification, and evaluation, to tire production and evaluation." [21]. Bridgestone Americas produced its first version of a guayule-driven natural rubber tire in 2015 [21]. Ultimately, the extracted guayule rubber leads to excessive guayule resin amounts accompanied by such a produced rubber.

2.4. GUAYULE PROCESSING

Natural rubber is chemically known as cis-1,4-polyisoprene. It comprises 400 to 50,000 isoprene units hooked up in a head-to-tail shape. An entire guayule shrub only contains 5–10% cis-1,4-polyisoprene (natural rubber) by weight [44]. The natural rubber extraction process takes much effort for implementation. One of the common methods used is that workers tap the shrub till the latex drops and is then collected in buckets [44]. The rubber extraction process requires the plant to be mature. The cultivation process takes 2–3 years to be ready for the rubber extraction process [44].

Bridgestone group's process center states four steps from harvesting to natural rubber extraction. Even though some resin is inevitably extracted with rubber, researchers attempt to optimize the rubber extracted involving little-to-no resin. Therefore, guayule resin can be separated to a great extent. Figure 2.1 illustrates the potential co-product utilization from Bridgestone guayule rubber extraction process [25].

The four steps are stated as follows:

1. Milling,

2. Rubber extraction,

3. Impurity removal, and

4. Solvent removal.

2.4.1. Milling. The literature revealed that the milling process could be implemented as follows:

1. Milling the dried material after cultivating for 2–3 years, harvesting, chipping and screening through 3.8 cm-mesh.
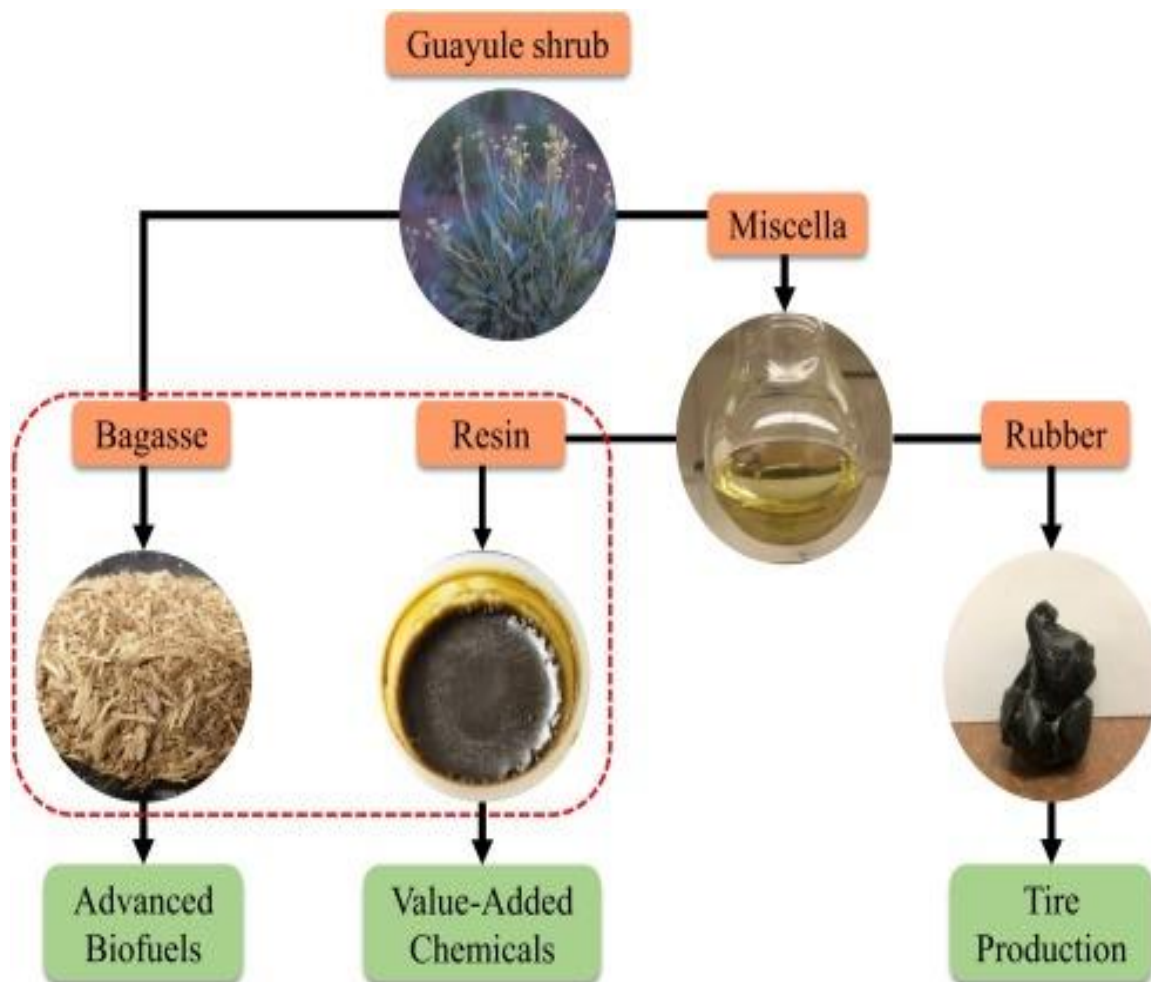
Figure 2.1 Schematic Diagram for Potential Co-Product Utilization from Bridgestone® Guayule Rubber Extraction Process [25].[1]

2. A desiccator is used at room temperature for the dried material for 4-week storage for moisture removal. Then, the dried material is milled using a ball mill. After pulverization, the material becomes less than 1.7 mm.

3. Afterward, it is stored for two weeks in a sealed vial at room temperature before the extraction process [47].

2.4.2. Guayule Rubber Extraction. There are two types of guayule rubber extraction: latex rubber extraction and bulk rubber extraction. The formation and storage of latex are comprised inside the guayule cells [46]. Guayule latex is composed of rubber and non-rubber components. Guayule latex rubber mostly had a lower viscosity compared to Hevea rubber. In other words, it had a lower molecular weight compared to Hevea rubber since it used to contain more than 8% resin [48]. Nevertheless, guayule latex rubber could be enhanced by maximizing resin extraction. On the other hand, bulk rubber is extracted directly from guayule shrub (e.g., by solvent extraction), having almost the same viscosity as latex rubber. Separating high molecular weight guayule rubber fraction (means high resin proportion separated from the rubber-resin mix) by a proper coagulation process could output a bulk viscosity of guayule rubber comparable to Hevea rubber [46].

2.4.2.1. Latex rubber extraction. Crushed harvested guayule latex is diluted by water (or any other liquid medium) at a solid to liquid proportions 1:5 to 1:20 [49], considering that 20% solid dispersion in the liquid medium could result in rubber with a comparable viscosity to the Hevea rubber [50].

2.4.2.2. Bulk rubber extraction. There are two mechanisms of bulk rubber/resin separation (flotation and solvent extraction). The flotation process is coagulation of latex in an aqueous medium. Solvent extraction is divided into two extraction techniques: sequential and simultaneous. The sequential process implies the following points:

- A polar organic solvent (e.g., acetone) is added and blended to the shrub.

- A less polar solvent removes rubber (e.g., hexane).

The simultaneous process implies the following points:

- A solvent washes the shrub (e.g., acetone-pentane azeotrope as a mixed system or xylene as a single compound) for a dilute solution (i.e., rubber-resin miscella).

- For high-molecular-weight rubber fraction coagulation, a polar organic solvent (e.g., acetone or methanol) is added to the miscella.

The simultaneous extraction process is better than the sequential extraction process to fractionate the rubber out of resin for high-molecular-weight rubber [46].

2.5. BRIDGESTONE GUAYULE RUBBER/RESIN EXTRACTION PROCEDURE

Schloman (2005) [46] reported the process that Bridgestone Americas applies to extract guayule rubber, which is as follows:

1. Guayule shrub is cut to 3–4-cm pieces.

2. The shrub tissue is compressed and sheared by a flaker.

3. An extraction solvent is blended with flaked shrub at 50℃ to form a slurry. A blend of hexane and acetone, or acetone-pentane azeotrope (liquid mixture), could be used. However, the extraction process's primary approach is the recycled rubber-resin miscella (solution).

4. Simultaneously, rubber and resin represent the liquid phase of the slurry. Bagasse, on the other hand, is separated by centrifugal force.

5. An amount of miscella is reused in the extraction process to continue the rubber extraction process as a solvent.

6. Fractionation process

   - Miscella is blended with acetone for the rubber coagulation process.

- Rubber is coagulated at the bottom of the fractionator (mixer-settler).

- Resin and rubber with low-molecular-weight are located in the fractionator upper portion and pumped out.

- The coagulated rubber is pumped from the downstream fractionator.

- A blend of pentane or hexane with acetone is used to separate the remaining resin and low-molecular weight rubber from the high-molecular-weight rubber.

- Solvent swollen-high molecular weight rubber passes by a devolatilizer, desolventizer (heat and reduced pressure) to separate the remaining solvent away from the final rubber product.

- The rubber is compressed in rectangular-shaped packages (30-35 kg).

These steps are described by Figure 2.2 as a flowchart depicting step by step the phases of the bagasse/resin/rubber separation process.

2.6. OVERVIEW ON GUAYULE RESIN

One guayule plant derivative is guayule resin, received from the manufacturer as illustrated in Figure 2.3. This byproduct is inevitably extracted during guayule rubber production [20, 26]. Each kilogram of the produced rubber, at the very least, corresponds to one kilogram of resin [26, 44]. The current value of guayule resin is almost nothing [26]. Some researchers see that about 25-50% savings in the guayule rubber production could be attributed to the exploitation of other associated byproducts such as resin and bagasse [24, 26].
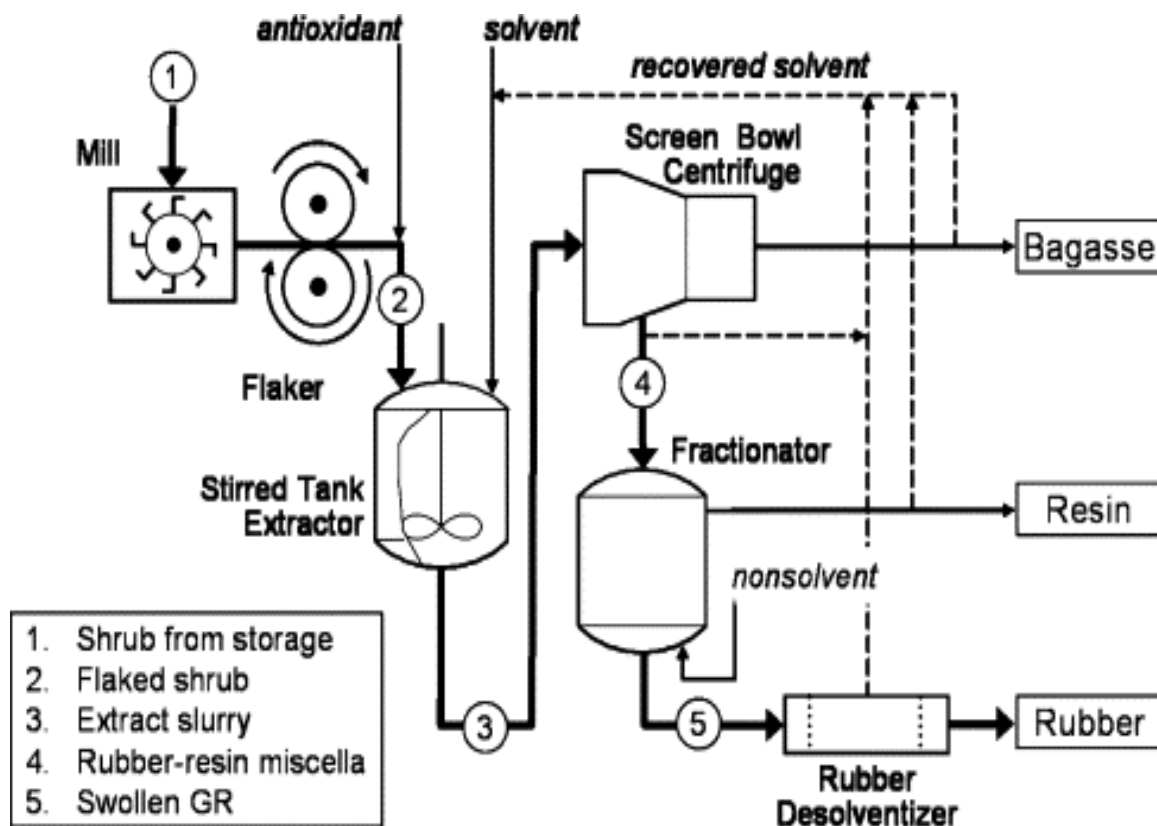
Figure 2.2 Stepwise Flowchart of Bagasse/Resin/Rubber Separation [46].[2]

Guayule resin is composed of volatile (3-5%) and non-volatile fractions (95-97%) [20, 26, 51, 52]. It is composed of complex mixtures of terpenes, fatty acid triglycerides, sesquiterpenes, and others [20, 22, 51, 53]. Further details regarding guayule resin's chemical composition are interpreted in the following subsection. Guayule resin is an inevitable extractable (byproduct) during the guayule natural rubber production [20, 28]. Even though some of the guayule resin components are volatile, they may have a high boiling point such as terpenes [26, 45]. Because of the solvent-based extraction process of guayule resin, a significant amount of low-molecular-weight guayule rubber (5,000-

10,000) is inevitably included in the extracted resin [22, 26]. Further details related to the guayule resin chemical characterization could be found in [20].

Figure 2.3 Guayule Resin.

Using guayule in the asphalt industry could benefit commercial value and a massive flexible pavement industry [26]. Investigations on guayule resin revealed an asphalt-like material [26]. It is very susceptible to temperature change: viscoelastic at room temperature, viscous at high temperatures, and solid at low temperatures [26]. Likewise, pure guayule resin provides rheological properties comparable to the conventional asphalt at specific grades [26, 28]. It could be distinct in the asphalt industry regarding sustainability and economics as it is a bio (renewable) material and a byproduct [20, 26].

2.7. REVIEW ON GUAYULE RESIN'S COMPOSITION

This subsection implies a reproduction of argumentation published in [18]. Since guayule resin denotes a bio-based byproduct extracted from guayule plant with the primary

product (guayule natural rubber), its composition is mainly hydrocarbons [20]. Such a composition could also be shown by the potential molecular formulas (MFs), as illustrated in Figure 2.4 [20, 54]. It is mainly composed of atoms of carbon (C), hydrogen (H), oxygen (O), and nitrogen (N). These elements are included in several chemical compounds such as Triterpenes [Argentatin: -A ($C_{30}H_{48}O_4$), -B ($C_{31}H_{50}O_3$), -C ($C_{31}H_{52}O_4$), -D ($C_{30}H_{50}O_3$), -E ($C_{30}H_{50}O_2$), -F ($C_{30}H_{42}O_3$), -G ($C_{30}H_{48}O_3$) and -H ($C_{30}H_{48}O_3$)], Sesquiterpenes [Guayulin: -A ($C_{24}H_{30}O_2$), -B ($C_{23}H_{30}O_3$), -C ($C_{24}H_{30}O_3$) and -D ($C_{23}H_{30}O_4$), and Partheniol ($C_{15}H_{24}O$)], and many others [20, 54].

Water and water-soluble contents in guayule resin rely on the extraction technique (e.g., sequential and simultaneous). Guayule resin employed in this research was extracted according to a simultaneous extraction reported in the literature as homogeneous and almost contains no water-soluble materials [55]. Unlike simultaneous extraction, sequential extraction is noticeably heterogeneous and involves entrained water-soluble matter [55]. Literature reported that the water-soluble matter attributed to the sequential extraction technique could be 2–3% [51].

2.8. REVIEW ON GUAYULE RESIN IN FLEXIBLE PAVEMENT

Guayule resin was introduced into the flexible pavement as a recycling agent [22, 43, 45]. The literature revealed that biomaterials could be extracted from the guayule plant as modifiers to virgin asphalt [45]. Likewise, high concentrations of RAP and/or RAS and non-petroleum-based recycling agent (i.e., bio-based recycling agent) were used associated with little-to-no virgin asphalt [43].

Major Guayule Resin Composition

Volatile Fraction
3-5%

Non-volatile Fraction
95-97%

Terpenes/Hydrocarbon
(monoetrpene = 2 isoprene = 2 x C_5H_8)

Water Soluable

Water Insoluable

α-Pinene
MF: $C_{10}H_{16}$

β-Pinene
MF: $C_{10}H_{16}$

Camphene
MF: $C_{10}H_{16}$

α-Phellandrene
MF*: $C_{10}H_{16}$

β-Phellandrene
MF: $C_{10}H_{16}$

Sabinene
MF: $C_{10}H_{16}$

β-Myrcene
MF: $C_{10}H_{16}$

Bornyl Acetate
MF: $C_{12}H_{20}O_2$

Cinnamic acid
MF: $C_9H_8O_2$

Polyphenol
MF: N/A;
it has C, H, and O

Polysaccharide

Terpenes/Hydrocarbon
(monoetrpene = 2 isoprene = 2 x C_5H_8)

Fatty acid triglyceride
(20–25%)

Sesquiterpene

Triterpene
[Derivatives of $C_{30}H_{48}$ (i.e., 3-terpene ($C_{10}H_{16}$)]

Alkaloid
[organic/contains N atoms/contains neutral acidic proprties

β-Ocimene
MF: $C_{10}H_{16}$

Limonene
MF: $C_{10}H_{16}$

Linoleic (60–65%)
MF: $C_{18}H_{32}O_2$

Linolenic (10–15%)
MF: $C_{18}H_{30}O_2$

Palmitic (10%)
MF: $C_{16}H_{32}O_2$

Oleic (10%)
MF: $C_{18}H_{34}O_2$

Stearic (1%)
MF: $C_{18}H_{36}O_2$

Guayulin A
MF: $C_{24}H_{30}O_2$

Guayulin B
MF: $C_{23}H_{30}O_3$

Guayulin C
MF: $C_{24}H_{30}O_3$

Guayulin D
MF: $C_{23}H_{30}O_4$

Partheniol
MF: $C_{15}H_{24}O$

Argentatin A
MF: $C_{30}H_{48}O_4$

Argentatin B
MF: $C_{31}H_{50}O_3$

Argentatin C
MF: $C_{31}H_{52}O_4$

Argentatin D
MF: $C_{30}H_{50}O_3$

Argentatin E
MF: $C_{30}H_{50}O_2$

Argentatin F
MF: $C_{30}H_{42}O_3$

Argentatin G
MF: $C_{30}H_{48}O_3$

Argentatin H
MF: $C_{30}H_{48}O_3$

Guayulamine A
MF: N/A

Guayulamine B
MF: N/A

Figure 2.4 Potential chemical components of guayule resin [18].[3]

Lusher and Richardson compared guayule-based recycling agents to petroleum-based recycling agents such as cyclogen [43]. Acetone-extracted guayule rubber resin (residual resin) accomplished an accepted recycling agent comparable to the cyclogen used

---

[3] MF: molecular formula; N/A: not available.

as a petroleum-based recycling agent for a long time [45]. In other words, the residual resin

could be a future rejuvenating agent as a component of the reclaimed asphalt binder blend

instead of a costly and environmentally harmful petroleum-based recycling agent. The

researchers optimized the proportions among RAP, RAS, and the novel bio-based recycling

agent to yield a rejuvenated recycling binder that could encounter the challenges against

high-, intermediate-, and low-temperature resistances with considering the original, rolling

thin film oven (RTFO), and pressure aging vessel (PAV) conditions according to the

identified specifications [43]. When used as a recycling agent, one of the drawbacks of the

residual resin was the relatively high mass loss compared to the conventional asphalt

considering the short-term aging simulated by the RTFO at 163℃ [22, 43, 45].The

literature experimentally revealed the applicability of using acetone-extracted guayule

rubber resin as a substitute bio-based recycling agent instead of a commonly used

petroleum recycling agent (cyclogen) [43]. Even though the market involves several bio-

based recycling agents, guayule resin has the potential to be competitive due to two

benefits: (a) its potential to add diversity to the market as a domestic source and (b) the

success of domestic guayule derivatives' commercialization [22].

2.9. REVIEW ON ASPHALT, RUBBER AND ASPHALT RUBBER

2.9.1. Chemical Bonding of Asphalt. The literature clarified that the conventional

asphalt had symmetric and asymmetric C−H stretches in CH_2 and CH_3 at wavenumbers

ranging 3000–2800 cm^{-1} [56]. It involved four distinct peaks in this range (around 2954

cm^{-1} [57, 58], 2924 cm^{-1} [57, 59], 2870 cm^{-1} [57, 58], and 2853 cm^{-1} [57, 59, 60]). Other

peaks were formed around 1458 cm^{-1} [57, 59, 60] and 1376 cm^{-1} [57, 60, 61] for the same

functional group, indicating symmetric and asymmetric bends of CH_3 [62, 63]. Such functional groups were compatible with the elemental composition of the conventional asphalt (around 80% carbon and 10% hydrogen) [56]. Other distinct peaks were observed at 1730 cm^{-1} and 1032 cm^{-1} for C=O (carbonyl) [57, 59, 60] and S=O (sulfoxide) [57, 61, 64], respectively, representing the main functional groups responsible for the oxidative aging through asphalt life cycle. The aromatic peak was associated with C=C at 1603 cm^{-1} [57, 60, 61]. Four carbon atoms in a row were observed at 721 cm^{-1} [56].

2.9.2. Significance of Asphalt Rubber. This subsection implies a reproduction of argumentation published in [27]. In the U.S., the conventional asphalt was cheaper than asphalt rubber (AR). However, the sharp worldwide price increase of crude oil reflected the conventional asphalt price around 2008 when its cost reached about $300 per ton [65]. Around that time, the low cost of AR (with 20% CRM) remarkably made it attractive [65]. In the 2015 Crumb Rubber Report, Caltrans reported, "The total percentage of asphalt containing CRM increased from 26.7 percent to 41.3 percent (3,738,054 tons to 4,175,289 tons) from 2014 to 2015" [66]. This represented, on average, 14.56 lb of CRM per ton of the California paving materials in 2015 [66]. The U.S. Tire Manufacturers Association (USTMA) reported consumption of ground rubber of about 62 million tires (about 1013 thousand tons) out of 255 million generated tires in 2017 [67, 68]. This ground rubber represented about 25% of the overall scrap tires in that year. About 12% of such ground rubber was used in the asphalt industry [67, 68]. In recent years, the cost of conventional asphalt is over $550 per ton [26]. This price is expected to increase shortly due to the diminishment of worldwide crude oil [3, 32]. Asphalt replacement is inevitable for sustainable, flexible pavement [26].

2.9.3. Review on CRM Composition. The CRM comprises rubber/elastomers, carbon black, metallic components, and other additives. Their proportions differ according to the tire type (car, truck/bus, or mix) [69]. In other words, the CRM includes natural rubber (cis−isoprene, mainly responsible for elasticity), synthetic rubber (styrene-butadiene rubber [SBR], mainly responsible for thermal stability), metallic elements (containing 15–20% polar components, highly reactive), and carbon black and textiles (organic fillers) [56].

Regarding Fourier transform infrared spectroscopy (FTIR) analysis of CRM, the literature claimed that four strong sharp peaks were formed for N−H stretches between 3500–3000 cm^{-1} corresponding to amines. The NH$_2$ asymmetric stretch was formed in a wavenumber range of 3500–3420 cm^{-1}. The peak of NH$_2$ symmetric stretch could be found in a wavenumber range of 3500–3420 cm^{-1}. The peak of NH$_2$ scissors stretch could be found at 1637 and 1616 cm^{-1}. Aromatic secondary amine could be formed at 3414 cm^{-1}, and saturated secondary amine or amide could be found at 3238 cm^{-1} [56]. On the other hand, the concentration of sulfur in CRM was about 1–2%, depending on the tire type [69, 70]. Sulfur in CRM could be attributed to either C−S or S−S functional groups [56]. Since the absorbance of N−H stretch in CRM was significantly high, it was not easy to identify the sulfur bonds as their absorbance was very low through the wavenumber range of 500–700 cm^{-1}. Likewise, CRM contained aliphatic C−H stretch in the region of 3000–2800 cm^{-1}, which had short peaks for the last-mentioned reason. The SBR peak was formed at 965 cm^{-1}, indicating =C−H in phase out-of-plane bending of trans-1,4-butadiene and masked by N−H scissoring vibration as reported by Nivitha et al. [56].

2.9.4. Asphalt Rubber Compatibility. The CRM was used as an asphalt modifier for a long time due to its compatibility with asphalt. Though the primary asphalt rubber interaction was physical, the chemical interaction could occur [56]. Typically, it needs higher interaction temperatures to be observed (170–200℃) since the devulcanization and/or depolymerization may occur, causing a rubber dissolution in asphalt [71]. It was rarely seen at lower than this range of interaction temperatures [56]. The gel permeation chromatography (GPC) showed a reduction in chain length of rubber when interacted with asphalt, indicating its depolymerization in the internal asphalt structure [72, 73].

This paragraph implies a reproduction of argumentation published in [18]. Nivitha et al. [56] investigated the crumb rubber modified asphalt (asphalt rubber) using FTIR, concluding a similarly formed spectrum for both conventional asphalt and asphalt rubber, except for a few distinct peaks. Only one amine peak was observed at 3300 cm^{-1}, indicating secondary amine/amide. With heating to more than 100℃, amines reacted with carboxylic acid yielding ammonium carboxylate salt, losing water molecules to produce a secondary amide. Accordingly, it was expected that this could also occur as carboxylic acid was present in asphalt. The SBR peak was formed at 965 cm^{-1} in asphalt rubber, similar to its formation in the CRM, i.e., no observed peak shift [56].

The following two paragraphs imply a reproduction of argumentation published in [26].

The CRM has two effects on asphalt modification, as exampled in Figure 2.5. One of them is the liquid phase, which corresponds to the interaction effect, meaning no effect of the CRM particle (residue) on the binder's performance. The other is the whole matrix, which involves the dispersed CRM residue's particle effect in the binder's matrix

performance. Previous studies depicted a relatively higher performance attributed to the whole matrix [74]. It is important to study the behavior of both on the binder performance. In other words, the particle effect indicates the effect of the residual CRM particles after the interaction on the overall binder matrix; however, the interaction effect represents the influence of the dissolved CRM in the binder liquid phase [75]. Whole matrix and liquid phase scales were considered in this study to reveal the different effects (particle reside vs. interaction) on the guayule-based binders.
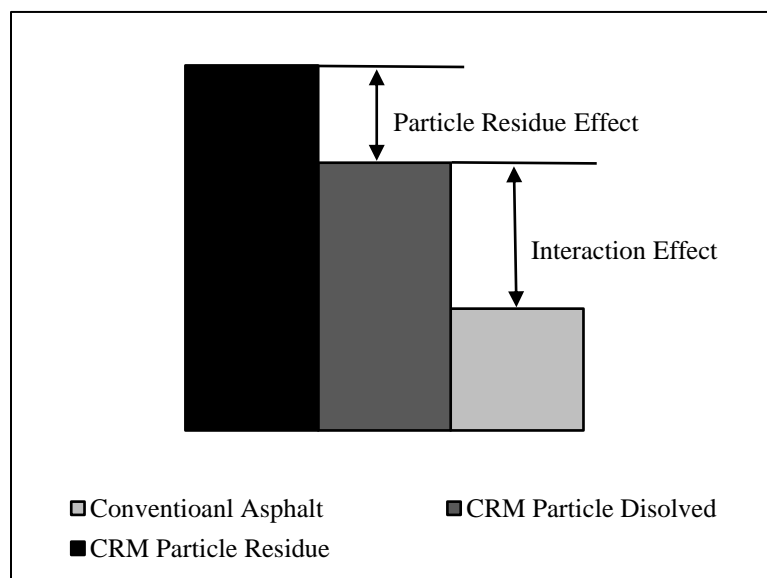
Figure 2.5 An example of the Contribution of Interaction Effect against CRM Particle Residue Effect on the Asphalt-Rubber Binder's Performance [75].

Recent studies on asphalt rubber have focused on the effect of material parameters and interaction parameters. Some researchers declared that the temperature is the primary interaction parameter affecting the CRM dissolution in asphalt rubber [76, 77]. A 190℃ interaction temperature had potential to develop the liquid phase of the asphalt-rubber

binder [76, 77]. Besides, a 3000 rpm interaction speed had the potential to result in a more homogenous asphalt rubber [76, 77]. The CRM was difficult to entirely dissolve in asphalt due to its cross-linked structure [71]. The above-mentioned specific interaction parameters were proven attributed to the formation of a three-dimensional (3D) network structure, which was significantly effective in terms of the binder rheological properties enhancement [78]. In the current study, the use of guayule resin as an asphalt alternative was sought. The CRM was used as a modifier/enhancer triggering an innovative binder that could compete against conventional binder performances for sustainable, flexible pavement.

2.10. BINDER BLEND'S SEPARATION TENDENCY

This subsection implies a reproduction of argumentation published in [27]. One significant problem encountered with asphalt rubber is the limited storage time after its production [79, 80] due to its poor storage stability [81, 82]. Subsequently, this kind of binder does not offer widespread application because of the time limitation of the asphalt processing [82]. One of the crucial solutions, in this regard, is the mobilization of the required equipment (blending unit, metering unit, storage tanks, etc.). However, the associated costs are relatively high, reflecting the overall cost of asphalt rubber production [79].

Storage stability of the asphalt rubber was analyzed and enhanced in the literature [81-84]. The literature showed a significant storage instability associated with the asphalt rubber's whole matrix, unlike its liquid phase [84]. The storage instability is attributed to parameters that are explained by Stoke's law, as depicted in Equation (1) [81, 82]:

$$v_t = \frac{2a^2 \Delta \rho g}{9\eta} \tag{1}$$

where:

v_t Terminal (sedimentation) velocity

a   Dispersed particle radius

$\Delta \rho$ Density difference between Newtonian liquid medium and dispersed particles

η Liquid-medium viscosity

The sedimentation velocity is directly proportional to the dispersed particle (residue) radius and density difference between the Newtonian phase and dispersed particles. On the other hand, it is inversely proportional to the liquid-medium viscosity. Consecutively, the separation tendency of a modified asphalt needs to be investigated due to its composition of two or more different materials. In the current study, the separation tendency of the novel guayule-based binder was investigated on the whole matrix scale and liquid phase scale and compared to asphalt and asphalt rubber.

2.11. ENERGY CONSUMPTION IN ASPHALT INDUSTRY

Energy consumption of producing asphalt concrete is generally attributed to many factors such as moisture included in the mineral aggregates, mixing temperature, production capacity per hour, and production delays via the day as a waste of time [85]. Likewise, the sort of plant, either batch- or drum-plant, affects the hot mix asphalt (HMA) production energy consumed [85]. Going widely with asphalt production not only implies the previously mentioned factors, but it also includes the virgin binder extraction itself,

including the distillation process of the crude oil and the energy used to extract the virgin binder as well as the energy needed to keep asphalt warm or hot to prevent its solidification [86]. On the other hand, mineral aggregates used require drying to remove moisture and to mix with asphalt binder [86]. The aggregate particles also need to be crushed and stockpiled to be blended with warm/hot asphalt binder [86]. In addition, energy consumed for transportation and construction must be considered [86]. However, the drying and mixing process (material production) is the most considerable energy consumed compared to the transportation and construction processes [86]. Figure 2.6 shows the typical percentages of the energy used in the asphalt pavement industry. However, the entire process differs according to individual project conditions.

To summarize, energy consumed in the asphalt industry comprises many factors attributed to binder and aggregate (e.g., aggregate moisture content, mix temperature, production capacity, and delays) [85]. Likewise, energy is consumed via transportation and construction processes [86]. However, the drying and mixing process (material production) is the most considerable portion of the energy consumed compared to the transportation and construction processes (typically 75%) [86]. Even though energy consumption differs upon the project size itself, studies reported, on average, 3 GJ per ton as energy consumption for HMA [85]. On the other hand, warm mix asphalt (WMA) [87], since it is a way to reduce the energy used by reducing the mixing temperature to be 140–150℃, consumes about 80% (about 2.4 GJ) on average, compared to HMA [86]. Asphalt binder needs to be heated at 150℃ to 190℃, and studies reported electrical consumption, on average, is 8 kW per ton [88, 89]. As a result, for a 1-h binder heating (150°C to 190°C),

the energy consumed is, on average, 28.8 MJ [88, 89], considering that moving up the temperature from 150°C to 190°C increases the energy consumed.
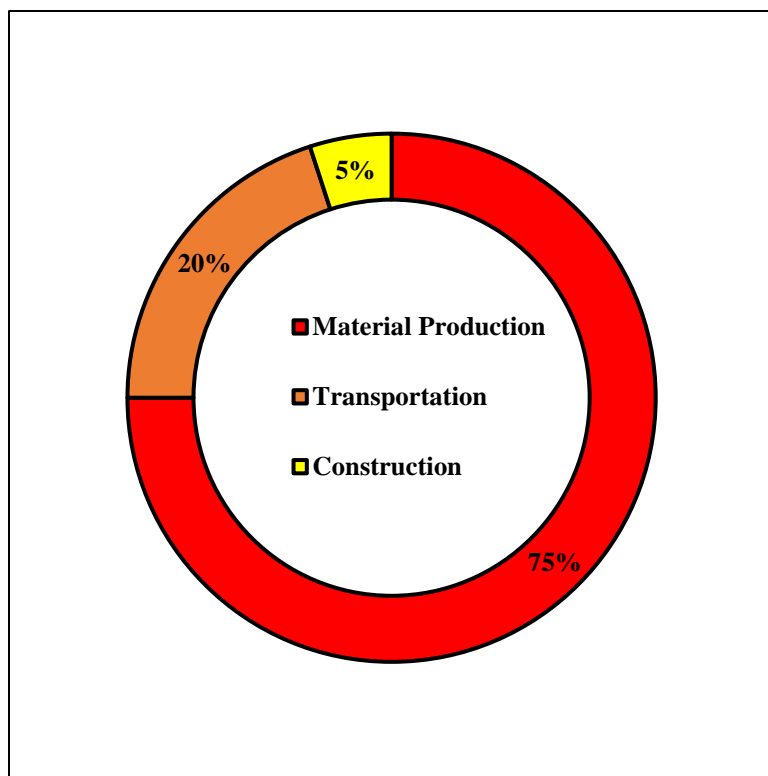
Figure 2.6 Typical Energy-Consumed Distribution in the Asphalt Pavement Industry [86].

The literature mentioned above is an initiative to encourage bio-binders in the flexible pavement industry. Bio-binders could offer encouraging substitutes to the conventional asphalt cement concerning the low viscosity benefits, regardless of the bio-oil source [9, 13]. Research disclosed that bio-oils have provided a similar tendency to the conventional asphalt binder [9, 13]. Nevertheless, they had potential to offer comparable viscosities at relatively lower temperatures. This behavior is desirable in the flexible

(asphalt) pavement construction process to yield lower energy consumption, thus lower construction expenses [9]. Subsequently, guayule resin, as an innovative bio-based asphalt alternative [90], could provide a relatively lower viscosity in comparison with asphalt; reflecting reduced production temperatures; hence, savings in plant energy consumption and environmental emissions are predicted [2, 13]. It is distinguished with saving energy, cutting emissions from production, paving operations, and improving conditions for workers [91] because of reducing the harmful gases emitted [92]. This is followed by lowering the construction expenses [13].

3. EXPERIMENTAL CONSIDERATIONS

3.1. OVERALL APPROACH

Figure 3.1 illustrates the overall approach followed for the innovative binder characterization. For material variability, variant materials were considered: two asphalt grades, two guayule resin (or guayule hereafter) batches, and one crumb rubber modifier (CRM). The two standard asphalt grades were PG52-28 (critical grade PG57-29) and PG64-22 (critical grade PG67-25). The two guayule batches were initially investigated and found PG55-16 and PG58-11. The grades are recognized based on the critical grade temperatures hereafter in this study, meaning pass/fail temperatures according to the Superpave criteria. The CRM size is represented by CRM #30–40 [2] (i.e., passed mesh #30 and retained on mesh #40 according to the US standard system [78]). Multiple samples were prepared based on asphalt (A), guayule (G), asphalt-guayule (AG), guayule-rubber (GR), asphalt-rubber (AR), and asphalt-guayule-rubber (AGR) binders [2]. A high shear mixer (HSM), heating mantle, and temperature controller were used for the binder interaction process [2]. Guayule was heat-treated with stirring at 160°C using the HSM until no foaming (bubbling) was noticed, indicating no additional moisture or light-weight volatiles involved, as investigated in this study [2, 15, 28]. As recommended in the literature, the blending technique was applied [26, 93-95]. The investigations included the effect of variant material parameters on the designated binders' behaviors.

Physical, mechanical, and compositional investigations were conducted to characterize the innovative binder. The major tests are demonstrated in Table 3.1. The Superpave criteria and other advanced tests were followed to evaluate the designated bin-
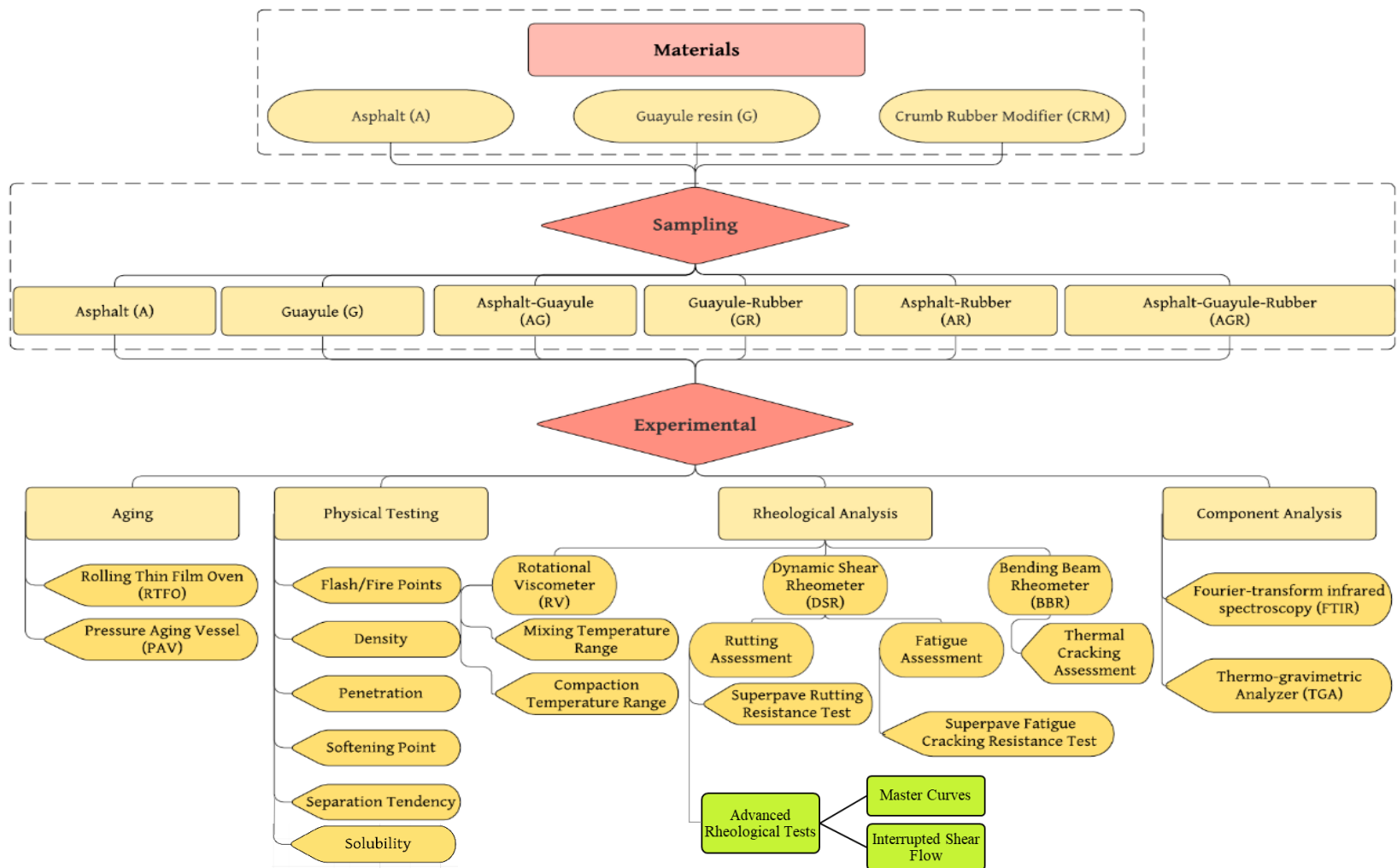
Figure 3.1 Overall Approach Flowchart.

ders. The compositional investigations involved component and thermo-gravimetric analysis using FTIR and thermo-gravimetric Analyzer (TGA).

To investigate the binder for oxidative aging caused during the construction process (production) and through its life, it was simulated in the laboratory using the RTFO and PAV. As discussed hereafter, mix performance investigations followed the binder investigations to validate the field's binder performance.

3.2. STATISTICAL CONSIDERATIONS

To fulfil the statistical satisfaction of the experimental design conducted in this study, two, three, or more replicate samples were tested for each test according to the requirements of each standard/specification. The outliers of samples were eliminated in case of applying three or more replicate samples using the statistical outlier analysis to preliminary avoid any significantly statistical data. Accordingly, the t-statistic was calculated based on Equation (2) and (3). The largest calculated t-statistic was compared to the critical t-statistic based on a 5% significance level according to ASTM E178 [96]. Nevertheless, some standards/specifications allowed testing two replicate samples such as AASHTO T 315 [97] for the DSR data analysis. In that case, the limits recommended in such a standard was considered. For instance, the performance-related parameters in AASHTO T 315 [97] required an acceptable range of two test results to be 4.6% for original (unaged) binder ($|G^*|/\sin\delta$), 7.2% for RTFO residue ($|G^*|/\sin\delta$), and 11.2% for PAV residue ($|G^*|/.\sin\delta$). These parameters were established based on a single-operator precession (repeatability). ASTM C670 [98] reported that "These values were established based on the difference between two test results that is expected to be exceeded with a

probability of about 5 % in the normal and correct operation of the test method; used as an index of precision of the test method." In general, the results were established in tables and figures based on averages and standard deviation (or coefficient of variation or acceptable range of two test results) considered through the precision and bias statements of a specific standard/specification requirements (as available). For brevity, an example was illustrated in Chapter 4 along with the error bars.

$$t_{max} = \frac{x_{max} - x_{avg}}{\sigma} \tag{2}$$

$$t_{min} = \frac{x_{avg} - x_{avg}}{\sigma} \tag{3}$$

3.3. DETAILED EXPERIMENTAL CONSIDERATIONS

The designated binders involved a wide range of material parameters that revealed the initiative role of guayule in the binder blend establishment. The designated binders represent control asphalts (As), pure guayules (Gs), asphalt-guayule (AGs), guayule-rubber (GRs), asphalt-rubber (ARs), and asphalt-guayule-rubber (AGRs) binders. The novel binder was assessed based on partial and full replacements.

Guayule was utilized in partial asphalt replacement (20–75% replacement). Two critical asphalt grades (PG57-29 and PG67-25), two guayule batches (PG55-16 and PG58-11), and CRM #30–40 were used. The material variability here comprised the control A, AG, AGR, and AR binders.

Table 3.1 The Purpose of the Major Tests for Binder Characterization.

Property & Tool	Purpose
Dynamic viscosity by RV	Binder's viscosity assessment at temperatures higher than 100℃ using the rotational viscometer to evaluate binder's workability and mixing and compaction temperature ranges during the construction process.
Rheological analysis at high and intermediate temperatures by DSR	Binder's rheology assessment at high and intermediate temperatures using the dynamic shear rheometer (DSR) as follows: - Critical high temperature: for rutting resistance assessment based on the Superpave criteria. - Critical intermediate temperature: for fatigue cracking resistance assessment based on the Superpave criteria. - Master curve: to evaluate the binder's behavior at a wide range of frequency sweep and temperature sweep. - Interrupted Shear Flow: one of the techniques used by several researchers to evaluate the formation and enhancement of 3D network structure, which indicated a higher binder performance than that of no apparent 3D network structure formation [78, 84, 99, 100].
Rheological analysis at low temperatures by BBR	Binder's rheology assessment at low temperatures using bending beam rheometer (BBR): - Critical low temperature: for thermal cracking resistance assessment. - ΔT_c (difference between critical T_S and critical $T_{m\text{-value}}$), which indicates the binder aging susceptibility to thermal cracking potential [101].
Component analysis by FTIR	FTIR is one of the most common techniques to evaluate the compositional changes to the modified binders. Here, it helped understand the following terms: - Compositional analysis of guayule resin. - Compositional changes among asphalt, guayule, and CRM interactions; or any two of them. - Quantitate analysis of the oxidative aging behavior. - Separation tendency verifications
Thermo-gravimetric analysis by TGA	TGA was employed to analyze the following terms: - Guayule decomposition and moisture inclusion - CRM: as received and extracted residue from liquid binders after interactions. - Separation tendency verifications

Guayule was also considered for full asphalt replacement (100% replacement). Two guayule batches (PG55-16 and PG58-11) and CRM #30–40 were assigned. The material variability here comprised considerations of G and its enhancement by CRM (guayule-rubber or GR).

Partial and full replacement considerations were involved in two experiments, which were (1) soft-asphalt soft-guayule experiment (first experiment) and (2) stiff-asphalt stiff-guayule experiment (second experiment).

3.3.1. First Experiment: Soft-Asphalt Soft-Guayule. In this experiment, the raw materials and sampling were presented in [2], which were included/reused in this subsection.

3.3.1.1. Raw materials. This experiment established sampling based on soft asphalt (control), soft guayule, and CRM, as listed in Figure 3.2. According to the Superpave criteria, the soft asphalt cement was brought from Conoco Phillips terminal in Granite City, Illinois [2]. Guayule resin was received from Bridgestone Americas as the first soft batch [2]. The CRM was received in multiple gradations from Liberty Tire Recycling [2]. However, the only CRM particles' gradation used was CRM #30–40, according to the US standard system [2, 84].

3.3.1.2. Samples. To evaluate guayule as an innovative asphalt alternative, multiple samples were prepared. An example of a binder's sample designation recognized through this study is shown in Figure 3.3. The designated binders included soft asphalt (A1), soft guayule (G1), soft asphalt-guayule (AG1), soft guayule-rubber (GR1), soft asphalt-rubber (AR1), and soft asphalt-guayule-rubber (AGR1) binders, as listed in Figure

3.4. The soft asphalt-guayule blend was blended for 120 min [labeled AG1(50:50)120]. The GR1, AR1, and AGR1 were blended under two conditions: one with 20% CRM and the other with 10% CRM (by wt. of the liquid portion: soft asphalt, soft guayule, or soft asphalt-guayule blend). The 20% CRM-involved binders were blended for 240 min [GR1(83:17)240, AR1(83:17)240A, and AGR1(42:42:16)240A]. The 10% CRM-involved binders were blended for 360 min [GR1(91:9)360, AR1(91:9)360B, and AGR1(45:45:10)360B]. However, to assess the effect of CRM on the AGR1 blends, a 10% CRM-involved binder was designated at 240 min (labeled AGR1(45:45:10)240). To compare the effect of guayule on asphalt, two other blends were designated — AGR1(68:23:9)360 and AGR1(23:68:9)360 — for comparison to AGR1(45:45:10)360B. All designated binder proportions of the first experiment are presented in Table 3.2.

Figure 3.2 First Experiment Raw Materials [2].
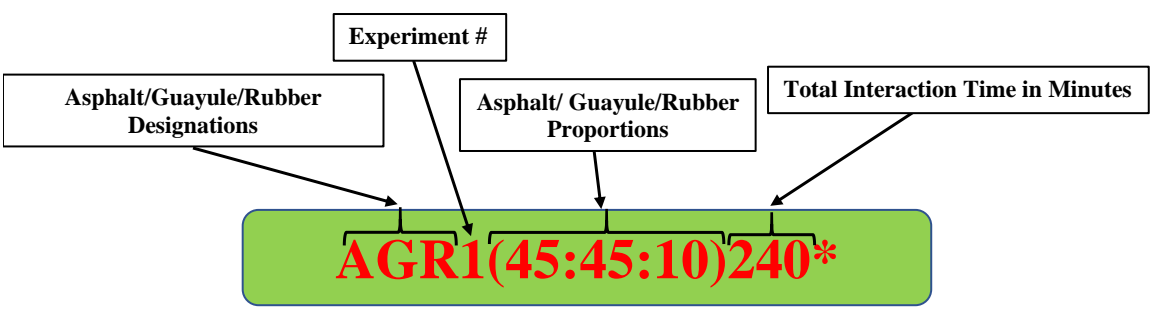
Figure 3.3 An Example of Binder Designation. [4]
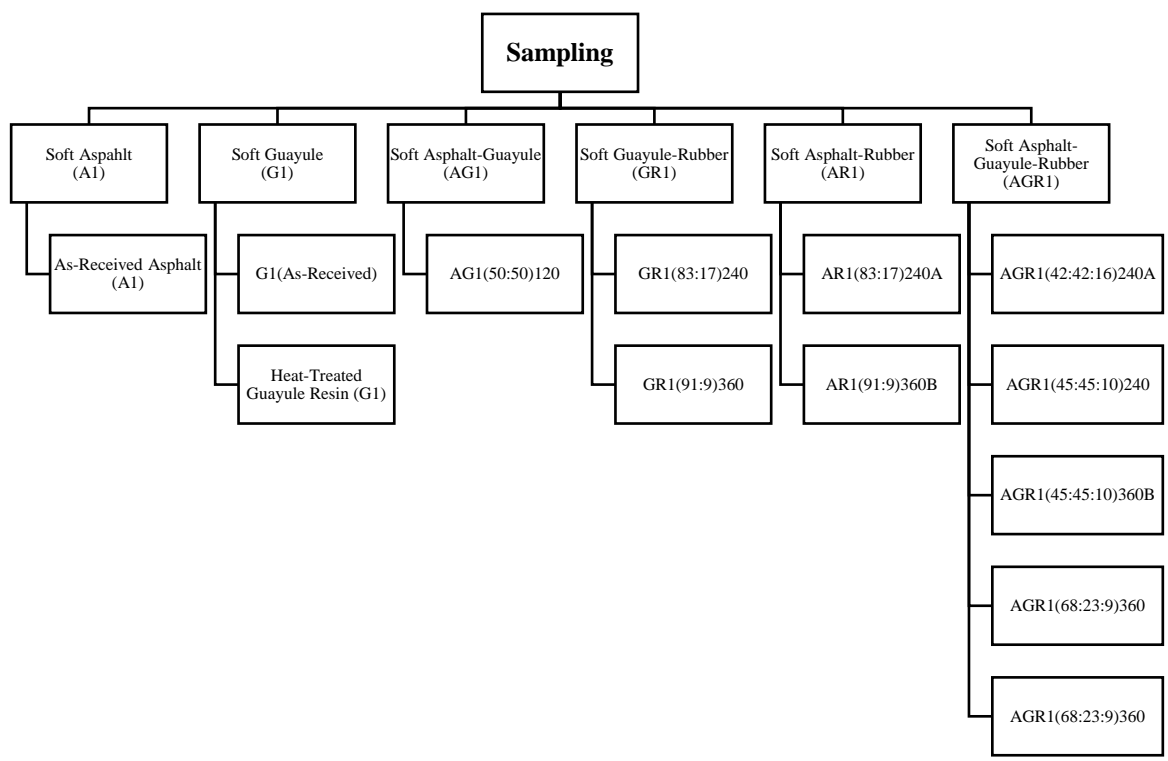
Figure 3.4 First Experiment Sampling Flowchart.

---

[4] *If a letter (e.g., A) added at the end of designation, it denotes a corresponding binder, meaning asphalt replaced guayule portion in the same experiment (same CRM concentration and same scenario of interactions).

Table 3.2 Binder Codes and Proportions of the First Experiment [2].[5]

| Group | Binder Code | Binder Proportions | | | | |
		A1% by wt. of blend	G1%	CRM%	AR1%	CRM% by wt. of A1
A1	A1	100				
G1	G1(As-Received)		100			
	G1		100			
AG1	AG1(50:50)120	50	50			
GR1	GR1(83:17)240		83.3	16.7		
	GR1(91:9)360		90.9	9.1		
AGR1	AGR1(42:42:16)240A	41.65	41.65	16.7	58.4	20
	AGR1(45:45:10)240	45.45	45.45	9.1	54.6	10
	AGR1(45:45:10)360B	45.45	45.45	9.1	54.6	10
	AGR1(68:23:9)360	68.2	22.8	9.1	77.3	20
	AGR1(23:68:9)360	22.8	68.2	9.1	31.8	10
AR1	AR1(83:17)240A	83.3		16.7	100	20
	AR1(91:9)360B	90.9		9.1	100	10

3.3.1.3. Sample preparation. High shear mixer (HSM), heating mantle, and temperature controller were used for binder interaction processes. Guayule was stirred and heat-treated at 160℃ using the HSM until no more foam (bubbles) was evident, thus indicating absences of moisture and preliminary low-molecular weight volatiles [15, 28]. The CRM was also oven-dried before any interaction with asphalt and/or guayule. Figure 3.5 shows the guayule stages from barrel to heat treatment. The interactions in this experiment were conducted at 190℃ and 3000-rpm for various durations as recognized in each binder designation. All material portions (asphalt, guayule, and/or rubber) were added from the beginning of the interaction.

---

[5] A1: soft asphalt cement; G1(As-Received): as-received guayule from the manufacturer; G1: heat-treated soft guayule; AG1: soft asphalt-guayule blend; GR1: soft guayule-rubber blend; AR1: soft asphalt-rubber blend; AGR1: soft asphalt-guayule-rubber blend.

Figure 3.5 Guayule Resin Stages from Barrel to Heat Treatment.

3.3.2. Second Experiment: Stiff-Asphalt Stiff-Guayule. In this experiment, the raw materials and sampling were presented in [26], which were included/reused in this subsection.

3.3.2.1. Raw materials. In this experiment, binder blends were made from stiff asphalt, stiff guayule, and CRM, as shown in Figure 3.6. The control asphalt source was Philips 66 Company, IL. The source of CRM was Liberty Tire Recycling LLC. Different sizes of CRM were obtained. However, it was sieved, and the selected gradation was CRM #30–40, according to the US standard system [2 , 81, 102, 103]. Stiff guayule was provided by Bridgestone Americas and produced from a mix of three different batches (2016-7-1-RES-12, -13, and -14), which was found stiffer than the first batch mentioned in the first experiment.

For brevity, typical characteristics of the used control asphalt (A2) and guayule (G2) are illustrated in Table 3.3, which could indicate the preliminary physical properties of the novel guayule as an asphalt-like material.
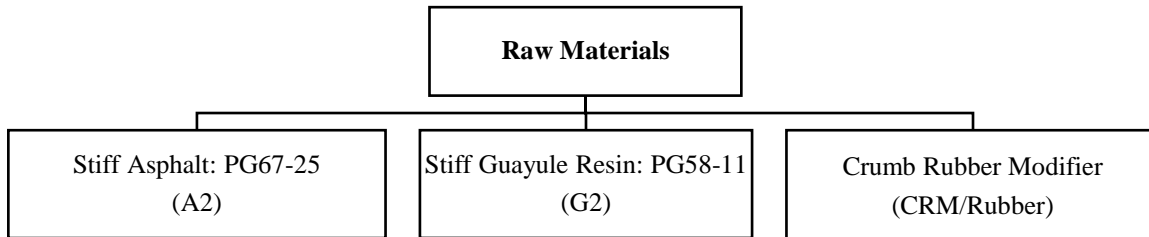
Figure 3.6 Second Experiment Raw Materials Flowchart.

Table 3.3 Properties of control asphalt (A2) vs. heat-treated guayule (G2) [18].

Property	A2	G2	Method
Flash Point [°C]	320	242	ASTM D92 [104]
Fire Point [°C]	330	261	ASTM D92 [104]
Density at 25°C [g/dm^3]	1028	1038	ASTM D70 [105]
Penetration at 25°C	50/60	40/50	ASTM D5 [106]
Viscosity at 135°C [Pa.s]	0.403	0.203	ASTM D4402 [107]
Softening Point [°C]	47	48	ASTM D36 [108]

3.3.2.2. Samples. To evaluate guayule as an innovative asphalt alternative, multiple samples were prepared based on stiff asphalt (A2), stiff guayule (G2), stiff asphalt-guayule (AG2), stiff guayule-rubber (GR2), stiff asphalt-rubber (AR2), and stiff asphalt-guayule-rubber (AGR2) binders, as listed in Figure 3.7. Additionally, binder codes and proportions are listed in Table 3.4. Nine AGR2 blends were designated. This experiment involved three major groups of interactions among stiff asphalt, stiff guayule, and CRM as follows: (1) 25% AR2+75% G2, (2) 50% AR2+50% G2, and (3) 75% AR2+25% G2. Each group of those included three subgroups. For example, 25% AR2+75% G2 contained 25% AR2 plus 75% G2 (by wt. of blend). The CRM in this experiment was established based on a proportion of the asphalt portion added at the beginning. Subsequently, the 25% AR2

was divided into three subcategories as follows: 10% CRM, 15% CRM, and 20% CRM (by wt. of asphalt). As justified hereafter, five of nine were designated to proceed in most discussions through this study, which were AGR2(23:75:2)100A, AGR2(44:50:6)100B, AGR2(42:50:8)100C, AGR2(68:25:7)100D, and AGR2(62:25:13)100E. Thus, these designated binders were rheologically compared to their corresponding ARs (same CRM concentration and same scenario of interactions) to investigate the AGR2s' contribution while considering that G2 had a PG-HT of 58℃, and A2 had a PG-HT of 67℃. Therefore, adding guayule to the AR binder would likely negatively affect the final product's rheological properties upon the different proportions of asphalt, rubber, and guayule. These ARs were AR2(98:2)100A, AR2(94:6)100B, AR2(92:8)100C, AR2(93:7)100D, and AR2(87:13)100E. To compare the AGR2s and AR2s, physical tests were implemented and represented by the high-temperature grade in terms of whole matrices (WMs) and liquid phases (LPs).

3.3.2.3. Sample preparation. Oven-dried CRM was added to the preheated asphalt cement (A2). The asphalt-rubber portion was mixed for 40 min interaction time at 190℃ interaction temperature and 3000 rpm interaction speed. This asphalt-rubber portion was distributed in three cans with respect to the design proportions (CRM concentrations of 10%, 15%, and 20%, by wt. of asphalt portion).

Guayule was heat-treated at 160℃ and 600 rpm until no bubbling (foaming) to ensure no moisture was inside, the so-called heat-treatment process. Part of the heat-treated guayule was distributed in the three cans containing the asphalt-rubber portion (25% AR2, 50% AR2, and 75% AR2). As such, guayule was poured in concentrations of 75%, 50%,

and 25%, respectively. Each blend of the AGR2 was mixed for additional 60 min at 160°C and 600 rpm as a final step for AGR2 blends' preparation

Sampling

A2

G2
- G2(As-Received)
- Heat-Treated Guayule Resin (G2)

GR2
- GR2(87:13) 100
- GR2(75:25) 100

AGR2

Whole Matrix (WM)

25%AR2+75%G2
- AGR2(23:75:2) 100A
- AGR2(22:75:3) 100
- AGR2(21:75:4) 100

50%AR2+50%G2
- AGR2(45:50:5) 100
- AGR2(44:50:6) 100B
- AGR2(42:50:8) 100C

75%AR2+25%G2
- AGR2(68:25:7) 100D
- AGR2(65:25:10) 100
- AGR2(62:25:13) 100E

Liquid Phase (LP)
- AGR2(23:75:2) 100A(LP)
- AGR2(44:50:6) 100B(LP)
- AGR2(42:50:8) 100C(LP)
- AGR2(68:25:7) 100D(LP)
- AGR2(62:25:13 100E(LP)

AR2

Whole Matrix (WM)
- AR2(98:2) 100A
- AR2(94:6) 100B
- AR2(92:8) 100C
- AR2(93:7) 100D
- AR2(87:13) 100E

Liquid Phase (LP)
- AR2(98:2) 100A(LP)
- AR2(94:6) 100B(LP)
- AR2(92:8) 100C(LP)
- AR2(93:7) 100D(LP)
- AR2(87:13) 100E(LP)

Figure 3.7 Second Experiment Sampling Flowchart.

The ARs were designated to correspond to the five mentioned-above (designated) AGR2s. That's why they were prepared using the same approach as explained above, except for diluting the asphalt-rubber portion with extra asphalt (instead of guayule) to end up with the same CRM concentration and same interaction speed, time, and temperature.

Considering the preparation of the guayule-rubber (GR2) blends, the same process of the AGR2 blend was followed except for the asphalt (A2) portion, which was replaced by guayule (G2).

Table 3.4 Binder Codes and Proportions of the Second Experiment [18, 26].[6]

| Group | Brief Code | Binder Proportions | | | | |
| | | A2% | G2% | CRM% | AR2% | CRM% |
		by wt. of blend				by wt. of A2
A2	A2	100				
G2	G2(As-Received)		100			
	G2		100			
GR2	GR2(87:13)100		87.5	12.5		
	GR2(75:25)100		75	25		
AGR2	AGR2(23:75:2)100A	22.7	75	2.3	25	10
	AGR2(22:75:3)100	21.7	75	3.3	25	15
	AGR2(21:75:4)100	20.8	75	4.2	25	20
	AGR2(45:50:5)100	45.5	50	4.5	50	10
	AGR2(44:50:6)100B	43.5	50	6.5	50	15
	AGR2(42:50:8)100C	41.7	50	8.3	50	20
	AGR2(68:25:7)100D	68.2	25	6.8	75	10
	AGR2(65:25:10)100	65.2	25	9.8	75	15
	AGR2(62:25:13)100E	62.5	25	12.5	75	20
AR2	AR2(98:2)100A	97.7	0	2.3	100	2.4
	AR2(94:6)100B	93.5	0	6.5	100	7
	AR2(92:8)100C	91.7	0	8.3	100	9.1
	AR2(93:7)100D	93.2	0	6.8	100	7.3
	AR2(87:13)100E	87.5	0	12.5	100	14.3

3.4. BINDER INVESTIGATIONS

The Superpave requirements were first followed in this study to evaluate the designated binders. Such designated binders were exposed to tests that addressed the construction process (mixing and compaction requirements), rutting, fatigue, and thermal cracking resistances through viscosity, high-, intermediate-, and low-temperature measurements [2]. Moreover, more advanced rheological tests were applied to assess

[6] A2: stiff asphalt cement; G2(As-Received): as-received guayule from the manufacturer; G2: heat-treated stiff guayule; GR2: stiff guayule-rubber blend; AR2: stiff asphalt-rubber blend; AGR2: stiff asphalt-guayule-rubber blend.

designated guayule-based binders such as frequency sweep (master curve) test and interrupted shear flow test. These tests were employed to evaluate the novel binder's applicability with frequency sweep and temperature sweep at an advanced level of testing.

The study investigated designated guayule-based binders' separation tendency since the binder storage is desirable at high temperatures for broader applications [27, 82]. Separation tendency is meant here to be assessed in two scenarios: (a) liquid phase separation (liquid residue after interaction) and (b) whole matrix storage stability (overall matrix including liquid residue and CRM particle residue) [27].

In addition to the physical and rheological analysis mentioned above, component analysis was presented to understand the compositional changes influencing the novel binder to chemically understand the clue behind the presented rheological performance in various conditioning: as-received materials, after blending (interaction), after aging (oxidation) by RTFO, and PAV [2]. The component analysis covered the component exchanges among asphalt, guayule, and CRM residue. Therefore, the novel material could be engineered for the desired characteristics.

3.4.1. Physical Testing. This subsection implies a reproduction of methods presented in [26, 27].

3.4.1.1. Density. To investigate the separation tendency of the novel binder, the density was measured for designated AGRs (whole matrices and liquid phases) and compared to their control asphalt and the corresponding ARs (whole matrices and liquid phases). All densities were measured at 25℃. The binder density ($\Delta\rho$) was calculated as illustrated in Equation (4) according to ASTM D70 [105].

$$\Delta\rho = \frac{C - A}{(B\text{-}A) \text{ - } (D\text{-}C)} x \ 1000 \qquad (4)$$

where:

      A   Wt. of pycnometer (plus stopper)

      B   Wt. of pycnometer filled with water

      C   Wt. of pycnometer partially filled with binder

      D   Wt. of pycnometer filled with binder and water

3.4.1.2. Separation tendency. The separation tendency was investigated for designated AGRs (whole matrices and liquid phases) and compared to their control asphalt and the corresponding ARs (whole matrices and liquid phases). According to ASTM D7173 [109], the lab-simulated storage was implemented. Fifty grams of each designated binder was decanted in a standard aluminum tube, kept sealed (to prevent the introduction of air) in an oven at 163℃ for 48h, placed immediately in a freezer at -20℃ for 4h to make the sample solid enough for cutting into about three equal fractions (top, middle, and bottom), as shown in Figure 3.8. The separation index (SI) was determined by complex shear moduli (G*s) of the top and bottom fractions to judge the separation tendency. The SI determination is interpreted in Equation (5) [81, 82, 84].

$$SI = \frac{\text{Max} \ (G^*_{top}, G^*_{bottom}) - G^*_{avg}}{G^*_{avg}} \ x \ 100 \qquad (5)$$

where:

      SI   Separation index

G^*_{top} Complex shear modulus of the top fraction

G^*_{bottom} Complex shear modulus of the bottom fraction

G^*_{avg} Average complex shear modulus of the top and bottom
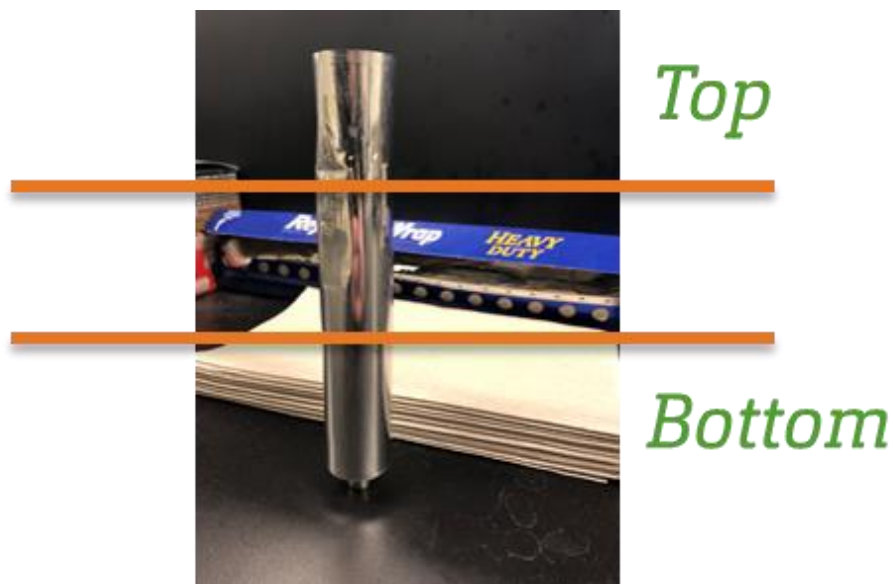
                        fractions

Figure 3.8 Aluminum Tube Divided into Three Portions (Top, Middle, and Bottom).

3.4.1.3. CRM and liquid phase extractions, solubility, and phase separation.
The CRM and liquid phase extractions were implemented for designated AGRs and compared to their corresponding ARs with respect to the methodology of previous researchers [76, 77, 81, 94, 103, 110].

The CRM extraction stepwise is interpreted, as follows:

    1. As shown in Figure 3.9, 10±2 g of the binder was diluted in 100 g of trichloroethylene for 25 min,

2. The binder solution passed through mesh #200 (75µm),

3. Retained CRM particles were washed with extra trichloroethylene until the filtrate became colorless,

4. Washed CRM particles were kept in an oven at 60°C for 12h to ensure a complete solvent removal.

Figure 3.9 Technical Steps from the CRM Extraction Procedures.

The liquid phase extraction stepwise is interpreted, as follows:

1. The required amount of the binder was heated to 165˚C,

2. That heated binder was drained through mesh #200 (75µm) in the oven at 165˚C for 25 min,

3. The extracted liquid phase was stored at -12˚C immediately to prevent any unwanted aging or reaction.

Liquid phase-rubber residue separation aimed to investigate several properties such as:

- Binder's liquid phase density, viscosity, and storage stability. Therefore, the liquid phase was required.

- Component analysis of AGRs and corresponding ARs by FTIR and TGA. Therefore, the liquid binder and rubber residue were acquired.

- Reduction of the dispersed CRM particle radius and the CRM composition analysis by FTIR and TGA. Therefore, the CRM residue was extracted.

3.4.1.4. Solubility.   Regarding the new biomaterial (guayule), the solubility test was applied according to ASTM D2042/AASHTO T 44 [111, 112]. Likewise, the same test was implemented for an AG blend. This test could indicate whether lumps of guayule were retained. To conduct this test, the AG blend was prepared with proportions of 50:50, mixed at 3000 rpm and 190°C for 120 min. This basic solubility test resulted in almost 100% solubility, either for pure guayule in trichloroethylene or the AG blend in trichloroethylene, and no attributed coagulation was noticed. Since this test might not entirely represent the guayule solubility in asphalt, an issue might still be there regarding the asphalt-guayule compatibility. The separation tendency test, according to ASTM D7173 [109], was implemented for the same AG blend. As discussed later, the SI equaled 1.5%, indicating almost no asphalt-guayule phase separation. Accordingly, the potential of high compatibility between asphalt and guayule existed. It was believed by many researchers that there is a strong relationship between compatibility and solubility [113-117]. As a result, one could say that the guayule had the potential to be soluble in asphalt.

3.4.2. Rheological Analysis.   This subsection implies a reproduction of methods presented in [2, 18, 26, 27].

3.4.2.1. Dynamic viscosity. Following AASHTO T 316/ ASTM D4402 [107, 118], a Brookfield rotational viscometer (RV) was used to obtain representative viscosity measurements of designated guayule-based binders, corresponding ARs, and control asphalts at different temperatures by applying a 20-rpm revolution speed. Some binders were shown on dynamic viscosity in the temperature domain diagrams such as designated A, G, AG, GR, and AGR binders. Accordingly, the mixing and compaction temperature ranges were determined based on viscosity values of 0.170±0.020 Pa.s and 0.280±0.030 Pa.s, respectively [119]. The influence of guayule on material viscosity through various material parameters was measured. To investigate the separation tendency of the novel binder, the dynamic viscosity was also measured for designated liquid phases of AGRs and compared to their corresponding ARs, control asphalt, and pure guayule at a specific temperature (163℃).

3.4.2.2. Rheological analysis at high and intermediate temperatures. A dynamic shear rheometer (DSR) was used to investigate the designated binders' rheological behaviors at high and intermediate temperatures, by which the rutting and fatigue resistances, respectively, were evaluated. Rutting resistance was assessed, in which measurements of G* and phase angle (δ) as well as the Superpave rutting parameter ($|G^*|/\sin\delta$) were provided. Consequently, the critical PG-HTs (critical high temperatures) of the designated binders were determined based on the original (unaged) and RTFO-aged materials. Fatigue resistance was evaluated by determining the critical PG-ITs (critical intermediate temperatures) of the designated binders based on the PAV-aged materials. According to the Superpave criteria, the critical high temperature of an unaged binder

corresponded to a 1.0-kPa $|G^*|/\sin\delta$; however, it corresponded to a 2.2-kPa $|G^*|/\sin\delta$ for the RTFO-aged binder. The critical intermediate temperature of a PAV-aged binder corresponded to a 5000-kPa $|G^*|.\sin\delta$. AASHTO T 315 was followed [97]. Parallel plate test geometry was selected based on the standard and literature. A 25-mm testing diameter was employed for the high-temperature resistance assessment, and an 8-mm testing diameter was used for the intermediate-temperature resistance assessment. Each sample was heated to be easily poured into a silicone mold. After being cool enough to handle, it was laid down and pressed between the parallel plate geometry, then trimmed to achieve the required diameter for accurate rheological measurements. As recommended in the literature, a 2-mm gap was employed for the binders comprising CRM residue [120-122]. This gap was applied to ensure particles did not affect the oscillation process [120, 121, 123]. Otherwise, the standard gap was employed for the liquid binders, 1 mm for high-temperature measurements, and 2 mm for intermediate-temperature measurements [97]. The strain control mode was used. The strain values in percent were applied in the linear viscoelastic region of each investigated material, which selected to be 12% for unaged binders, 10% for RTFO-aged binders, and 1% for PAV-aged binders.

As binder grading may not be sufficient to evaluate the binder performance since it is controlled by specific parameters such as a frequency of 10 rad/s, advanced rheological tools were applied, which were master curve tool as a function of frequency sweep and temperature sweep, and interrupted shear flow tool. The master curve is an excellent tool to show the effect of wide ranges of frequencies and temperatures on the binder behavior. Subsequently, the frequency sweep test was applied at multiple temperatures to build up

the master curves of designated AGRs to study their behaviors under the loading rate change. In the frequency sweep tests, the applied shear strain did not exceed 1% to ensure the linear viscoelastic region. Master curves were provided for storage modulus (G′), loss modulus (G″), δ, and |G*|/sinδ rheological parameters.

The interrupted shear flow test was applied for designated AGR liquid phases. Previous researchers studied the formation of a 3D network structure [78, 84, 99, 100]. Those references [78, 84, 99, 100] declared that the 3D network structure formation indicated a higher binder performance than that of no apparent 3D network structure formation. Regarding the rheological analysis limitations, this was evident by the creation of a peak overshoot of shear stress with the application kickoff; hence, steady-state shear flow with time was clarified by Ragab et al. (2013) and Ragab and Abdelrahman (2018) [78, 84]. In this research, this test was applied at a temperature of 64°C after a isothermal time of 30 min and attributed to a shear rate of 2 s^{-1} [78, 84, 99, 100] [99, 100]. The initial stress growth was applied for 60 s and then applied again (second stress growth) for the same duration [100] after the rest time to follow its development and trend up to recovery. Upon multiple experimental trials, the rest time was selected to be 5 s, 10 s, 20 s, 30 s, 40 s, and 50 s, as the required information for analysis was obtained through this range which was a rapid time for binder's full recovery compared to the literature. One continuous test was conducted for each binder sample with a rest time of 5 min since it was more than enough to ensure getting the original sample state with the second stress growth [84].

3.4.2.3. Rheological analysis at low temperatures. A bending beam rheometer (BBR) was employed to assess the designated binders' low-temperature performances,

following AASHTO T 313 [124]. According to the Superpave criteria, the creep stiffness (S(t)) and m-value (rate of change of stiffness with loading time) were determined after a 60-s loading time at the low-test temperature, which simulated the performance criteria after 2h at 10℃ higher than the field temperature by the principle of time-temperature superposition. By Superpave criteria, the stiffness is specified to be no more than 300 MPa (indicating adequate limits of thermal stresses), and the m-value is specified to be no less than 0.3 (indicating adequate ability to relax stresses) [125, 126]. Both stiffness and m-value ensure no expected thermal cracking through the pavement life cycle. The critical low temperature is determined by passing stiffness and m-value requirements (higher critical low temperature). In this study, most designated binders were exposed to different test temperatures that respectively corresponded to 10℃ higher field temperatures [125, 126].

The ΔT_c parameter represents the difference between the critical low temperatures based on stiffness (S(t)) and m-value at a test time of 60 s [101, 127]. This parameter defines the slope of the stiffness curve as a function of temperature [101]. The negative values indicate that m-value dominates [101]. Literature mentioned that wider ranged negative values refer to a higher prediction of premature thermal cracking [101].

The ΔT_c parameter was used in this study to reveal the resistance of the guayule-based binders to thermal cracking against the control asphalt binders, besides the critical low-temperature parameters (S(t) and m-value).

3.4.2.4. Aging methods. All designated binders were RTFO- and PAV-aged. The typical base asphalt procedures were followed with no changes in either RTFO aging or

PAV aging to address the current specifications of conventional asphalt. To simulate short-term aging (construction process) and long-term aging (end of in-service pavement life cycle), RTFO according to ASTM D2872 [128] and PAV according to ASTM D6521 [129], respectively, were followed. The RTFO was run at 163℃ and 4000 ml/min for 85 min. The PAV was run for 20h at 2.1 MPa and 100℃. The RTFO was used to demonstrate the mass loss of the designated binders because it mimicked the loss of volatiles and oxidative aging through the construction process [17]. The literature showed that the mass change in conventional asphalt through such an approach reached ±1% (the lower the grade the higher the mass loss). Conversely, the literature reported that the mass losses attributed to the bio-binders were higher than those in conventional asphalt due to moisture, lightweight volatiles, or both [17].

3.4.2.5. Aging resistance evaluation. To evaluate aging resistance considering the RTFO aging, the RTFO aging susceptibility (AS) was determined. The AS was calculated using Equation (6) based on |G*|/sinδ before and after aging [130].

$$RTFO\ Aging\ Susceptibility\ (AS) = \frac{\frac{|G^*|}{\sin\delta}_{after\ aging}}{\frac{|G^*|}{\sin\delta}_{before\ aging}} \tag{6}$$

The |G*|/sinδ before aging was taken 1.0 kPa, and its corresponding critical high temperature was used to determine the |G*|/sinδ after RTFO aging.

3.4.3. Component Analysis. This subsection implies a reproduction of methods presented in [2, 18, 26, 27].

3.4.3.1. Compositional changes by FTIR. The Nicolet iS50 FTIR instrument was employed to investigate the composition analysis of asphalt, guayule, asphalt-guayule, as-received CRM, extracted CRM from AGR2s, and their corresponding AR2s, in addition to the liquid binders extracted from AGR2s and AR2s. The FTIR was beneficial to illustrate what components were dissolved in the solution or migrated from CRM to liquid binder (asphalt, guayule, and asphalt-guayule blend) and vice versa. Previously, the FTIR was used by many researchers to investigate asphalt rubber and polymer modified asphalt to show the solubility (or dissolution) of polymer/rubber components in the liquid binder of the modified asphalt [56, 61, 64, 131].

Nicolet iS50 FTIR presented more representative results due to its pure material dependency (without solvent dilution) [77, 95], which is equipped with a diamond attenuated total reflectance (ATR) sample cell [120]. The ATR technique was used because of lower effort, faster testing, and no solvent dilution required [27], unlike the KBr disk technique (the so-called transmission mode) [77, 95]. The mechanism of ATR relies on multiple internal reflections of the infrared light by a trapezoidal and oblong non-absorbing prism [132]. A tiny sample was pulled on the diamond surface for a sufficient thickness [132]. Regardless of the sample thickness, the absorption spectrum requires a few-micrometer penetration depth [132]. The infrared spectra were collected based on an accumulation of 32 scans with a resolution of 4 cm^{-1} [12, 17, 133]. The multiple reflections aimed to enhance the resultant absorption spectrum [132]. The spectra were obtained in a wavenumber ranged from 4000 to 400 cm^{-1} [12, 17, 133].

3.4.3.2. Oxidative aging investigation. The mechanism of organic compound aging is known from the literature, explaining how a chemical compound can transfer from most reduction to most oxidation. To summarize, a hydrogen atom could be replaced by OH bond (formulating alcohol). Further oxidation could occur by implanting a carbonyl bond, which replaces hydrogen and OH group (formulating ketones). The most oxidized compound here could be accomplished with C=O and O−H (formulating acid). This oxidation process is attributed to the disappearance of CH_2 radical while C−O, C=O, and O−H stretches and CH_3 are formulated, indicating oxidative aging [17]. The C−O, C=O, and O−H stretches typically belonged to alcohols, esters, and acids in bio-binder. Such functional groups in guayule and guayule-based binders could negatively affect the binder performance at intermediate and low temperatures, as revealed hereafter in this study.

A quantitative assessment of short- and long-term aging of a designated AGR, its corresponding AR, and the control asphalt (A) was provided. Aging rates were investigated based on carbonyl and sulfoxide aging behaviors to understand the oxidative aging mechanism of the novel binder in compliance with conventional asphalt's oxidative aging investigations discussed in the literature. Several studies reported that the oxidative aging of asphalt through RTFO and PAV aging was associated with carbonyl and sulfoxide bonds in the conventional asphalt [60, 133, 134], which were recognized around 1700 and 1030 cm^{-1} wavenumbers, respectively [12]. Carbonyl and sulfoxide provided insights into the morphological behavior on the chemical bonding level [16]. The FTIR indices' changes with aging (between 2000 and 600 cm^{-1}) were studied. Based on the literature, the total area of spectral bands between 2000 and 600 cm^{-1} was assigned to determine aging

behavior's quantitative analysis [12, 16, 132]. Equations (7) and (8) were employed for the quantitative analysis of carbonyl index ($I_{C=O}$) and sulfoxide index ($I_{S=O}$), respectively [16].

$$I_{C=O} = \frac{\text{Area of carbonyl band around 1700 cm}^{-1}}{\text{Area of spectral bands between 2000 and 600 cm}^{-1}} \tag{7}$$

$$I_{S=O} = \frac{\text{Area of sulfoxide band around 1030 cm}^{-1}}{\text{Area of spectral bands between 2000 and 600 cm}^{-1}} \tag{8}$$

3.4.3.3. Thermo-gravimetric analysis by TGA. TGA is a common approach used to investigate the composition analysis of composite materials [135]. The TGA composition analysis was utilized in the literature in this area [77, 95, 136, 137]. TA Q50 TGA was utilized to recognize the guayule decomposition and moisture inclusion. Likewise, it was used to analyze the as-received CRM and extracted CRM particle residue from designated AGRs and their corresponding ARs to show the released constituents of CRM into the binder's liquid phase, as utilized by previous researchers in this regard [74, 78, 81, 95, 138]. Two methods were employed according to material nature: ramp method and stepwise isothermal thermo-gravimetric (SITG) method [81].

The ramp method (the most common technique) was used to analyze materials containing distant thermal decomposition of their components. In this technique, the sample was heated to a predetermined temperature utilizing a constant heating rate that models the mass loss as a function of temperature [57]. Due to the significant thermal decomposition gaps of CRM, the ramp method was sufficient to analyze as-received CRM and extracted CRM from designated binders. For CRM, an amount of 20-25 mg was analyzed with a 20°C/min heating rate starting from the room temperature up to 600°C.

According to the literature, CRM has four major components: oily components, natural rubber, synthetic rubber, and filler components (e.g., carbon black). Each component has its range of decomposition temperature. The first region corresponds to the oily components and is from 25℃ to 300℃, the second region corresponds to natural rubber and is from 300℃ to the temperature corresponding to the minimum point between the two peaks in the derivative thermo-gravimetric (DTG) curve, and the last region is the filler components at 500℃ [18, 27, 57, 77, 81, 95].

The other method (SITG) is a better TGA approach in case of the closeness of the decomposition temperatures of a multi-component material [57, 81, 139]. In this method, the sample is subjected to a programmed heating method to ensure that material decomposition distinction occurs with no overlap. Consequently, it was employed for the TGA of guayule as the ramp method was carried out with no distinctive outcomes. Nevertheless, the ramp method was employed as a rapid technique to indicate the 100% material's decomposition to recognize the decomposition temperature range. The SITG method was also employed to analyze the thermal stability of designated top and bottom portions (after the separation tendency test) of a binder's liquid phase to verify the status of the liquid phase separation. In this method, 20-25mg was analyzed at a 20℃/min heating rate, starting at room temperature until maximum decomposition temperature. The applied heating system involved a kickoff from the ambient temperature through 600℃ and a heating rate of 20℃/min until reaching a mass loss of more than 1%/min, followed by an isothermal condition until reaching a mass loss of less than 0.5%/min.

3.5. MIX PERFORMANCE VALIDATION

This subsection implies a reproduction of methods presented in [90][7]. The innovative binder cannot be fully assessed without investigating the binder-aggregate mix. As a result, the guayule-based mix performance was investigated employing field-simulated laboratory mixes. Mix testing involved assessments considering moisture susceptibility, rutting resistance, fatigue cracking resistance, and thermal cracking resistance [140]. Designated binders were investigated through mixes based on the hypotheses followed above with the designated binders. A job mix formula was followed to explore the designated guayule-based binders in the field-simulated lab mixes.

3.5.1. Materials. This subsection implies the binder designation for mixture preparation, aggregate gradation, and the investigated mixtures.

Table 3.5 Binders' Data for Mix Experiment.[8]

Binder Code	Proportions			Performance Grade[1] [℃]		
	A%	G%	CRM%	PG-HT[2]	PG-IT[3]	PG-LT[4]
A2	100			67	20	-25
G2		100		58	31	-11
GR2(87:13)100		87.5	12.5	61	32	-10
GR2(75:25)100		75	25	64	33	-8
AGR2(62:25:13)100E	62.5	25	12.5	73	22	-16

3.5.1.1. Binder preparation. Binders were designated to evaluate the performance of the guayule-based binder through the mixture [140]. The designation implied five binders, which were control asphalt (PG67-25), pure guayule (PG58-11), one AGR2 blend (AGR2(62:25:13)100E), and two guayule-rubber blends (GR2(87:13)100 and GR2(75:25)100). The critical performance grades of the designated binders were reported in Table 3.5 based on the outcomes revealed in Section 4.

3.5.1.2. Aggregate gradation. According to AASHTO M 323 [141] and MoDOT 403 [142], a job mix formula was followed to investigate the guayule-based binders in the field-simulated lab mixtures. Five individual aggregates were employed to make an accepted aggregate blend with the MoDOT's Superpave mix design procedure. The five aggregate types and proportions were as follows: three Potosi Dolomite Formation (29% of 9/16″ clean, 29% of 3/8″ clean, and 15% of screenings), 25% of manufactured sand (crushed gravel), and 2% of mineral fillers (-#200). The aggregate blend had a 12.5-mm (1/2″) nominal maximum aggregate size, named SP125 in the Superpave mix design procedure. Figure 3.10 illustrates the combined aggregate gradation, compared to the Superpave and MoDOT specification limits: Superpave upper and lower specification limits (USL and LSL, respectively), and MoDOT 403 SP125 USL and LSL.

3.5.1.3. Investigated mixes. Figure 3.11 shows a flowchart of the five designated mixtures for investigations. The five mixtures were determined to address the effect of the binder replacements on the mixture performance. Mixture IDs were defined underneath the flowchart. The pure asphalt mixture (A2-Mix) was selected to be compared with the AGR2 mixture (AGR2(62:25:13)100E-Mix). On the other hand, guayule was investigated in

mixtures as a full asphalt alternative. Based on its performance limitations, a pure guayule mixture (G2-Mix) was assessed. Figure 3.12 shows the pure guayule mix as loose and compacted mixtures. Two guayule-rubber mixtures were designated to analyze the performance changes by CRM addition in two different concentrations (12.5% and 25%, by wt. of blend), named GR2(87:13)100-Mix and GR2(75:25)100-Mix, respectively.
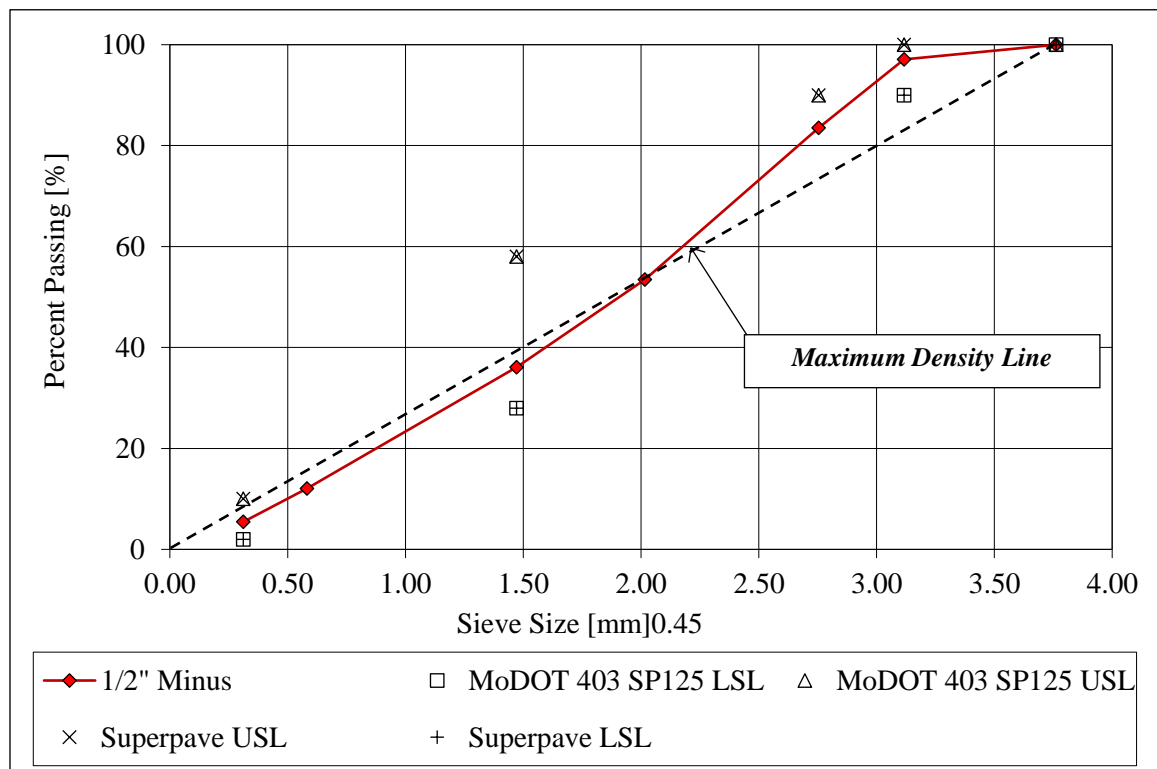
Figure 3.10 Aggregate Gradation [90].

To determine the air content (V_a) of each compacted mixture, the theoretical maximum specific gravity (G_{mm}) and bulk specific gravity (G_{mb}) were determined,

according to AASHTO T 209 [143] and AASHTO T 166 [144], respectively. Table 3.6

illustrates the G_{mm} value of each designated mixture.

```
                          ┌─────────────┐
                          │  Mixtures   │
                          └─────────────┘
```

Asphalt Mix A2-Mix[1]	Pure Guayule Mix G2-Mix[2]	Guayule-Rubber Mix (1) GR2(87:13)100-Mix[3]	Guayule-Rubber Mix (2) GR2(75:25)100-Mix[4]	Asphalt-Guayule-Rubber Mix AGR2(62:25:13)100E-Mix[5]

[1]A2-Mix: included PG67-25 control asphalt (A2).
[2]G2-Mix: included PG58-11 pure guayule (G2).
[3]GR2(87:13)100-Mix: included GR2 blend (87.5% G2 and 12.5% CRM, by wt. of blend).
[4]GR2(75:25)100-Mix: included GR2 blend (75% G2 and 25% CRM, by wt. of blend).
[5]AGR2(62:25:13)100E-Mix: included AGR2 blend (62.5% A2, 25% G2, and 12.5% CRM, by wt. of blend).

Figure 3.11 Investigated Mixtures [90].

Figure 3.12 Pure Guayule Mixture (G2-Mix): Loose (Left) and Compacted (Right) [90].

Table 3.6 G_{mm} Values of Designated Mixtures [90].

Designated Mix	G_{mm} [Unitless]
A2-Mix	2.526
G2-Mix	2.540
GR2(87:13)100-Mix	2.550
GR2(75:25)100-Mix	2.546
AGR2(62:25:13)100E-Mix	2.549

3.5.2. Methods. This subsection implies interpretations regarding mixing and compaction requirements for mixture preparation and involved mixture tests.

3.5.2.1. Mixing and compaction temperatures. As interpreted in Subsection 3.3.2.1, the RV was used to determine the mixing and compaction temperature ranges. The mixing and compaction temperatures' investigation is discussed in Section 4. However, Table 3.7 demonstrates the accepted temperature ranges used to proceed with mixture experiment, according to viscosity values of 0.170±0.020 Pa.s and 0.280±0.030 Pa.s, respectively [119]. The applied mixing and compaction temperatures are also stated between two brackets.

Table 3.7 Mixing and Compaction Temperatures [140].

Designated Mix	Temperature Range [℃]	
	Mixing	Compaction
A2-Mix	152-158 (155)[9]	135-143 (143)
G2-Mix	141-146 (143)	121-127 (127)
AGR2(62:25:13)100E-Mix	176-181 (176)	164-169 (165)
GR2(87:13)100-Mix	146-153 (150)	132-138 (135)
GR2(75:25)100-Mix	172-178 (176)	159-165(165)

---

[9] The number between the two brackets indicates the selected temperature for mixing/compaction.

3.5.2.2. Mixing and compaction processes. The individual aggregates were oven-dried until a constant mass was achieved, indicating no further moisture inside, then combined. The mixing temperature was used for mixing pans, mixing paddles, combined aggregate, and asphalt binder. AASHTO R 30 [145] was followed for mix design and short-term aging simulation procedures. A mechanical mixer was employed to prepare the loose mixtures at the optimum asphalt content based on the control asphalt mix design, P_b = 4.7%. A Superpave gyratory compactor was used to prepare the Superpave mix cores, according to AASHTO T 312 [146], in which G_{mb} was determined based on each V_a requirement.

3.5.2.3. Mixture tests. Mixture tests were selected to address the major distresses (rutting, fatigue cracking, and thermal cracking) in addition to moisture susceptibility evaluations [140]. Figure 3.13 illustrates the used mixture tests in this study, associated with the followed standards/specifications. Superpave recognized the modified Lottman test to assess moisture susceptibility. Therefore, it could be an initial indicator to predict the applicability of the guayule-based mixtures against moisture damage (stripping). Even though many researchers employed this standard method of moisture sensitivity assessment, there is a belief that it is not highly correlated to the field performance [147]. The Hamburg Wheel Tracking test (HWT) test is not a standard method recognized by Superpave. Nevertheless, the HWT test could be a representative tool to evaluate the moisture susceptibility besides the associated rutting potential. The rut test by asphalt pavement analyzer (APA) is a common technique directly relevant to the rutting resistance assessment used in this study. The concept of fracture energy was utilized to predict

cracking potential in the designated mixes at intermediate and low temperatures. The Semi-Circular Bend (SCB) test was employed to evaluate the intermediate temperature cracking. The Disk-Shaped Compact Tension (DCT) test was used to assess the thermal cracking resistance at low temperatures. The DCT test is more reliable than the SCB tests regarding the thermal cracking assessment because of the long crack path that provides adequate time to analyze the crack propagation at low temperatures [148]. However, the validity of the DCT test applications was only offered at low temperatures up to +10℃ [149].

Tensile strength ratio (TSR) test. Regarding moisture susceptibility, the Modified Lottman test is included in the Superpave Mix Design procedures [126]. In this study, AASHTO T 283 [150] was followed to investigate the moisture susceptibility of the five designated mixtures. Six-core specimens were made with a 6.5–7.5% V_a and divided into two sets (dry and wet). The first set involved three dry cores (control), and the other set involved three wet cores (conditioned), which were exposed to vacuum saturation of 70–80% with water. The wet set was exposed to one freezing cycle for 16h at -18℃ and one thaw cycle in a 60℃ water bath for 24h. Afterward, both sets were conditioned in a 25℃ water bath for 2h before testing. The indirect tensile strength was measured (using a load rate of 2 inch/min), and averages were calculated to acquire the tensile strength ratio (TSR), according to Equation (9) [126]. Many agencies recommended the TSR to be no less than 70% [126].

$$\text{TSR} = \frac{\text{Indirect Tensile Strength of Conditioned set}}{\text{Indirect Tensile Strength of control set}} \tag{9}$$
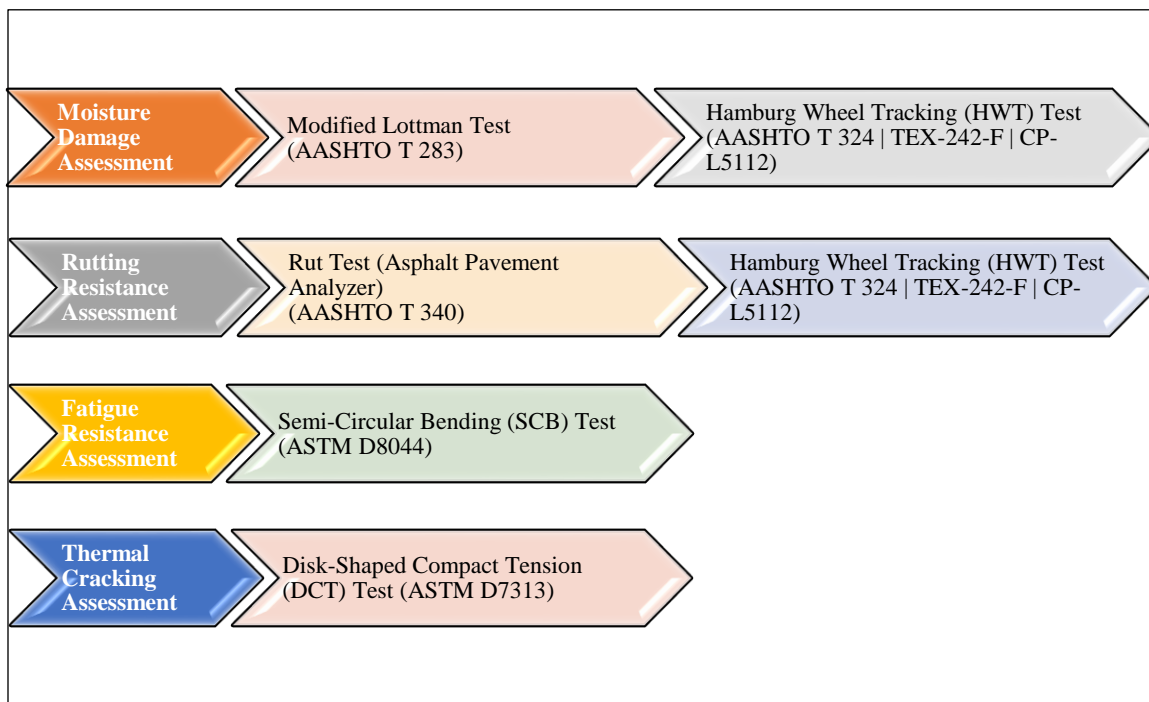
Figure 3.13 Flowchart of Mixture Tests [90].

Rut test. The mixture's rutting susceptibility was investigated using the APA. The rut test was carried out according to AASHTO T 340 [142]. Based on their performance grades, a 64℃ testing temperature was chosen to compare stiffer mixtures (A2-Mix, AGR2(62:25:13)100E-Mix, and GR2(75:25)100-Mix). A 58℃ testing temperature was selected to compare softer mixtures (GR2(87:13)100-Mix and G2-Mix). Stiffer and softer mixtures were recognized according to the binders' PG-HTs. The core samples — involving a V_a of 6.5–7.5% — were installed in the molds and set in the APA chamber for 6h before testing to ensure the isothermal condition. Eight thousand passes were applied based on 60 cycle/min at the test temperature. Figure 3.14 shows technical steps from the rut test procedures conducted by the APA.

Figure 3.14 Technical Steps from the Rut Test Procedures [90].

Hamburg wheel tracking (HWT) test. The HWT test was employed to investigate moisture susceptibility and the associated potential rutting of the designated mixtures using the modified APA. Moisture damage could occur for many reasons such as cohesion failure induced by moisture [147]. AASHTO T 324 reported that the agency specified the testing temperature [151]. Colorado Department of Transportation (CDOT) test criteria (CP-L5112) specified the test temperature based on the binder's PG-HT (i.e., 40℃ for PG52, 45℃ for PG58, 50℃ for PG64, and 55℃ for PG70 or higher) [152]. The lab-compacted specimen is required to contain a $6\pm2\%$ V_a. CDOT defined the failure when the rut depth surpassed 4 mm at 10,000 passes [153]. Texas Department of Transportation (TxDOT), TEX-242-F, specified a constant temperature of $50\pm1℃$ regardless of the binder grade [154]. The lab-compacted specimen is required to contain a $7\pm1\%$ V_a. The test outcome is considered a failure if the rut depth exceeds 12.5 mm [152]. TxDOT identified the minimum number of passes according to the binder grade (i.e., 10,000 passes for PG64 or lower, 15,000 passes for PG70, and 20,000 passes for PG76 or higher) [152]. In this study, the HWT test was mainly carried out with monitoring the outcomes according to the two

specifications to a great extent. Figure 3.15 shows technical steps from the HWT test procedures.
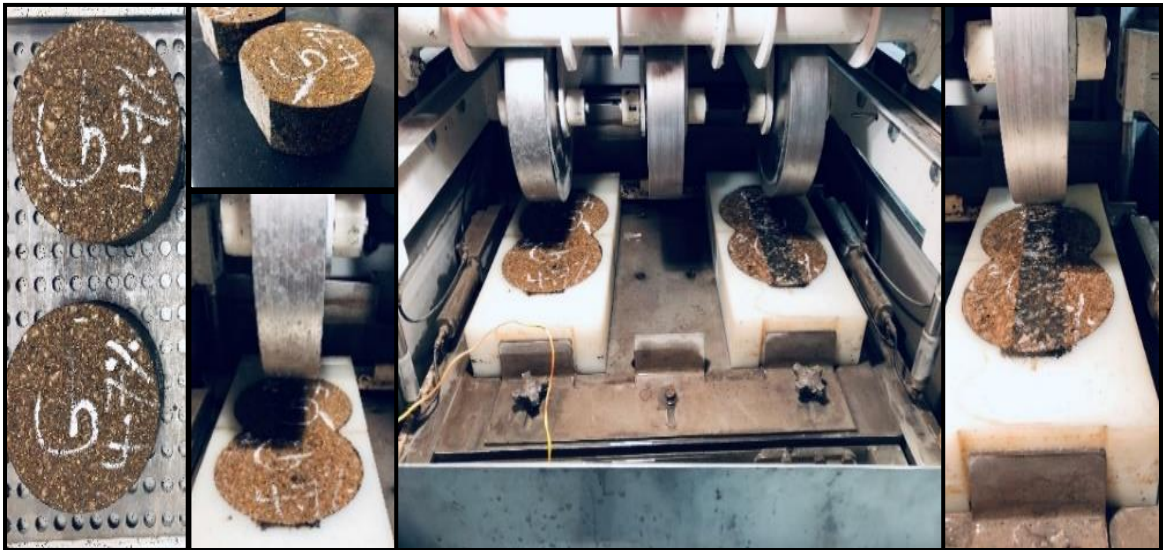
Figure 3.15 Technical Steps from the HWT Test Procedures [90].

Semi-circular bend (SCB) test. The concept of the SCB test was introduced by Mull et al. (2002) [155] to evaluate asphalt mixtures involving CRM. Afterward, this concept was utilized to investigate fatigue fracture resistance of asphalt mixtures in Louisiana [156, 157]. In this study, the five designated mixtures were analyzed using the SCB test at 25℃. This test is highly recommended by Louisiana Transportation Research Center [158] and found suitable by several researchers to estimate the mixture's fatigue fracture resistance [156]. The 25℃ test temperature was used in the literature to address the intermediate temperature cracking [156-159]. At a rate of 0.5 mm/min, the three-point bending test was

conducted, according to ASTM D8044 [160], in which the specimen represented a half-disk with a notch cut depth parallel to the loading and vertical axis. The specimen was loaded monotonically up to fracture failure occurrence [156, 160]. The applied contact load was 0.045 kN. The target V_a was 6.5–7.5% [160]. Louisiana Department of Transportation and Development (LADOTD) recommended three sets of specimens with notch depths of 25, 32, and 38 mm [156-160]. Technical steps from the SCB test procedures are shown in Figure 3.16. The critical strain energy release rate (J-integral or J_c) end result parameter, illustrated in Equation (10), was utilized to evaluate the fatigue fracture resistance. The J-integral is a function of the rate of change of strain energy per notch depth (dU/da) [156]. Several studies revealed that softer binders might reduce fracture resistance at intermediate temperatures [156, 158, 161].

$$J_c = -\left(\frac{1}{b}\right) \frac{dU}{da} \tag{10}$$

where:

J_c Critical strain energy release rate, kJ/m^2

b   Specimen thickness, mm

a   Notch depth, mm

U   Strain energy to failure (area under the load-displacement curve to peak load), N.mm

dU/da   change of strain energy with notch depth (strain energy-notch depth slope)

Figure 3.16 Technical Steps from the SCB Test Procedures [90].

LADOTD recommended a minimum of 0.45 kJ/m2 to indicate a threshold acceptance of a mixture's resistance to fatigue fracture cracking [158]. Studies reported that the higher the Jc value, the higher the fracture resistance to fatigue cracking [162].

Disk-shaped compact tension (DCT) test. The DCT test was selected to investigate the fracture energy (G_f) at low temperatures, illustrated in Equation (11) [149], to evaluate the thermal fracture properties of the designated mixtures. Technical steps from the DCT test procedures are shown in Figure 3.17. The target V_a was 6.5–7.5%. Literature reported that the quality of the DCT results goes down when temperatures go higher than +10°C [149]. The better DCT fracture energy outcomes were associated with softer binders at low temperatures [163, 164]. Based on the literature, the test temperature was selected to be 10°C greater than the PG-LT [149, 165]. Besides measuring at 10°C greater than the PG-

LT, measurements at different low temperatures were taken to further investigate the effect of low-temperature change on some designated mixtures. ASTM D7313 [149] was followed to conduct this test. A constant crack mouth opening displacement (CMOD) rate of 0.017 mm/s (approximately 1 mm/min) controlled the DCT test [149, 165]. The seating (contact) and post-peak loads were applied 0.1 kN. The specimen geometry was set concerning ASTM D7313 [149]. Specimens were temperature-conditioned in the DCT instrument's environmental chamber for 2h to ensure the isothermal condition [149].

$$G_f = \frac{Area}{B(W - a)} \tag{11}$$

where:

G_f Fracture energy, J/m^2

Area   Area under the load-CMOD curve up to 100 N, N.m

B   Specimen thickness, m

W-a   Ligament length, m
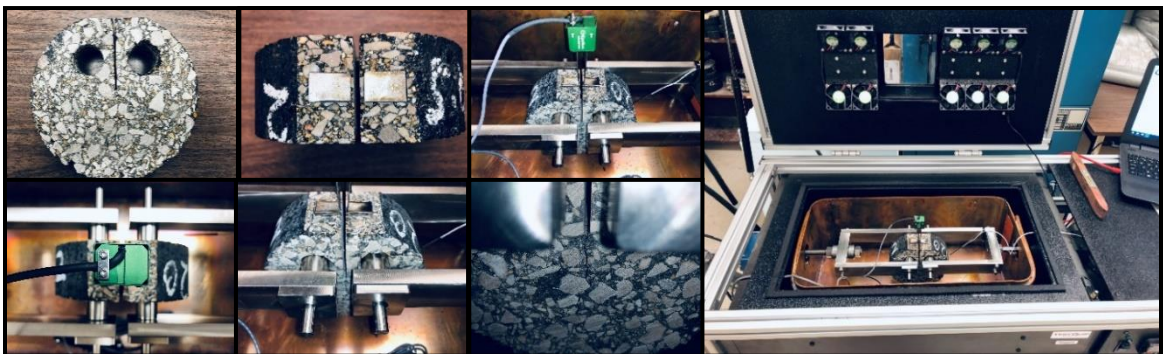
Figure 3.17 Technical Steps from the DCT Test Procedures [90].

Studies reported a threshold G_f value of 400 J/m^2 to indicate an acceptable threshold value of fracture energy to resist low-temperature cracking [165] to allow short-term aged specimens to be utilized [163].

4. BASIC RHEOLOGICAL ANALYSIS BASED ON THE SUPERPAVE CRITERIA

This section aimed to investigate guayule in partial and full asphalt cement replacement from the perspective of the standard rheological asphalt characterization recognized by the Superpave criteria. The investigated binders included soft and stiff control asphalt (A), guayule (G), asphalt-guayule (AG), guayule-rubber (GR), asphalt-rubber (AR), and asphalt-guayule-rubber (AGR) blends. Superpave criteria were employed to evaluate the designated binders in this section. The designated binders were exposed to tests covering the construction process (mixing and compaction requirements), rutting resistance, fatigue cracking resistance, and thermal cracking resistance through viscosity, and high-, intermediate-, and low-temperature measurements. Therefore, the investigation involved as-received materials, after blending (interaction), after RTFO aging, and after PAV aging.

4.1. FIRST EXPERIMENT: SOFT-ASPHALT SOFT-GUAYULE

This subsection implies a reproduction of results presented in [2].

4.1.1. Mixing and Compaction Requirements. Figure 4.1 illustrates the mixing and compaction temperature ranges for the soft asphalt (A1), soft guayule (G1), and soft asphalt-guayule (AG1(50:50)120) binders. Despite the same high-temperature grade for A1 and G1 (both PG52, standard), G1 presented a relatively lower viscosity than A1, thus reflecting reduced production temperatures, saving plant energy consumption, and lowering environmental emissions were predicted [13]. For instance, at 135℃, the viscosity

was 0.149 Pa.s for G1 and 0.244 Pa.s for A1. The A1 and G1 had mixing temperature ranges of 140–146℃ and 129–136℃, respectively. They had compaction temperature ranges of 129–134℃ and 114–120℃, respectively. The trendline of AG1(50:50)120 — comprised of 50% asphalt and 50% guayule — was located closer to the G1 trendline. Such a trendline illustrated the domination of guayule in the overall blend's viscosity. The AG1(50:50)120 mixing and compaction temperatures yielded 132–139℃ and 119–125℃, respectively.
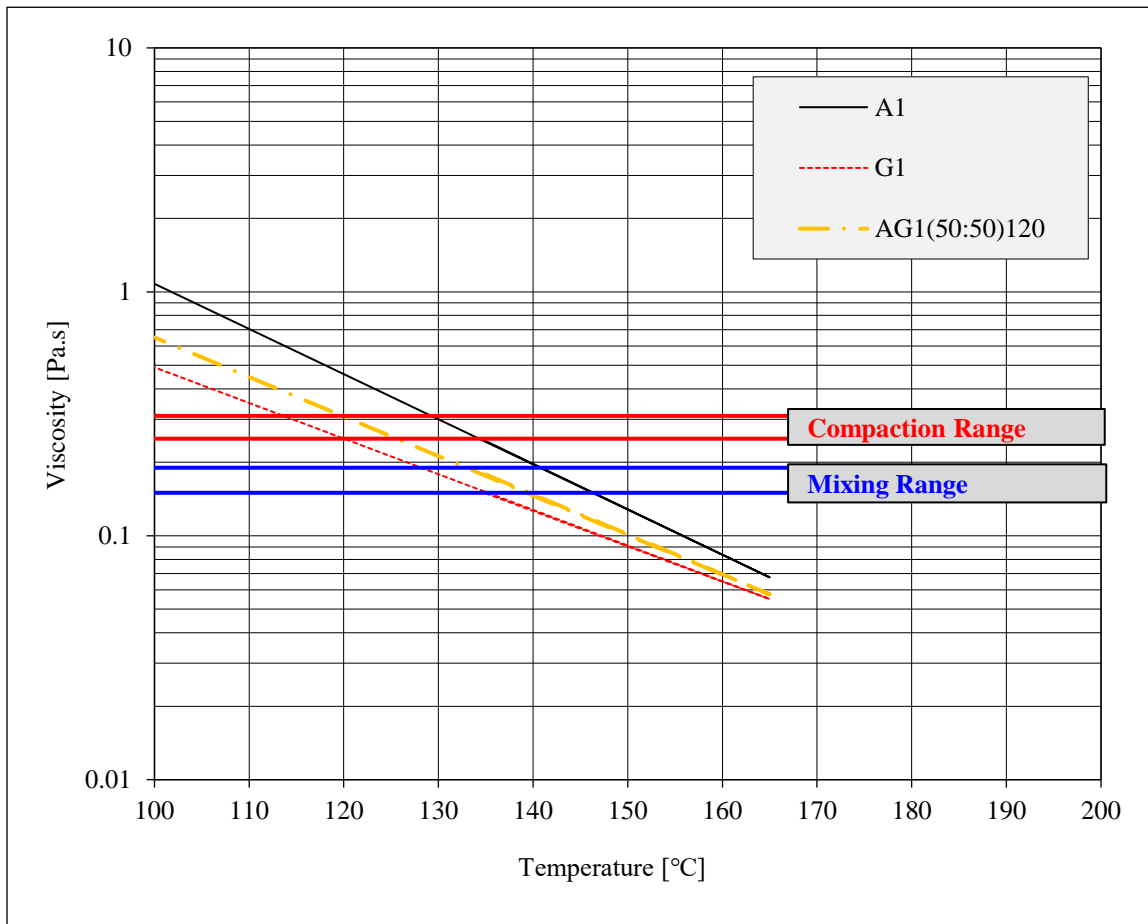
Figure 4.1 Mixing and Compaction Temperature Ranges: A1, G1, and AG1(50:50)120 [2].

4.1.2. Rutting Resistance. In this experiment, tested binders were categorized into 13 designated binders as listed in Table 4.1. The designated binders were investigated using the DSR to evaluate their basic rheological properties at a wide range of high temperatures. The G^*, δ, and $|G^*|/\sin\delta$ were determined for each binder before and after RTFO aging. The G^* parameter represents the binder stiffness, meaning the higher the G^*, the greater the stiffness. The δ parameter represents the binder viscoelastic behavior, meaning the higher the δ, the lower the elasticity. The binder is desired to be stiffer and more elastic at high temperatures to resist rutting, particularly at the early stages of the pavement life.

For brevity, in compliance with the statistical considerations mentioned in Subsection 3.2, Figure 4.2 shows the temperature sweep of the Superpave rutting parameter ($|G^*|/\sin\delta$) of the control asphalt (A1) and the heat-treated guayule (G1) as original (unaged) binders and RTFO-aged binders. Each data point in the chart represents an average of two test results with respect to AASHTO T315 [97] precision requirements according to the repeatability (single-operator precision), which is based on a probability of about 5% in the normal and correct operation of the test method; used as an index of precision of the test method [98]. The average values were calculated considering the acceptable ranges of two test results, which were 4.6% for $|G^*|/\sin\delta$ of original binder and 7.2% for $|G^*|/\sin\delta$ of RTFO-aged binder. The vertical line at each data point represents the error bar based on $\pm$ one standard deviation.

4.1.2.1. Major observations of basic rheological parameters at high temperatures. Considering comparable guayule and asphalt at high-grade temperatures (both PG52, standard), from Table 4.1, the following points reveal the major observations

based on the basic rheological parameters used for standard asphalt assessment (G* and δ)

at high temperatures:
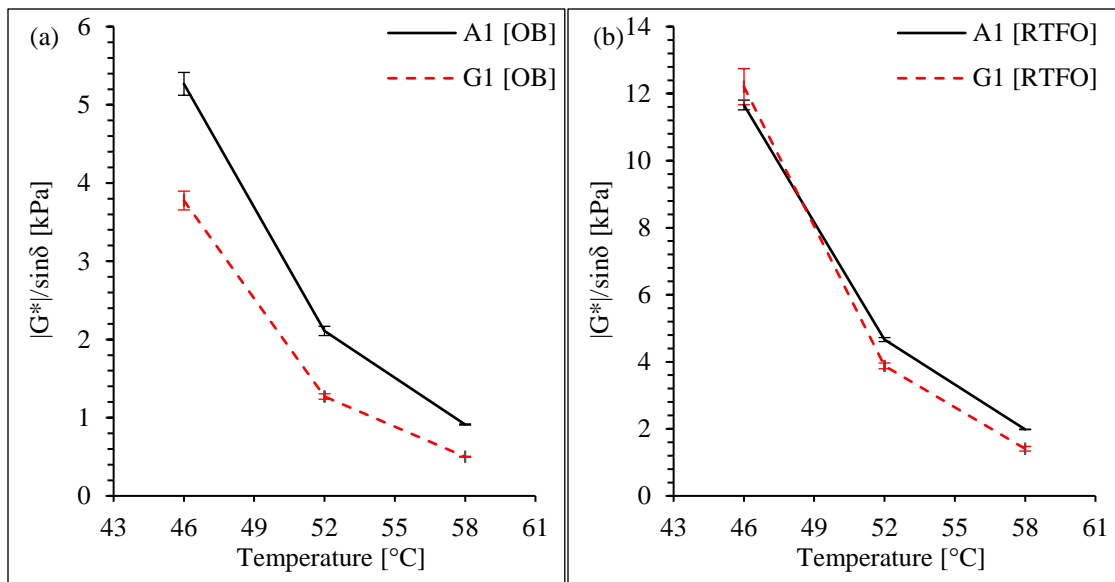
Figure 4.2 Example of Statistical Considerations: Average Values and Standard
Deviation Error Bars of |G*|/sinδ of A1 and G1 with Temperature Sweep: (a) Original
Binders [OB] and (b) RTFO-Aged Binders [RTFO].

- The heat treatment process revealed a considerable increase in guayule
  stiffness due to the potential removal of moisture and light molecular weight
  components in the as-received guayule. There was a little-to-no change in
  guayule's elastic behavior before vs. after RTFO aging or as-received vs.
  heat treated.

- After RTFO aging, guayule was stiffer than asphalt at lower temperatures
  (e.g., 46°C) but softer at higher temperatures (e.g., 58°C).

Table 4.1 Rheological Parameters of First Experiment at High Temperatures.

Binder Code	Temp [°C]	Unaged			RTFO-Aged		
		G* [kPa]	δ [°]	|G*|/sinδ [kPa]	G* [kPa]	δ [°]	|G*|/sinδ [kPa]
A1	46	5.2	84	5.3	11.5	79	11.7
	52	2.1	86	2.1	4.6	82	4.7
	58	0.9	87	0.9	2.0	84	2.0
G1(As-Received)	46	1.3	85	1.3	10.1	85	10.1
	52	0.4	87	0.4	3.2	87	3.2
	58				1.2	88	1.2
G1	46	3.8	86	3.8	12.2	86	12.2
	52	1.3	87	1.3	3.9	87	3.9
	58	0.5	88	0.5	1.4	88	1.4
AG1(50:50)120	46	2.6	86	2.6	8.7	85	8.7
	52	1.0	87	1.0	3.0	86	3.0
	58	0.4	87	0.4	1.1	87	1.1
GR1(83:17)240	46	4.7	74	4.9	14.8	71	15.7
	52	2.1	78	2.1	6.2	74	6.5
	58	1.0	81	1.0	2.8	76	2.9
	64	0.6	83	0.6	1.4	79	1.5
GR1(91:9)360	46	2.9	80	3.0	12.8	81	13.0
	52	1.2	83	1.2	4.5	83	4.6
	58	0.6	84	0.6	1.8	85	1.8
AGR1(42:42:16)240A	46	4.6	72	4.8	12.9	70	13.7
	52	2.2	76	2.3	5.8	72	6.1
	58	1.1	78	1.2	2.8	75	2.9
	64	0.6	80	0.6	1.4	77	1.5
AGR1(45:45:10)240	58	1.0	81	1.1	2.6	78	2.6
	64	0.5	83	0.5	1.3	80	1.3
AGR1(45:45:10)360B	46	4.9	76	5.0	13.8	74	14.4
	52	2.1	79	2.1	5.7	75	5.9
	58	1.0	82	1.0	2.5	78	2.6
	64				1.2	80	1.2
AGR1(68:23:9)360	46	4.7	78	4.8	9.6	77	9.9
	52	2.1	80	2.1	4.1	79	4.2
	58	1.0	83	1.0	1.9	81	1.9
	64	0.5	84	0.5			

Table 4.1 Rheological Parameters of First Experiment at High Temperatures (Cont.).

Binder Code	Temp [°C]	Unaged			RTFO-Aged		
		G* [kPa]	δ [°]	|G*|/sinδ [kPa]	G* [kPa]	δ [°]	|G*|/sinδ [kPa]
AGR1(23:68:9)360	46	2.8	81	2.8	10.6	80	10.7
	52	1.2	83	1.2	4.0	82	4.0
	58	0.6	84	0.6	1.6	83	1.6
AR1(83:17)240A	46	23.0	56	27.8	28.2	53	35.2
	52	13.0	59	15.2	16.8	54	20.7
	58	7.3	63	8.2	10.0	56	12.1
	64	4.1	68	4.5	6.0	58	7.1
	70	2.3	72	2.4	3.6	62	4.1
	76	1.3	75	1.4	2.2	65	2.4
	82	0.8	78	0.8	1.4	69	1.5
AR1(91:9)360B	46	10.4	71	11.0	21.3	64	23.6
	52	5.0	74	5.2	10.5	66	11.5
	58	2.4	77	2.5	5.3	69	5.7
	64	1.2	79	1.3	2.7	72	2.9
	70	0.6	82	0.7	1.4	74	1.5

- Before RTFO aging, guayule and asphalt had close elastic behaviors. However, after RTFO aging, asphalt elasticity increased but guayule elasticity retained the same as before its RTFO aging.

- The CRM raised guayule stiffness and elasticity, reflected on a higher rutting resistance evaluated by the Superpave rutting parameter, $|G*|/sin\delta$.

- The CRM relatively enhanced the rheological parameters at high temperatures of asphalt (higher G* and lower δ) than that of guayule. In this regard, further details are provided in the following subsection (4.1.2.2).

- It was noticed that the asphalt-guayule (AG1(50:50)120) blend yielded lower stiffness than either individual asphalt or individual guayule, whereas it yielded the same elasticity of guayule, indicating the domination of guayule on the blend's elasticity. However, CRM addition in the AGR1 blend enhanced the blend's stiffness and elasticity compared to either individual asphalt, individual guayule, or asphalt-guayule blend.

4.1.2.2. Critical high temperature. Figure 4.3 illustrates the critical high temperature of the designated binders (unaged and RTFO-aged) in descending order based on the RTFO-aged binders. The critical high temperatures for the unaged binders were measured at 1.0 kPa, and 2.2 kPa for the RTFO-aged binders [182]. The following conclusions were established according to the RTFO-aged binders since they simulate the first stages of the pavement service life. It seems that RTFO aging raised the high-temperature grade of most presented binders [18]. The virgin asphalt and virgin guayule had 57℃ and 54℃ critical high temperatures, respectively. The AG1(50:50)120 yielded a 54℃ critical high temperature, indicating asphalt, guayule, and asphalt guayule blend had the same high-temperature grade (PG52, standard). The control asphalt (A1) divided the chart into the left side (superior high-temperature performance) and the right side (inferior high-temperature performance). Considering the results, the softer binders were GR1(91:9)360, AGR1(23:68:9)360, G1, G1(As-Received), and AG1(50:50)120, thus indicating the negative effects of higher guayule concentration, less CRM concentration, or both, when compared to the right-side binders. It was evident by the resultant rheological properties that the RTFO-aged guayule almost yielded the same performance as the as-

received guayule (G1(As-Received)) and the heat-treated one (G1), indicating a reduction in moisture and volatiles of guayule that made the molecular structure of as-received guayule similar to that of the heat-treated guayule, complied with literature about bio-oils [16, 18].
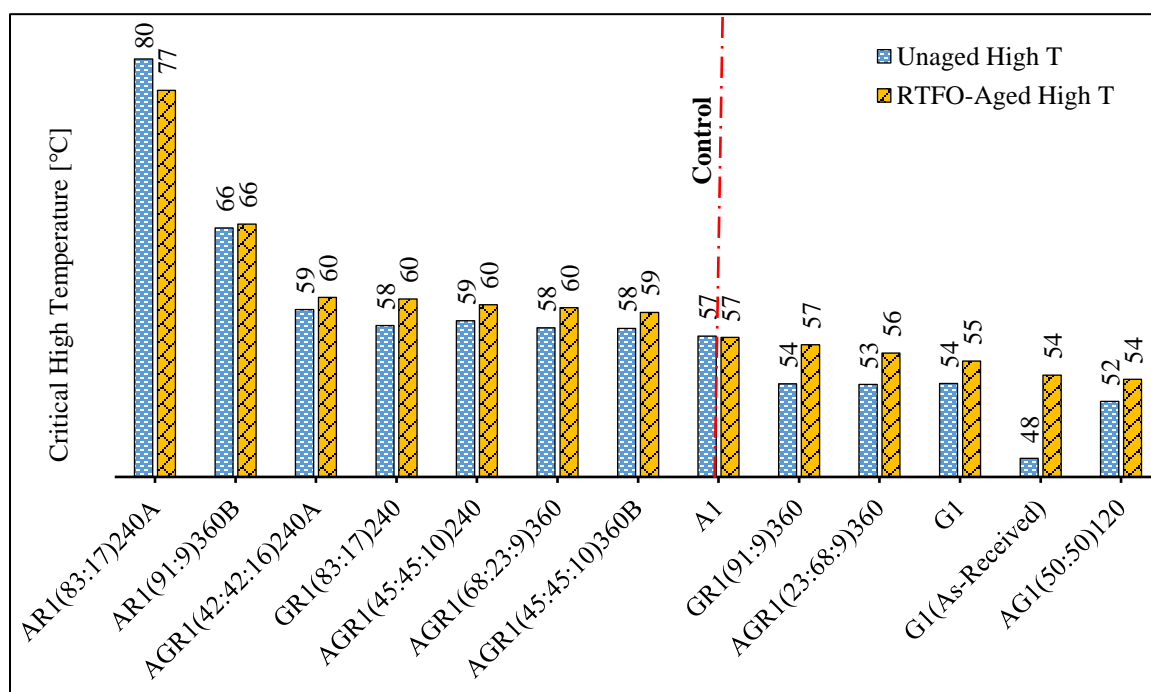
Figure 4.3 Critical High Temperatures for the Soft Designated Binders (Unaged and RTFO-Aged) Ranked in Descending Order Based on the RTFO-Aged Binders [2].

Rubber was reported to enhance the rheological properties of asphalt by resisting rutting distress [131]. The AR1(83:17)240A resulted in a 77℃ critical high temperature. However, the GR1(83:17)240 resulted in a 60℃ critical high temperature. The 20% CRM (by wt. of liquid binder) improved asphalt by four grades (about 34%, compared to the virgin binder) and guayule by one grade (about 11%), indicating that CRM provided more

enhanced asphalt rutting resistance than guayule, supported by the component analysis presented in Section 6. The AGR1(42:42:16)240A yielded a 60℃ critical high temperature, indicating the domination of guayule on the overall blend regarding rutting resistance, which was identical to the GR1(83:17)240. The AGR1(45:45:10)360B resulted in a 59℃ critical high temperature that provided an enhancement of 10% CRM addition compared to the AG1(50:50)120. The AGR1(68:23:9)360 and AGR1(23:68:9)360 resulted in 60℃ and 56℃ critical high temperatures. The critical high temperature of AGR1(45:45:10)360B was located between AGR1(68:23:9)360 and AGR1(23:68:9)360, indicating a consistent influence of the material parameter on the product performance. The greater influence of CRM enhancement on asphalt compared to guayule was recognized due to having the control asphalt and the virgin guayule in the same high-temperature grade (both PG52, standard).

  4.1.3. Aging Resistance. Figure 4.4 illustrates the AS of the designated binders ranked in ascending order. The AR1(83:17)240A binder had the highest aging resistance (AS = 1.8), and the GR1(91:9)360 binder had the lowest aging resistance (AS = 3.9). Consequently, adding 20% CRM to asphalt increased the aging resistance compared to the control asphalt (AS = 2.2). The AGR1(42:42:16)240A, AGR1(45:45:10)360B, AGR1(45:45:10)240, and AGR1(68:23:9)360 blends had approximately the same aging resistance (AS ~2.6), which were higher than the control asphalt's aging resistance. In AGR1s, the higher the CRM concentration, the higher the aging resistance. In this experiment, the lowest aging-resistant binders were AG1(50:50)120 (AS = 2.9), AGR1(23:68:9)360 (AS = 3.4), and GR1(91:9)360 (AS = 3.9).
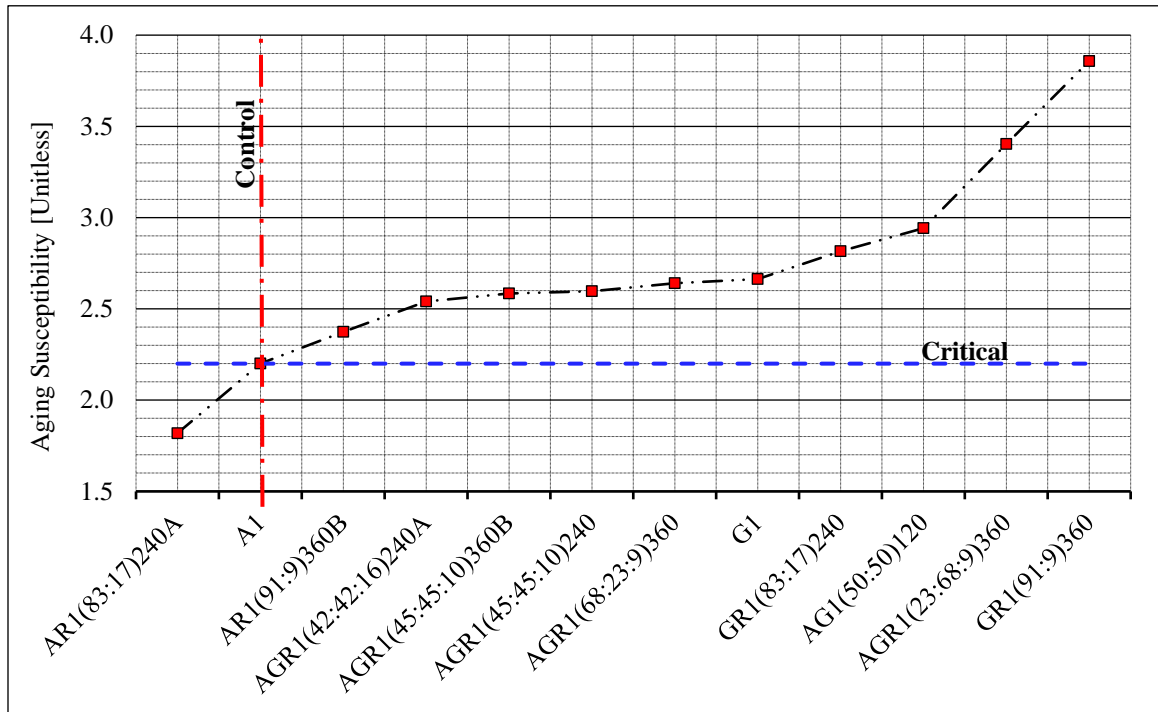
Figure 4.4 Aging Resistance for the Soft Designated Binders Ranked in Ascending Order [2].

4.1.4. Fatigue Cracking Resistance. The designated binders were investigated using the DSR to evaluate their basic rheological properties at variant intermediate temperatures. The G*, δ, and |G*|.sinδ were determined for each binder after PAV aging, as shown in Table 4.2. The binder is desired to be softer and more elastic at high temperatures to resist fatigue cracking particularly when approaching the end of the pavement life.

4.1.4.1. Major observations of basic rheological parameters at intermediate temperatures. The following points reveal the major observations based on the basic rheological parameters used for standard asphalt assessment (G* and δ) at intermediate temperatures:

Table 4.2 Rheological Parameters of First Experiment at Intermediate Temperatures.

| Binder Code | Temp [°C] | PAV-Aged | | |
		G* [kPa]	δ [°]	|G*|.sinδ [kPa]
A1	13	11440	38	7000
	16	7785	40	4980
	19	5238	42	3494
	22	3491	44	2423
	25	2225	46	1610
G1(As-Received)	22	10395	67	9561
	25	4940	74	4746
G1	22	10871	66	9956
	25	4873	74	4684
AG1(50:50)120	19	7186	56	5954
	22	4026	61	3537
	25	2173	66	1992
GR1(83:17)240	25	5477	70	5132
	28	2700	74	2596
GR1(91:9)360	22	10328	63	9208
	25	4724	71	4456
AGR1(42:42:16)240A	16	7057	49	5297
	19	4366	53	3472
	22	2584	57	2158
	25	1516	60	1314
AGR1(45:45:10)240	19	7252	48	5411
	22	4508	53	3591
AGR1(45:45:10)360B	16	15752	46	11305
	19	10111	51	7901
	22	5734	58	4843
AGR1(68:23:9)360	13	8864	43	6098
	16	5577	47	4087
	19	3449	51	2668
AGR1(23:68:9)360	16	13973	51	10806
	19	8403	57	7043
	22	4502	63	4024
AR1(83:17)240A	7	8741	39	5534
	10	5899	41	3871
AR1(91:9)360B	10	8587	40	5468
	13	6209	41	4093

- In compliance with high-temperature analysis, guayule provided lower elasticity than asphalt.

- Even though asphalt was stiffer than guayule at high temperatures, guayule possessed higher stiffness at intermediate temperatures, followed by a lower resistance to fatigue cracking.

- As expected, the as-received guayule yielded similar rheological parameters (G^*, δ, and $|G^*|.\sin\delta$) to the heat-treated guayule, indicating the effect of RTFO- and PAV-aging on the as-received guayule and made it comparable to the heat-treated guayule.

- The CRM significantly lowered asphalt stiffness but made a little-to-no change to its elastic behavior (significantly enhanced its resistance to fatigue cracking).

- The CRM slightly changed guayule stiffness and elasticity (almost no change in resisting fatigue).

- The CRM effect on asphalt-guayule blend mainly depended on the material concentrations.

4.1.4.2. Critical intermediate temperature. Figure 4.5 illustrates the critical intermediate temperatures of the designated binders ranked in ascending order. The virgin asphalt had a 16℃ critical intermediate temperature, and the virgin guayule had a 25℃ critical intermediate temperature. By assessing the critical high temperatures (discussed in Subsection 4.1.2) and critical low temperatures (discussed in Subsection 4.1.5), it was found that most designated guayule-based binders offered measured critical intermediate

temperatures higher than the average of high- and low-temperature grades plus 4℃, as defined by the Superpave criteria [126], thereby reflecting the compatibility of the Superpave criteria with the novel binder. As expected, the AG1(50:50)120 resulted in a 20℃ critical intermediate temperature that almost equaled the average of the asphalt and guayule critical intermediate temperatures. The addition of CRM to guayule did not change the critical intermediate temperatures of the guayule-rubber blends: both GR1(91:9)360 and GR1(83:17)240 resulted in 25℃ critical intermediate temperatures that were similar to the virgin guayule's critical intermediate temperature (25℃). Conversely, CRM significantly enhanced the virgin asphalt intermediate-temperature grade, resulting in 8℃ and 11℃ for AR1(83:17)240A and AR1(91:9)360B, respectively. Thus, high CRM concentration yielded enhanced intermediate-temperature performance of the AR1 blend. The AGR1 blends had enhanced intermediate-temperature grades compared to guayule and guayule-rubber blends because asphalt and CRM were both present. The AGR1(42:42:16)240A resulted in 16℃, and the AGR1(45:45:10)240 resulted in 20℃. Increasing the interaction times of AGR1(45:45:10) from 240 to 360 min negatively influenced the intermediate-temperature grade (22℃), making it undesirably stiffer. The effect of asphalt concentration was defined by comparing AGR1(68:23:9)360 to AGR1(23:68:9)360, which yielded 15℃ and 21℃, respectively.

4.1.5. Thermal Cracking Resistance. Figure 4.6a,b illustrates time-dependent creep stiffness (S(t)) and m-value, respectively, in the test temperature domain. Rubber offered negatively little-to-no change in the performance of guayule-rubber (GR1) binders. The GR1(83:17)240 and GR1(91:9)360 resulted in test temperatures of -6℃ and -4℃,

respectively, compared to the virgin guayule (-6°C). Rubber enhanced the critical low temperatures of AGR1 blends, meaning performance improved with a blend such as AGR1(42:42:16)240A (-16°C critical low temperature). The virgin asphalt had a lower critical temperature (-19°C) compared to the virgin guayule (-6°C), thus higher asphalt concentration yielded enhanced binder performance (e.g., AGR1(68:23:9)360 > AGR1(45:45:10)360B, which had critical low temperatures of -18°C and -12°C, respectively). Rubber in AR1 blends (AR1(83:17)240A and AR1(91:9)360B) enhanced the low-temperature performance, yielding -28°C and -25°C, respectively. As expected, a half asphalt to half guayule blend (AG1(50:50)120) led to a critical low temperature of -13°C; that was approximately the average of asphalt and guayule critical low temperatures. Such behavior indicated the simplicity of guayule influence when blended with asphalt concerning the low-temperature grade, unlike the degradation associated with the guayule-based binders at high-temperature performances. Two binders (AGR1(68:23:9)360 and AGR1(42:42:16)240A) were close to the virgin asphalt cement's critical low temperature, which were -18°C and -16°C, respectively.

Based on each binder's low-temperature grade, premature cracking could occur with the wide-ranged negative ΔT_c values. Accordingly, this could be attributed to AR1s such as AR1(83:17)240A and AR1(91:9)360B in this experiment, as shown in Figure 4.7. Conversely, guayule-based binders offered low-ranged negative ΔT_c values to little positive ΔT_c values. The higher the guayule concentration in the blend, the lower-ranged negative the ΔT_c parameter, indicating the guayule's low susceptibility to premature cracking at its low-temperature grade, unlike asphalt or AR1 binders.
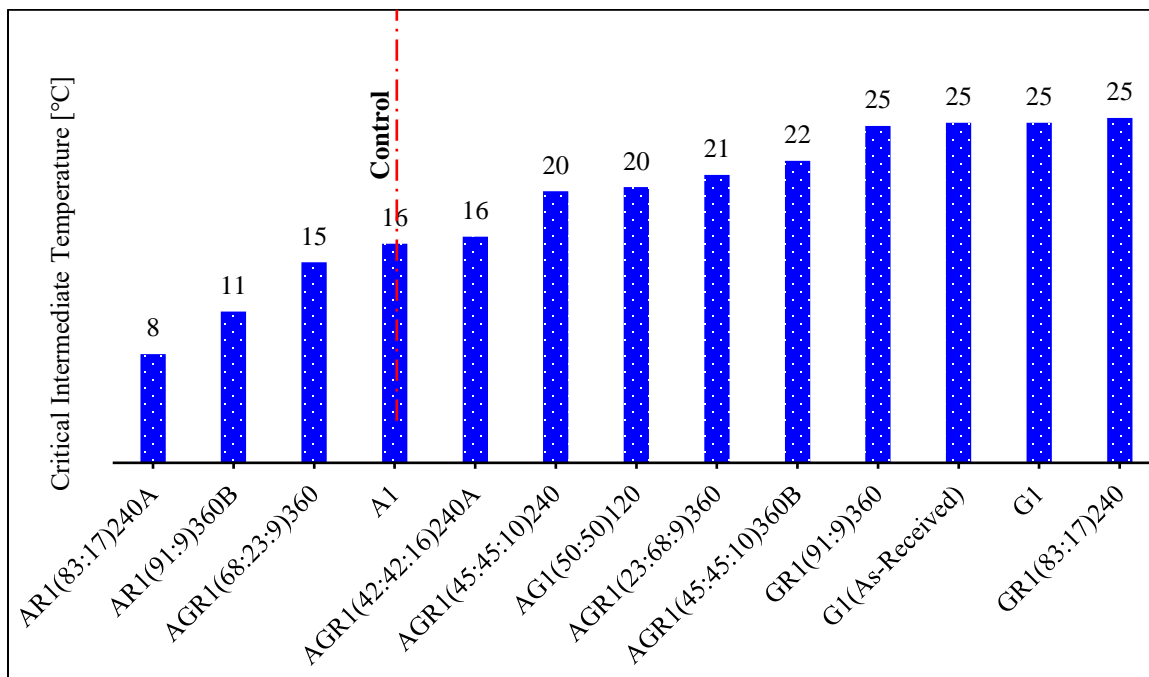
Figure 4.5 Critical Intermediate Temperatures for the Soft Designated Binders Ranked in Ascending Order [2].

4.1.6. Performance-related Correlations. Figure 4.8a,b summarizes correlations considering the effects of guayule (G1) and CRM concentrations on the performances of AGR1s and AR1s at high, intermediate, and low temperatures. As shown in Figure 4.8a(1), the CRM enhanced G1 performance-related properties at high temperatures. However, it was less effective compared to the impact of CRM on the A1 PG-HT. In other words, higher performance was attributed to AR2s compared to AGR2s. Less G2 concentrations with greater CRM concentrations in AGR2s led to enhancements to the PG-HTs, as shown in Figure 4.8b(1). Likewise, from Figure 4.8b(1), greater CRM concentrations led to enhancements to the PG-HT of G1, but not as much as asphalt-guayule PG-HT enhancements.
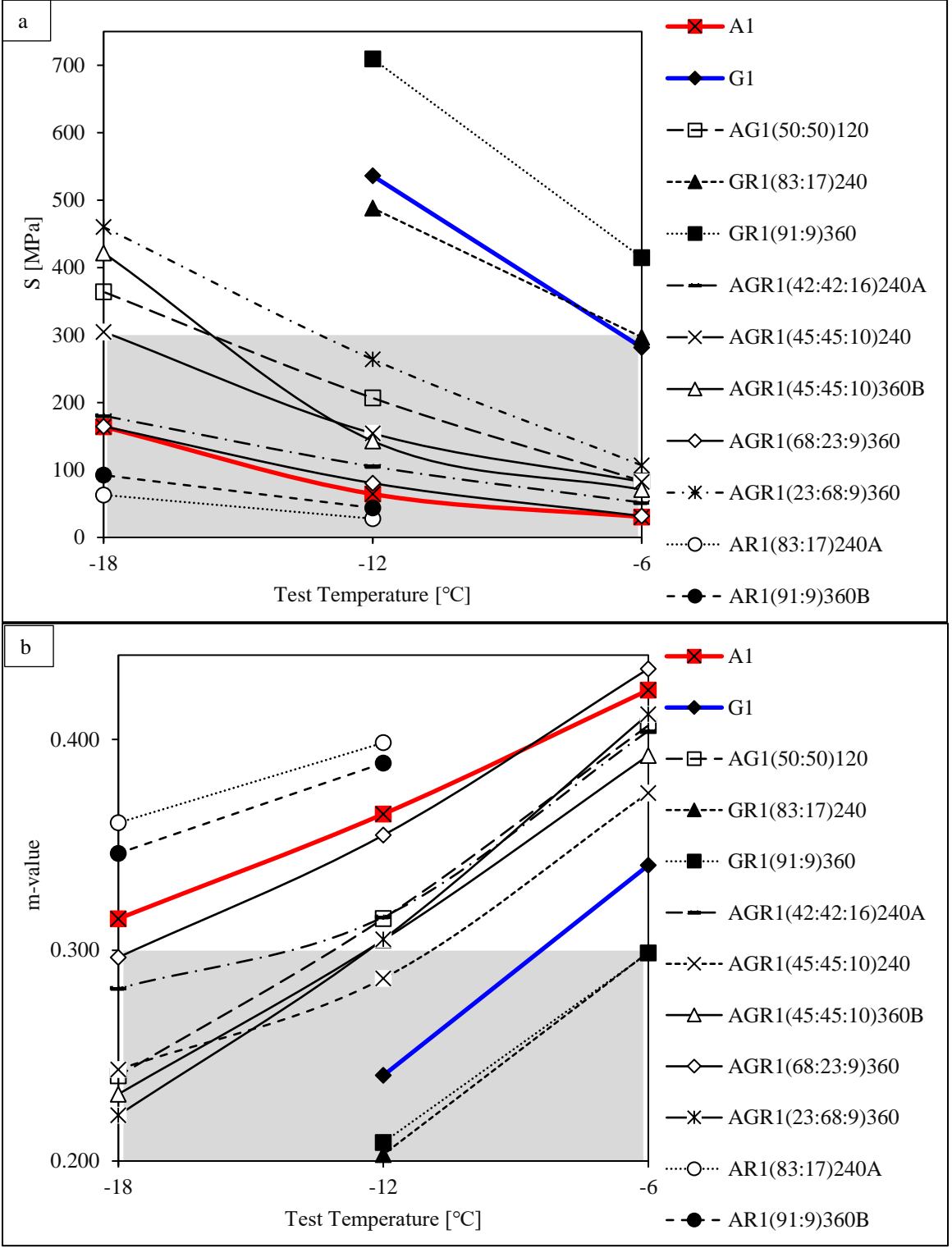
Figure 4.6 Low-Temperature Resistance for the Soft Designated Binders: (a) Stiffness (S(t)) and (b) m-value, both in the Test Temperature Domain [2].
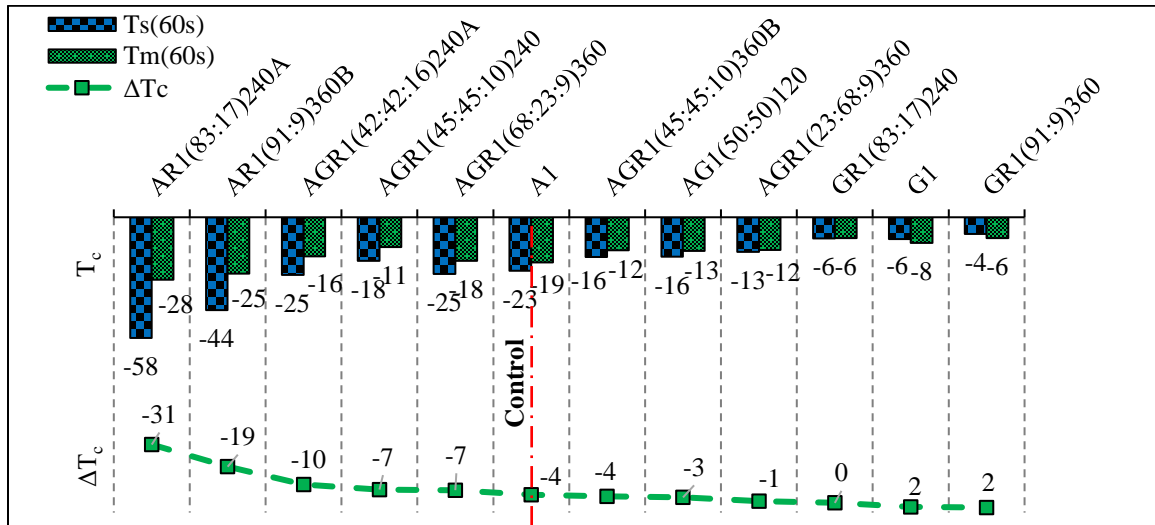
Figure 4.7 ΔT_c Chart for the Soft Designated Binders.

Greater CRM concentrations in AGR2s and AR2s enhanced their PG-ITs, as shown in Figure 4.8a(2). However, greater enhancements were attributed to AR2s due to the negative effect of the high PG-IT of G2 on AGR2s. The less effectiveness of CRM on guayule PG-IT can be shown in Figure 4.8b(2), in which almost no change in resisting fatigue by GR1 compared to G1. Less G2 concentrations with greater CRM concentrations in AGR2s led to enhancements to the PG-ITs of AGR2s, as shown in Figure 4.8b(2).

As shown in Figure 4.8a(3), increasing CRM concentrations in AGR2s and AR2s enhanced their PG-LTs. However, greater enhancements were attributed to AR2s due to the negative effect of the high PG-LT of G2 on AGR2s. As shown in Figure 4.8b(3), the trend of decreasing G2 concentrations with increasing CRM concentrations in AGR2s indicated enhancements to their PG-LTs. There was almost no change in resisting thermal cracking by GR1 compared to G1. This negative influence was due to the less effectiveness of CRM on the G1 PG-LT compared to the impact of CRM on the A1 PG-LT.
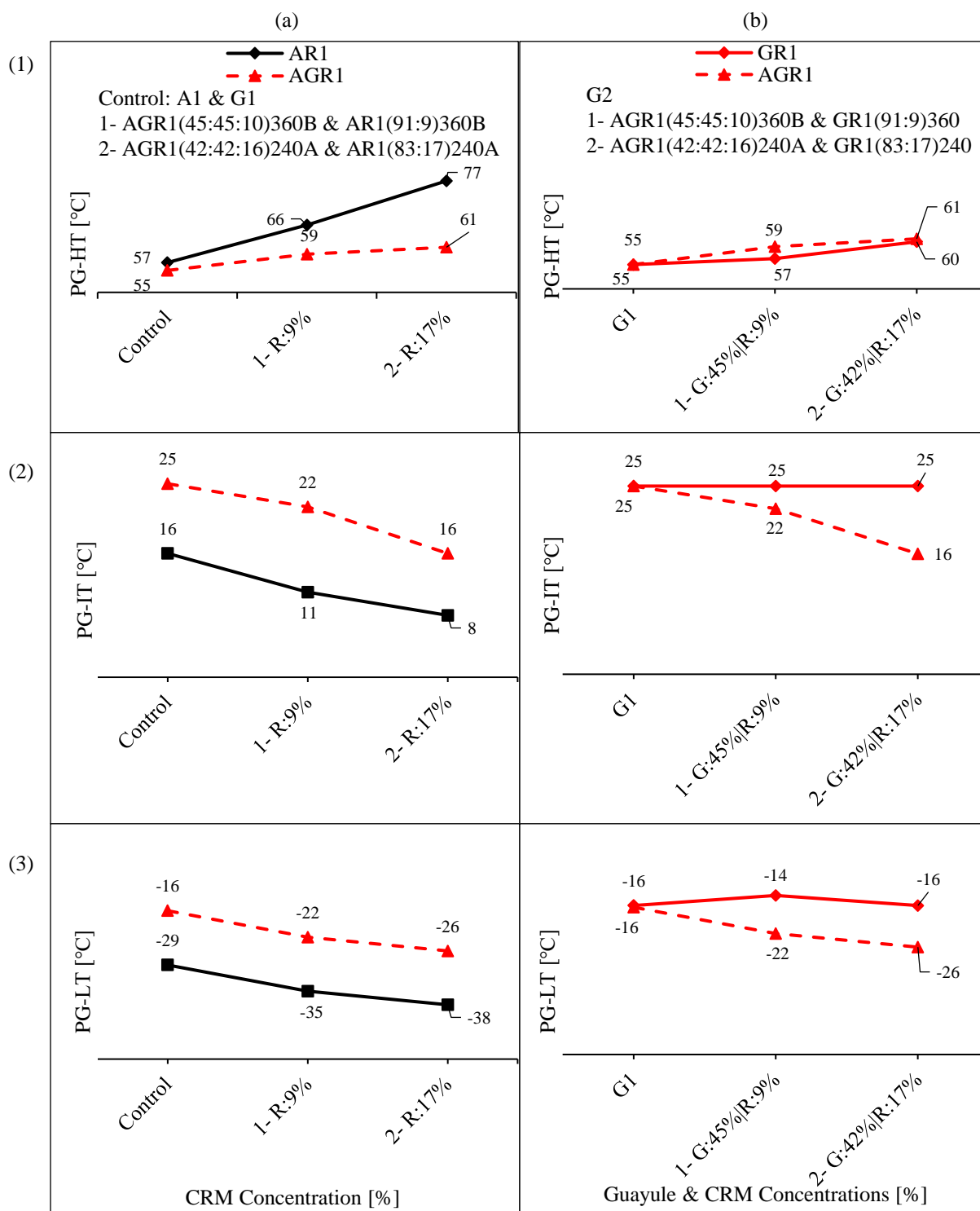
Figure 4.8 First Experiment Performance-related Correlations: (a) Effect of CRM Concentrations on Asphalt and Asphalt-Guayule and (b) Effect of Guayule and CRM Concentrations on Asphalt-Guayule and Guayule Performances; (1) RTFO PG-HT, (2) PG-IT, and (3) PG-LT.

4.1.7. Mass Loss. Guayule lost high volatile fractions during the RTFO aging compared to the virgin asphalt, as illustrated in Figure 4.9. Multiple volatile fractions such as α-pinene and β-pinene compounds, caused volatilization in guayule [25, 55]. Guayule lost 4.9% by weight, which agreed with the volatile fractions' concentrations of lightweight compounds mentioned in the literature (3–5%) [20]. In contrast, previous studies reported that the mass losses in bio-oils were related to further moisture losses [15, 166]. Nevertheless, guayule did not face a severe moisture problem, especially after the heat treatment and interaction process. Guayule most likely lost the involved volatile materials mentioned in the literature [20]. Such a mass loss was not associated with either A1 or AR1 binders; instead, it was associated with G1(As-Received), G1, AG1, GR1, AGR1 binders in different percentages.
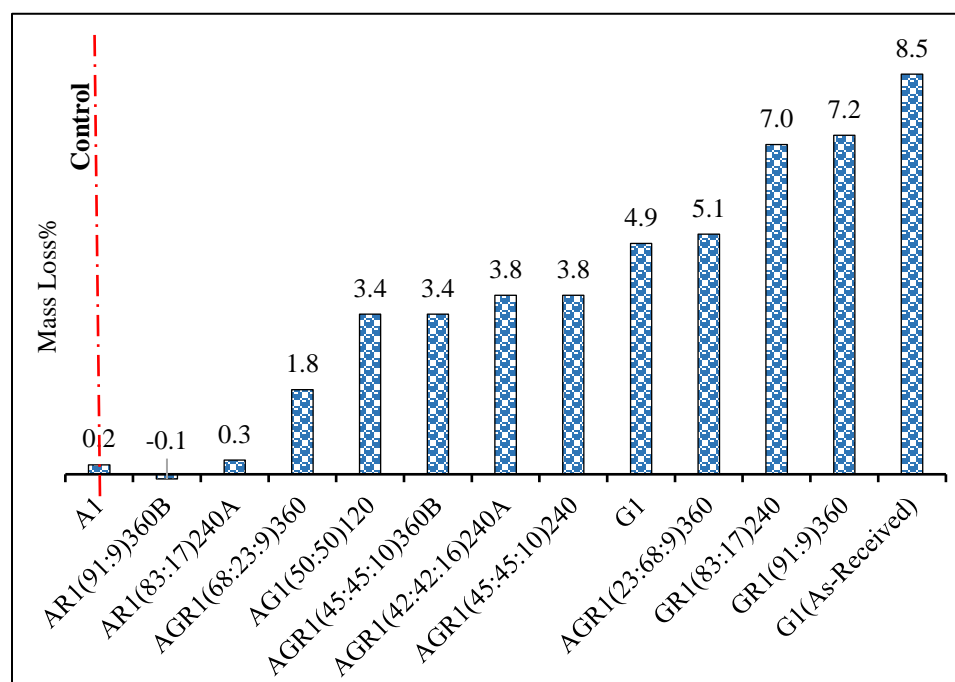
Figure 4.9 Mass Change for the Soft Designated Binders Ranked in Ascending Order [2].

Compared to the standard RTFO test's temperature (163℃) [167], lower RTFO temperatures are expected to minimize mass losses. Bio-binders generally provide lower mixing and compaction temperatures, as reported in the literature [9, 11, 14, 17]. For this reason, previous studies used lower RTFO-aging temperatures compared to the standard RTFO test's temperature, 163℃ [11, 14, 17]. However, in this study, guayule-based binders were conditioned according to the Superpave requirements (163°C) to mimic conventional asphalt conditioning, thereby yielding a high mass loss associated with the guayule-based binders. It was observed that guayule had a lower mass loss when compared to bio-oils reported in the literature [11, 15, 17]. The composition analysis demonstrated details related to mass losses of guayule-based binders in Section 6.

4.1.8. Summary. This subsection presented a large-scale evaluation of guayule in partial and full asphalt replacements based on the Superpave criteria. Guayule had a remarkably lower viscosity than asphalt at the same high-temperature grade, indicating savings in plant energy consumption and environmental emissions. Figure 4.10 illustrates the overall rheological performances of the designated soft binders required by the Superpave criteria. The two closest blends to the control asphalt (PG57-29) were AGR1(68:23:9)360 (PG60-28), and AGR1(42:42:16)240A (PG61-26). The virgin guayule yielded a lower grade (PG55-16). The CRM enhanced the virgin guayule's rheological behavior at high temperatures but not at intermediate or low temperatures. Dependency on a high concentration of guayule in the binder's blend would lead to insufficient fatigue and thermal-cracking resistances compared to the control asphalt, as clarified by the composition analysis presented in Section 6.
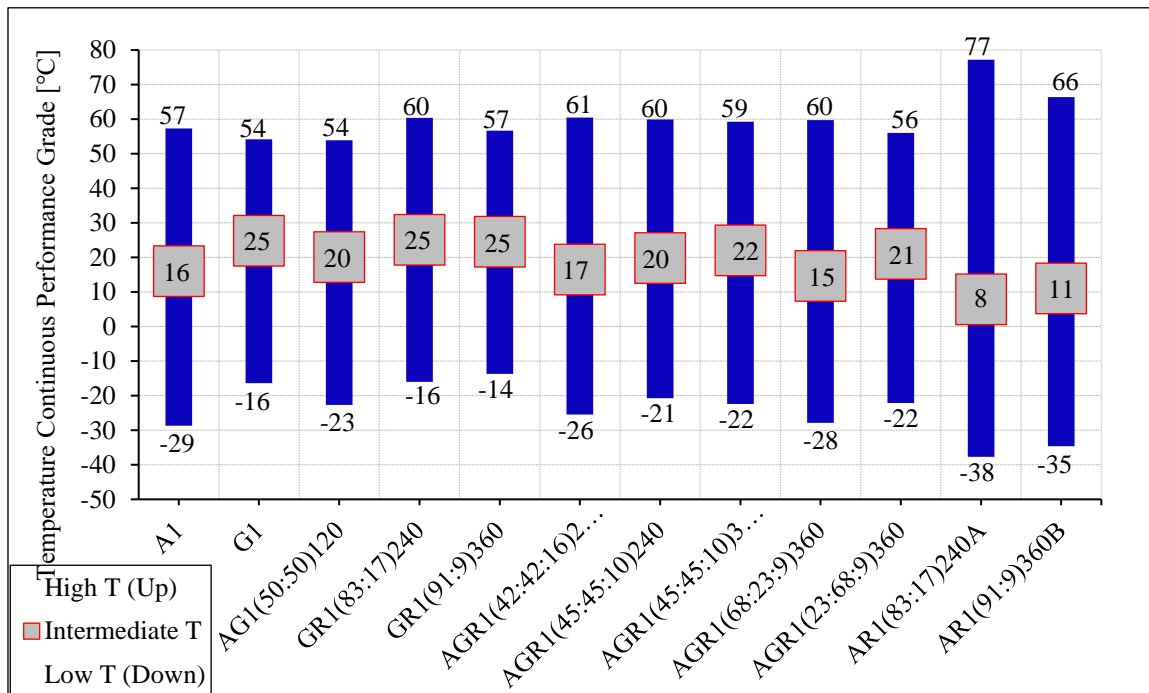
Figure 4.10 Temperature Continuous Performance Grades of the Soft Designated Binders [2].

4.2. SECOND EXPERIMENT: STIFF-ASPHALT STIFF-GUAYULE

4.2.1. Mixing and Compaction Requirements. Figure 4.11 illustrates the mixing and compaction temperature ranges for stiff asphalt (A2), stiff guayule (G2), stiff asphalt-guayule-rubber blend (AGR2(62:25:13)100E), and two stiff guayule-rubber blends (GR2(87:13)100, and GR2(75:25)100). The G2 had the lowest viscosity among others. For instance, at 135℃, the viscosity was 0.203 Pa.s for G2 and 0.403 Pa.s for A2. The A2 and G2 had mixing temperature ranges of 152–158℃ and 141–146℃, respectively. They had compaction temperature ranges of 135–143℃ and 121–127℃, respectively. The mixing and compaction temperatures of AGR2(62:25:13)100E were 176–181℃ and 164–169℃, respectively. Additionally, the effect of CRM addition on the pure guayule could be shown

in the GR2(87:13)100 mixing and compaction temperature ranges (146–153℃ and 132–

138℃, respectively), and the GR2(75:25)100 mixing and compaction temperature ranges

(172–178℃ and 159–165℃, respectively).
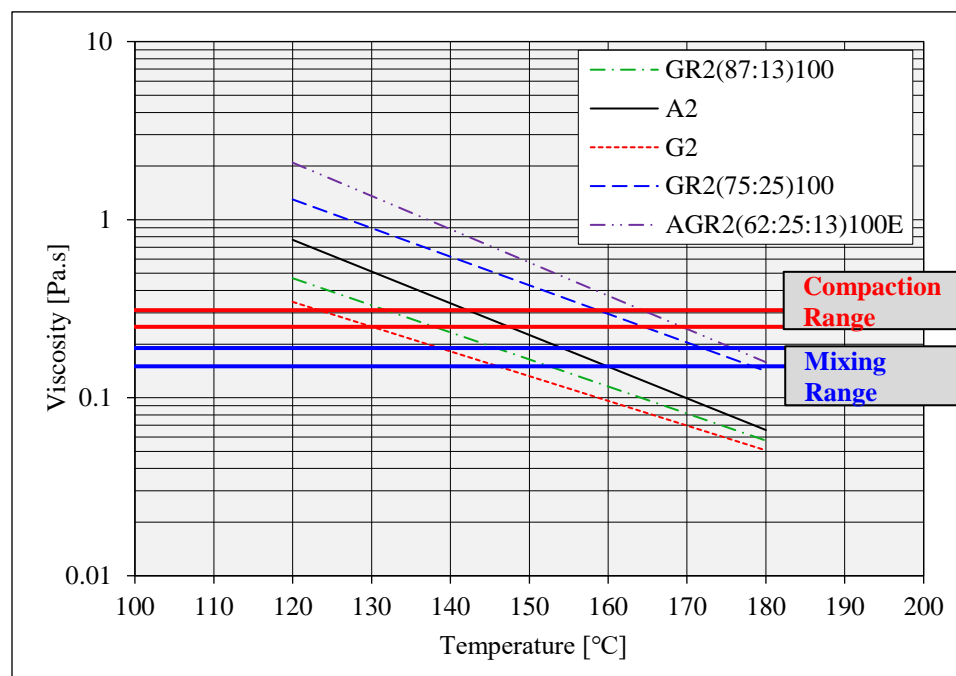
Figure 4.11 Mixing and Compaction Temperature Ranges: A2, G2,
AGR2(62:25:13)100E, GR2(87:13)100, and GR2(75:25)100.

4.2.2. Rutting Resistance. In this experiment, tested binders were categorized into

19 designated binders as listed in Table 4.3. The designated binders were investigated using

the DSR to evaluate their basic rheological properties at a wide range of high temperatures.

The G*, δ, and |G*|/sinδ were determined for each binder before and after RTFO aging.

4.2.2.1. Major observations of basic rheological parameters at high

temperatures. Considering that asphalt (67℃ PG-HT) is stiffer than guayule (58℃ PG-

HT), from Table 4.3, the following points reveal the major observations based on the basic rheological parameters, which are in compliance with the first experiment outcomes:

- The heat treatment process revealed a considerable increase in guayule stiffness due to the potential removal of moisture and light molecular weight components in the as-received guayule by the manufacturer. There was a little-to-no change in the guayule elasticity before vs. after RTFO aging or as-received vs. heat treated.

- RTFO aging raised asphalt elasticity, unlike guayule in which little-to-no change was occurred to guayule elasticity.

- The CRM raised guayule stiffness and elasticity, reflected on a higher rutting resistance evaluated by the Superpave rutting parameter, $|G^*|/\sin\delta$.

- The CRM provided asphalt with more enhancement to rheological parameters at high temperatures (higher G^* and lower δ) than guayule. In this regard, further details are provided in the following subsection (4.2.2.2).

- The addition of CRM into the AGR2 blend enhanced the blend's stiffness and elasticity compared to either individual asphalt or individual guayule in cases of high concentrations of asphalt and CRM (e.g., AGR2(68:25:7)100D, AGR2(65:25:10)100, and AGR2(62:25:13)100E). In other words, the higher the AR concentration, the greater the stiffens and elasticity.

Table 4.3 Rheological Parameters of Second Experiment at High Temperatures.

Binder Code	Temp [°C]	Unaged			RTFO-Aged		
		G* [kPa]	δ [°]	|G*|/sinδ [kPa]	G* [kPa]	δ [°]	|G*|/sinδ [kPa]
A2	46	15.0	81	15.0			
	52	6.2	83	6.2			
	58	2.7	85	2.7			
	64	1.2	87	1.2	3.1	83	3.1
	70	0.6	88	0.6	1.4	85	1.4
G2(As-Received)	46	5.1	85	5.1			
	52	1.7	87	1.7	9.4	84	9.5
	58	0.6	87	0.6	1.9	88	1.9
G2	46	9.5	85	9.5			
	52	2.7	86	2.7	9.1	85	9.1
	58	0.9	87	0.9	2.1	88	2.1
GR2(87:13)100	58	1.2	87	1.2	3.4	87	3.4
	64	0.6	87	0.6	1.3	88	1.3
GR2(75:25)100	58	2.4	86	2.4	5.6	85	5.6
	64	1.0	87	1.0	2.3	86	2.3
	70	0.5	87	0.5	1.0	87	1.0
AGR2(23:75:2)100A	46	10.9	84	10.9			
	52	3.6	85	3.6			
	58	1.2	87	1.2	2.7	86	2.8
	64	0.5	87	0.5	1.1	87	1.1
AGR2(22:75:3)100	46	10.8	82	10.8			
	52	3.7	84	3.7			
	58	1.4	86	1.4	3.1	84	3.2
	64	0.6	87	0.6	1.3	85	1.3
AGR2(21:75:4)100	46	11.0	82	11.0			
	52	4.0	84	4.0			
	58	1.5	85	1.5	2.6	86	2.6
	64	0.6	86	0.6	1.1	87	1.1
AGR2(45:50:5)100	46	13.3	81	13.3			
	52	4.7	84	4.7			
	58	1.8	85	1.8	4.1	81	4.2
	64	0.8	87	0.8	1.8	83	1.8
AGR2(44:50:6)100B	46	14.7	78	14.7			
	52	5.5	80	5.5			
	58	2.2	82	2.2	3.8	83	3.8
	64	1.0	84	1.0	1.6	84	1.6
	70	0.0	85	0.5			
AGR2(42:50:8)100C	46	15.5	76	15.5			
	52	5.9	79	5.9			
	58	2.4	81	2.4			

Table 4.3 Rheological Parameters of Second Experiment at High Temperatures (Cont.).

Binder Code	Temp [°C]	Unaged			RTFO-Aged		
		G* [kPa]	δ [°]	|G*|/sinδ [kPa]	G* [kPa]	δ [°]	|G*|/sinδ [kPa]
AGR2(42:50:8)100C	64	1.1	83	1.1	2.2	80	2.3
	70	0.5	85	0.5	1.1	81	1.1
AGR2(68:25:7)100D	46	19.6	75	19.6			
	52	7.7	79	7.7			
	58	3.2	82	3.2			
	64	1.4	85	1.4	4.0	75	4.2
	70	0.7	86	0.7	2.0	77	2.0
AGR2(65:25:10)100	46	24.6	70	24.6			
	52	10.5	72	10.5			
	58	4.7	76	4.7			
	64	2.2	79	2.2	4.8	72	5.0
	70	1.1	82	1.1	2.4	74	2.5
	76	0.6	84	0.6	1.3	76	1.3
AGR2(62:25:13)100E	46	24.5	68	24.5			
	52	10.9	70	10.9			
	58	5.1	73	5.1			
	64	2.5	77	2.5	5.8	69	6.2
	70	1.3	79	1.3	3.0	71	3.2
	76	0.7	82	0.7	1.6	74	1.7
AR2(98:2)100A	64	1.6	84	1.6	4.8	79	4.9
	70	0.8	86	0.8	2.2	82	2.2
	76				1.1	84	1.1
AR2(94:6)100B	64	2.6	80	2.6	9.3	68	10.1
	70	1.3	83	1.3	4.8	71	5.1
	76	0.7	85	6.7	2.5	74	2.6
	82				1.4	76	1.4
AR2(92:8)100C	64	3.2	77	3.2	10.0	66	10.9
	70	1.6	81	1.6	5.2	69	5.6
	76	0.8	83	0.8	2.8	72	2.9
	82				10.0	66	10.9
AR2(93:7)100D	64	2.7	79	2.7	8.9	70	9.4
	70	1.4	82	1.4	4.5	73	4.7
	76	0.7	84	0.7	2.3	75	2.4
	82				1.2	78	1.3
AR2(87:13)100E	64	5.4	70	5.7	15.6	59	18.3
	70	2.8	75	2.9	8.8	61	10.0
	76	1.5	79	1.5	5.0	64	5.6
	82	0.9	82	0.9	2.9	67	3.2
	88				1.7	70	1.9

4.2.2.2. Critical high temperature. In Figure 4.12, the critical high temperatures of the unaged and RTFO-aged binders were illustrated. The control asphalt (A2) divided the chart into the left side (superior high-temperature performance) and the right side (inferior high-temperature performance). It seems that RTFO aging raised the high-temperature grade of most presented binders [18]. The following interpretations in this subsection are according to the RTFO-aged binders since they simulate the first stages of the pavement service life. The A2 had a higher performance than G2, 67℃ PG-HT and 58℃ PG-HT, respectively [26]. The heat treatment process of guayule improved its performance against rutting [26]. It was evident by the resultant rheological properties that the RTFO-aged guayule yielded the same high-temperature performance as the as-received guayule (G2(As-Received)) and the heat-treated one (G2) (both 58℃), indicating a reduction in moisture and volatiles of guayule that made the molecular structure of the as-received guayule similar to that of the heat-treated guayule, complied with literature about bio-oils [16, 18]. This will be further investigated using the TGA analysis in Section 6. The AR2 interaction resulted in a better high-temperature performance than AGR2 interaction [18]. It seems rational due to the relatively lower critical high temperature of guayule (58℃), compared to 67℃ for asphalt [18], and the observably higher compatibility between asphalt and rubber. The influence of CRM enhancement on asphalt against guayule was evident with investigating asphalt and guayule having the same high-temperature grade (both PG52, standard) in Subsection 4.1. As expected, the higher the asphalt and CRM concentrations, the better the performance among the designated AGR2s [18]. Adding guayule to the AR binder resulted in a potential to positively equilibrate or

surpass the control asphalt performance at high temperatures (e.g., AGR2(68:25:7)100D and AGR2(62:25:13)100E), but others such as AGR2(23:75:2)100A resulted in performance away from achieving that of the control asphalt [26].
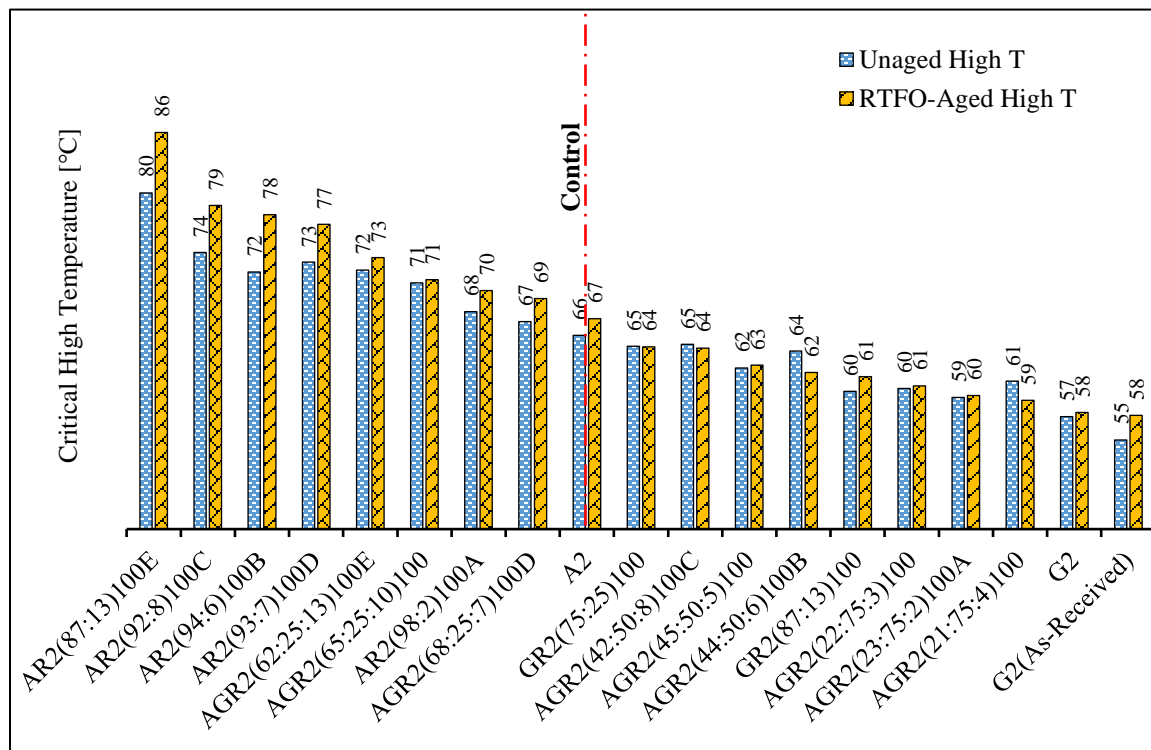
Figure 4.12 Critical High Temperatures for the Stiff Designated Binders (Original and RTFO) Ranked in Descending Order Based on the RTFO-Aged Binders [18].

4.2.3. Aging Resistance. Figure 4.13 illustrates the AS of the designated binders ranked in ascending order. The AGR2(44:50:6)100B binder had the highest aging resistance (AS = 1.6), and the AR2(94:6)100B binder had the lowest aging resistance (AS = 4.3). The control asphalt had an AS value of 2.7. Comparing this experiment to the above first experiment, the modified binder aging might depend on the asphalt grade. This could

be clearly shown when comparing Figure 4.13 to Figure 4.4. Here, the AR blends yielded the lowest aging resistances, and most asphalt-guayule -rubber and guayule-rubber blends yielded the highest aging resistances, as shown on the left- and right-hand sides of the control asphalt aging resistance.

From the two (soft and stiff) investigated experiments, it is not evident which kind of the designated binders was more susceptible to the RTFO aging whether asphalt rubber, guayule rubber or asphalt guayule rubber. For instance, from the first experiment, the superior asphalt resistance was associated with an AR1. On the contrary, from the second experiment, the inferior aging resistance was associated with an AR2.
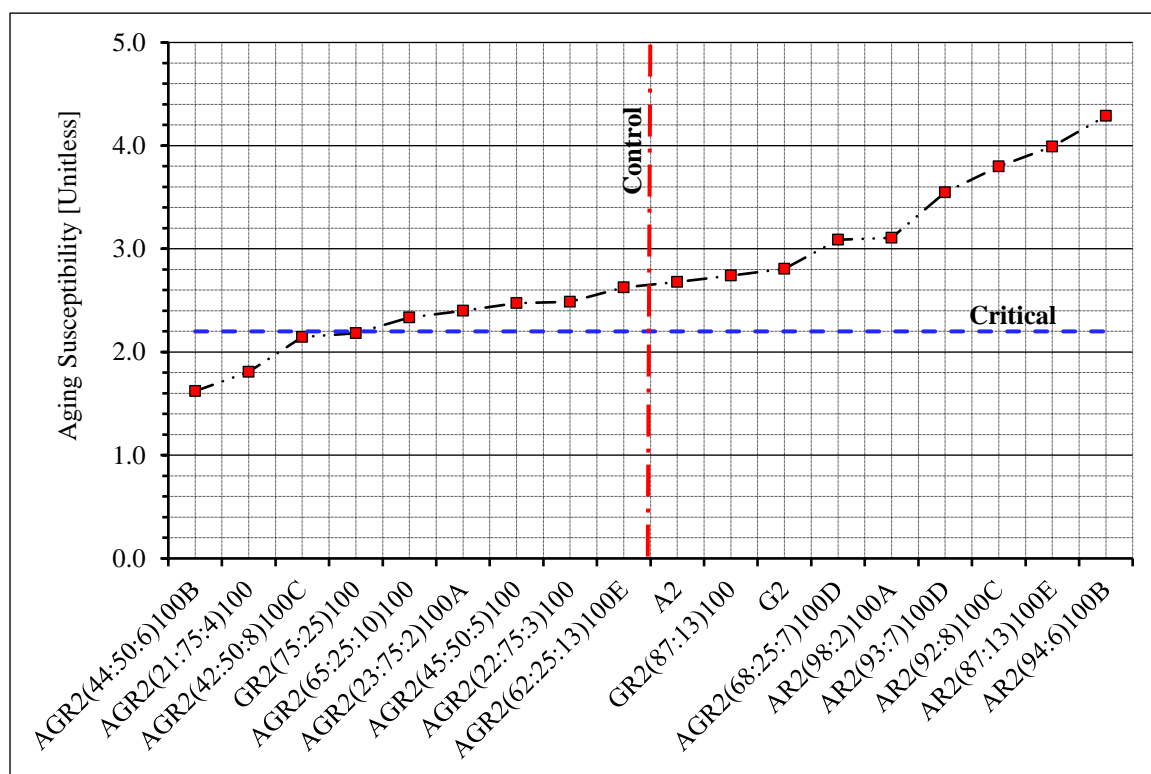
Figure 4.13 Aging Resistance for the Stiff Designated Binders Ranked in Ascending Order.

Table 4.4 Rheological Parameters of Second Experiment at Intermediate Temperatures.

Binder Code	Temp [°C]	PAV-Aged		
		G* [kPa]	δ [°]	|G*|.sinδ [kPa]
A2	19	8798	41	5826
	22	5980	44	4142
	25	4025	46	2905
	28	2687	48	2012
G2	25	19790	59	16998
	28	10210	67	9407
	31	4580	74	4396
GR2(87:13)100	31	7330	66	6712
	34	3420	72	3253
GR2(75:25)100	31	9370	62	8250
	34	4650	68	4305
	37	2330	71	2206
	40	1100	73	1052
AGR2(23:75:2)100A	25	14145	58	12055
	28	7405	66	6756
	31	3472	72	3304
AGR2(22:75:3)100	25	13427	58	11446
	28	7063	66	6432
	31	3311	72	3143
AGR2(21:75:4)100	25	13106	59	11264
	28	6940	66	6343
	31	3327	72	3159
AGR2(45:50:5)100	25	8307	56	6911
	28	4612	62	4068
AGR2(44:50:6)100B	25	9343	55	7638
	28	5287	60	4591
AGR2(42:50:8)100C	25	8536	55	6967
	28	4859	60	4207
AGR2(68:25:7)100D	25	5541	49	4189
	22	8652	45	6147
AGR2(65:25:10)100	22	7954	46	5717
	25	5115	50	3896
AGR2(62:25:13)100E	19	10237	43	6971
	22	6796	46	4916
	25	4394	50	3352
AR2(98:2)100A	19	9201	42	6097
	22	6253	44	4330
	25	4220	46	3039

Table 4.4 Rheological Parameters of Second Experiment at Intermediate Temperatures (Cont.).

| Binder Code | Temp [°C] | PAV-Aged | | |
		G* [kPa]	δ [°]	|G*|.sinδ [kPa]
AR2(94:6)100B	19	8692	39	5512
	22	6040	41	3998
	25	4166	44	2868
AR2(92:8)100C	16	9481	38	5899
	19	6565	41	4269
AR2(93:7)100D	16	11010	38	6784
	19	7632	40	4923
AR2(87:13)100E	13	11668	35	6720
	16	8273	37	4981

4.2.4. Fatigue Resistance. The designated binders were investigated using the DSR to evaluate their basic rheological properties at variant intermediate temperatures. The G*, δ, and |G*|.sinδ were determined for each binder after PAV aging, as shown in Table 4.4.

4.2.4.1. Major observations of basic rheological parameters at intermediate temperatures. The following points reveal the major observations based on the basic rheological parameters, which are in compliance with the first experiment outcomes:

- In compliance with high-temperature analysis, guayule offered lower elastic behavior than asphalt.

- Even though asphalt was stiffer than guayule at high temperatures, guayule possessed higher stiffness at intermediate temperatures, followed by a lower resistance to fatigue cracking.

- The CRM significantly lowered asphalt stiffness but made a little-to-no change to its elastic behavior (significantly enhanced its resistance to fatigue cracking).

- The CRM slightly changed guayule stiffness and elasticity (almost no change in resisting fatigue).

- The CRM effect on asphalt-guayule blend mainly depended on the material concentrations.

4.2.4.2. Critical intermediate temperature. Figure 4.14 illustrates the critical intermediate temperatures of the designated binders ranked in ascending order. The virgin asphalt had a 20℃ critical intermediate temperature, and the virgin guayule had a 31℃ critical intermediate temperature. By assessing the critical high temperatures (discussed in Subsection 4.2.2) and critical low temperatures (discussed in Subsection 4.2.5), it was found that most designated guayule-based binders offered measured critical intermediate temperatures equal to or higher than the average of high- and low-temperature grades plus 4℃, as defined by the Superpave criteria [126], thereby reflecting the compatibility of the Superpave criteria with the novel binder [2]. The addition of CRM to guayule offered a little-to-no change in the critical intermediate temperatures of the guayule-rubber blends: both GR2(87:13)100 and GR2(75:25)100 resulted in 32℃ and 33℃ critical intermediate temperatures, respectively, that were close to the virgin guayule's critical intermediate temperature (31℃) [2]. Rubber significantly enhanced the virgin asphalt critical intermediate temperatures [2]. Thus, high CRM concentration yielded enhanced intermediate-temperature performance in the AR blend [2]. The AGR2 blends had

enhanced intermediate-temperature grades compared to guayule and guayule-rubber blends because asphalt and CRM were both present [2].
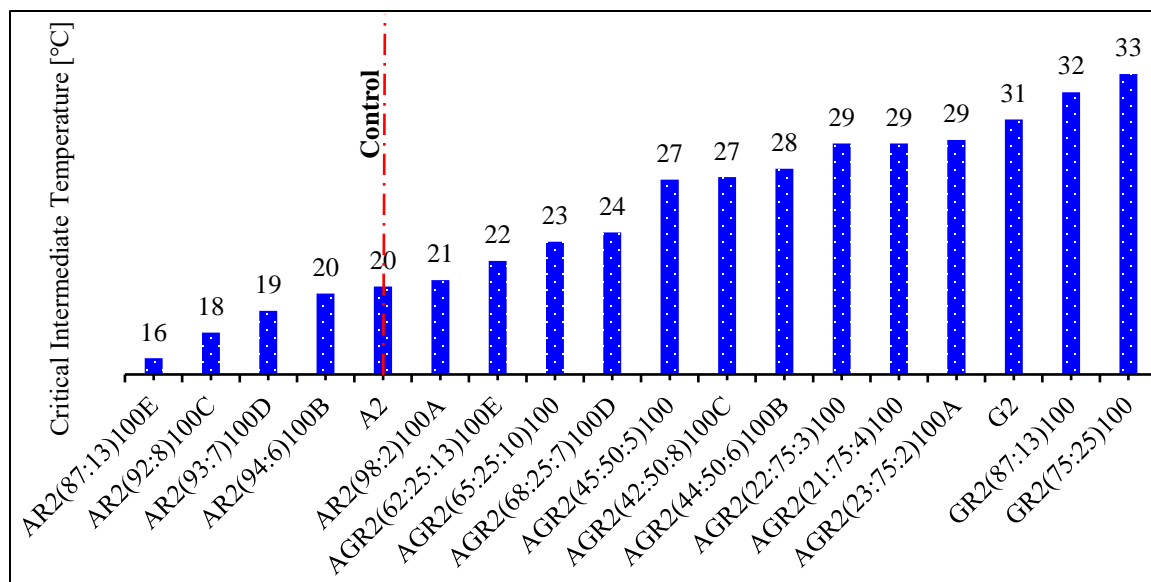
Figure 4.14 Critical Intermediate Temperatures for the Stiff Designated Binders Ranked in Ascending Order [18].

4.2.5. Thermal Cracking Resistance. Figure 4.15a,b illustrates time-dependent creep stiffness (S(t)) and m-value, respectively, in the test temperature domain. Rubber offered negatively little-to-no change in the performance of guayule-rubber (GR) binders. The GR2(87:13)100 and GR2(75:25)100 resulted in test temperatures of 0°C and 2°C, respectively, compared to the virgin guayule (-1°C). The virgin asphalt had a significantly lower critical temperature (-15°C) than the virgin guayule (-1°C), thus higher asphalt concentration yielded enhanced binder performance. For instance, considering almost the same CRM concentration in the blend, the AGR2(68:25:7)100D resulted in a -9°C critical

low temperature, whereas the AGR2(44:50:6)100B resulted in a -4 critical low temperature. Another example is that the AGR2(45:50:5)100 resulted in a -10°C critical low temperature, whereas the AGR2(21:75:4)100 had a -2 critical low temperature. The effect of CRM on the thermal cracking resistance was not evident in this experiment's AGR2 blends but could be shown from the first experiment in Subsection 4.1.5.

Based on each binder's low-temperature grade, premature cracking could occur with the wide-ranged negative ΔT_c values. Accordingly, this could be attributed to the A2, AR2, and AGR2 (involving a high concentration of asphalt) binders such as, ranked in ascending order, A2, AGR2(45:50:5)100, AGR2(65:25:10)100, followed by the AR binders in this experiment, as shown in Figure 4.16. Conversely, high-concentrated guayule-based binders offered low-ranged negative ΔT_c values to little positive ΔT_c values. The higher the guayule concentration in the blend, the lower-ranged negative the ΔT_c parameter, indicating the guayule's low susceptibility to premature cracking at its low-temperature grade, unlike asphalt or AR2 binders.

4.2.6. Performance-related Correlations. Figure 4.17a,b summarizes correlations considering the effects of guayule (G2) and CRM concentrations on the performances of AGR2s and AR2s at high, intermediate, and low temperatures. As shown in Figure 4.17a(1), increasing CRM concentrations in AGR2s and AR2s provided enhancements to the high-temperature performances. However, due to the relatively low PG-HT of G2 compared to A2, higher performance was attributed to AR2s compared to AGR2s. Less G2 concentration with greater CRM concentration in AGR2s led to enhancements to the PG-HTs of AGR2, as shown in Figure 4.17b(1).
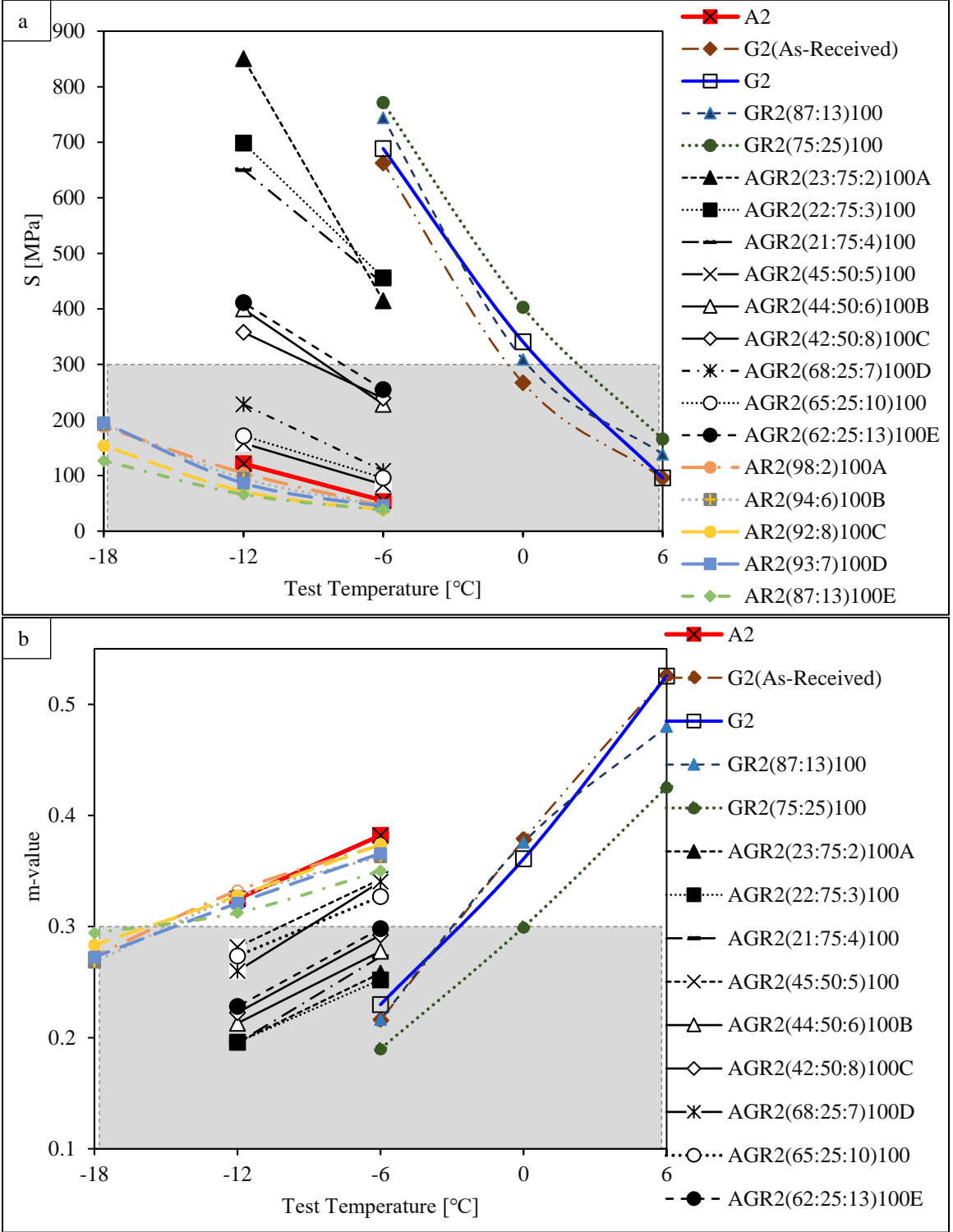
Figure 4.15 Low-Temperature Resistance for the Stiff Designated Binders: (a) Stiffness (S(t)) and (b) m-value, both in the Test Temperature Domain.
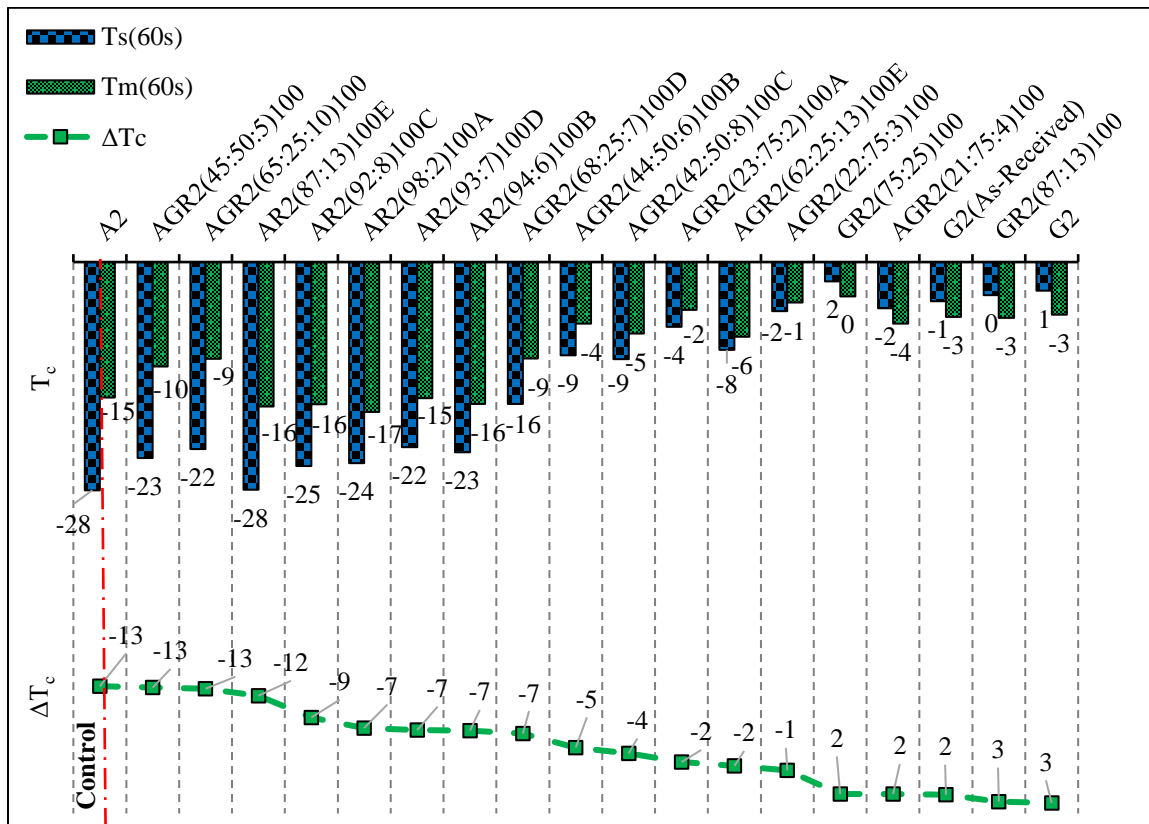
Figure 4.16 ΔT_c Chart of the Stiff Designated Binders.

Greater CRM concentrations in AGR2s and AR2s enhanced their PG-ITs, as shown in Figure 4.17a(2). However, greater enhancements were attributed to AR2s due to the low PG-IT of G2. Less G2 concentrations with greater CRM concentrations in AGR2s led to enhancements to the PG-ITs of AGR2s, as shown in Figure 4.17b(2).

As shown in Figure 4.17a(3), increasing CRM concentrations in AGR2s and AR2s enhanced their PG-LTs. However, greater enhancements were attributed to AR2s due to the low PG-LT of G2. As shown in Figure 4.17b(3), the trend of less G2 concentrations with greater CRM concentrations in AGR2s indicated enhancements to their PG-LTs
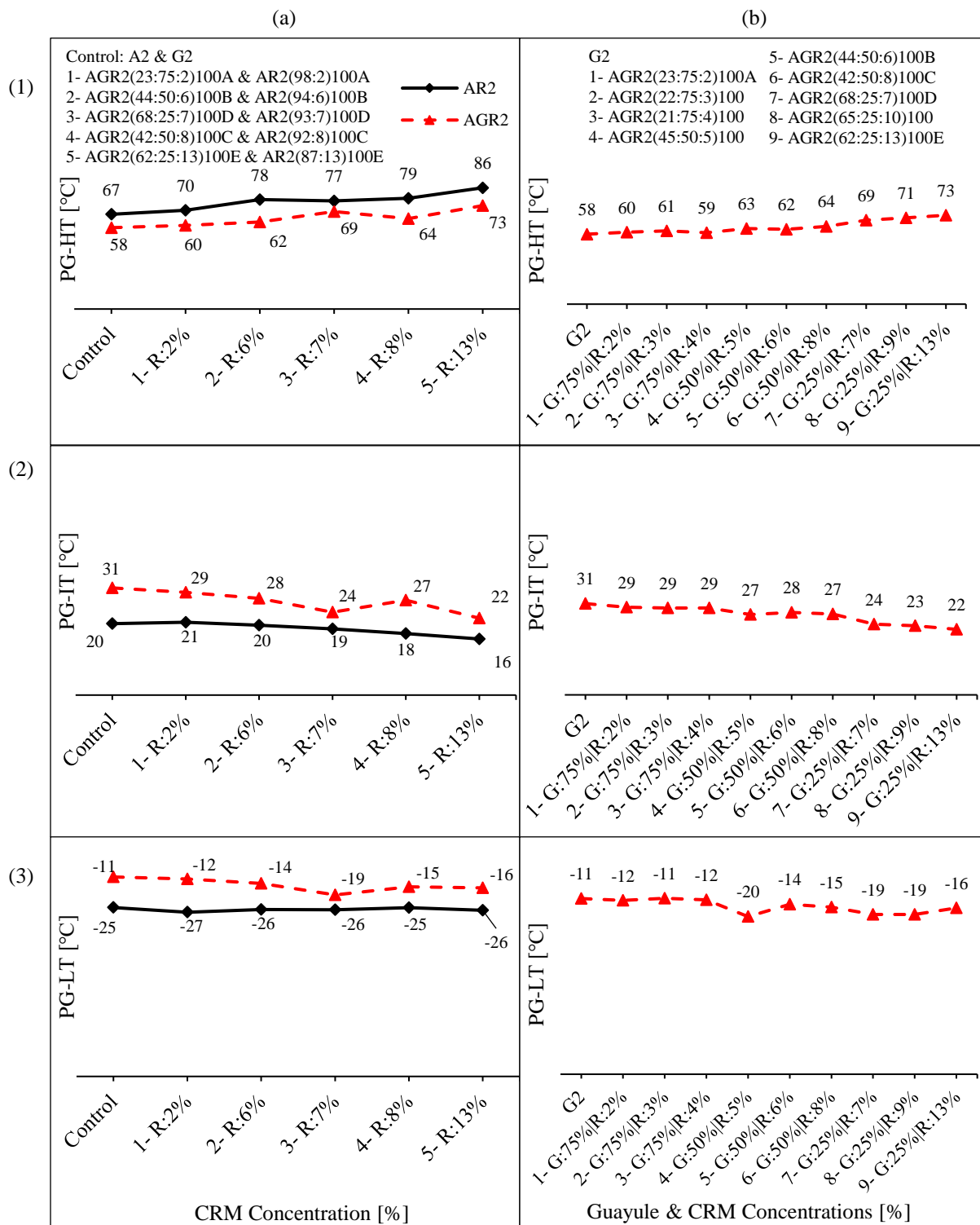
Figure 4.17 Second Experiment Performance-related Correlations: (a) Effect of CRM Concentrations on Asphalt and Asphalt-Guayule Performances and (b) Effect of Guayule and CRM Concentrations on Asphalt-Guayule Performances; (1) RTFO PG-HT, (2) PG-IT, and (3) PG-LT.
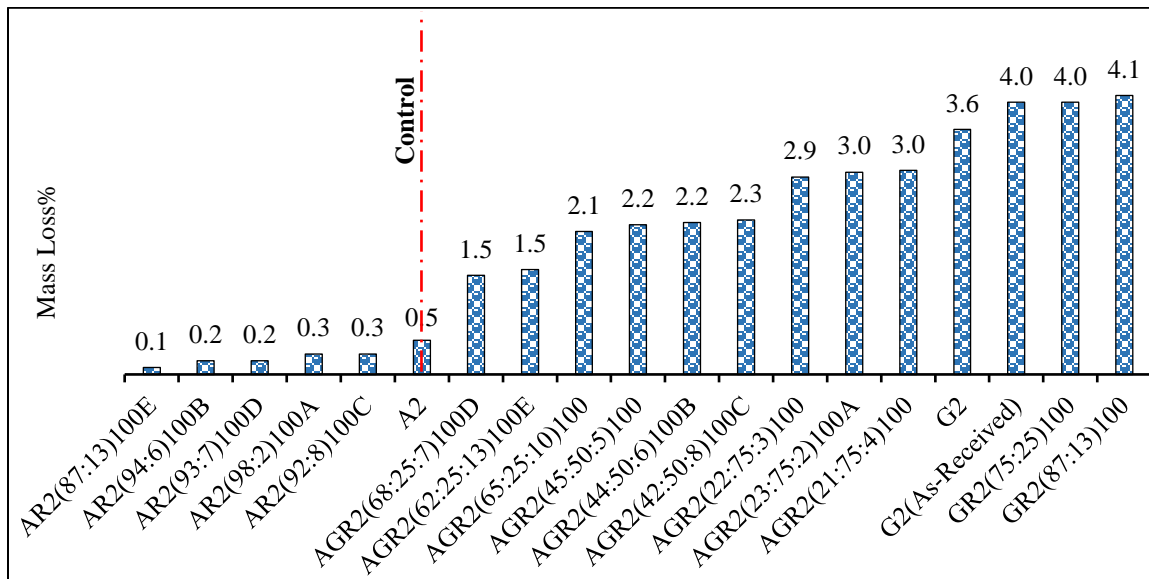
Figure 4.18 Mass Change for the stiff Designated Binders Ranked in Ascending Order [18].

4.2.7. Mass Loss. In Figure 4.18, the mass loss of the designated binders based on the RTFO aging was illustrated. The as-received guayule (G2(As-Received)) lost about 4.0% of its mass, but 3.6% (after the heat-treatment process) [6]. Due to the increase of asphalt and CRM concentrations, such a mass loss was relatively decreased in the guayule-based binders since their mass losses were much lower [6]. The mass loss of guayule was in agreement with the volatile-component concentrations, as mentioned in the literature [6, 20]. Guayule's moisture content seems to be less than 1%, which agrees with the TGA analysis implemented in a previous study by [26].

4.2.8. Summary. This subsection presented a large-scale evaluation of guayule in partial and full asphalt replacements based on the Superpave criteria with providing stiff binders compared to the first experiment binders discussed in Subsection 4.1. Guayule had

a remarkably lower viscosity than asphalt considering the different high-temperature grades in this experiment. Figure 4.19 illustrates the overall rheological performances of the designated stiff binders required by the Superpave criteria. In this experiment, binders provided enhanced performances at high temperatures compared to the control asphalt (PG67-25) such as AGR2(62:25:13)100E (PG73-16) and AGR2(68:25:7)100D (PG69-19). Even though these mentioned guayule-based binders did not accomplish the critical low temperature of the control asphalt, they provided an enhanced resistance against rutting. The CRM enhanced the virgin guayule's rheological behavior at high temperatures but not at intermediate or low temperatures in compliance with the first experiment discussed in Subsection 4.1.
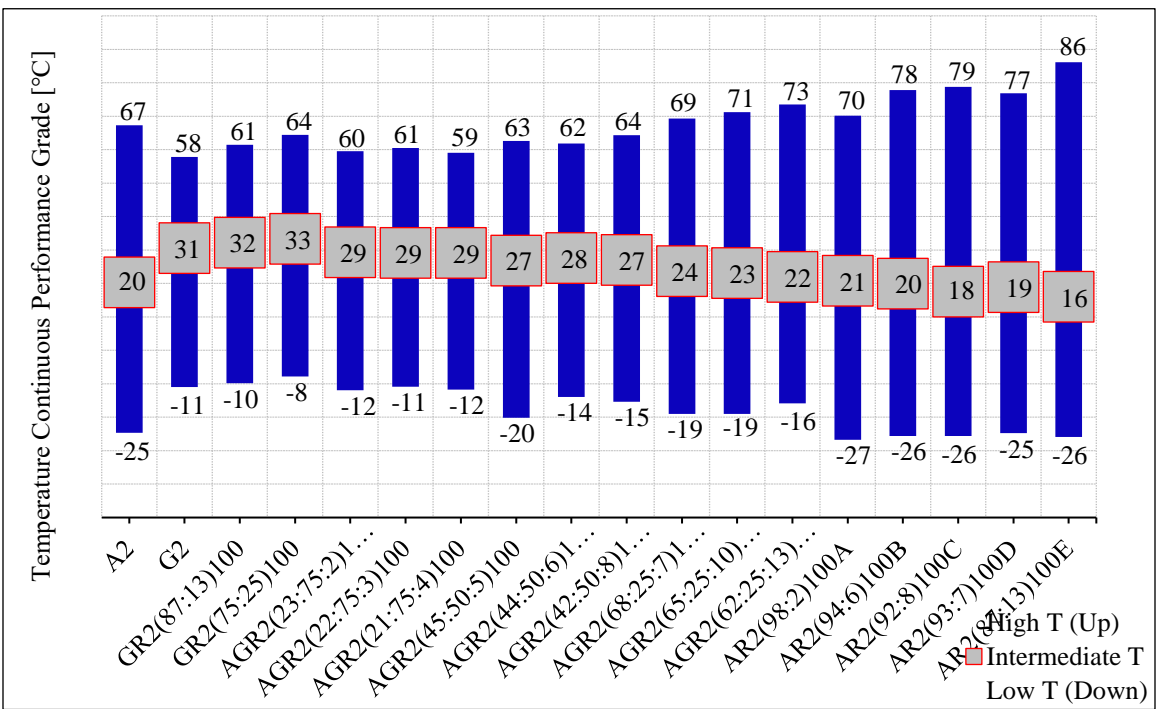
Figure 4.19 Temperature Continuous Performance Grades of the Stiff Designated Binders.

5. ADVANCED RHEOLOGICAL ANALYSIS

This section implies a reproduction of results published in [26]. Five of the nine AGR2 binders were designated to proceed in the following discussions, and they are tabulated with justification for selection in Table 5.1. The following subsections will consider the liquid phase vs. the whole matrix for the five designated AGR2s and their corresponding AR2s. The argumentation in this section was only discussed based on the original (unaged) binders.

Table 5.1 Selected Binders Attributed to the Justification for Selection [26].

Binder Code	Justification for Selection
AGR2(23:75:2)100A	High concentration of guayule (75% by wt. of blend). Low concentrations of asphalt and CRM. Accomplishing a lower PG-HT (60℃) compared to A2 (67℃).
AGR2(44:50:6)100B	Intermediate concentration of guayule (50% by wt. of blend). Intermediate concentrations of asphalt and CRM. Accomplishing a PG-HT of 62℃, near the standard PG-HT of A2 (64℃).
AGR2(42:50:8)100C	Intermediate concentration of guayule (50% by wt. of blend). Intermediate concentration of asphalt, but higher CRM. Accomplishing a PG-HT of 64°C, same standard PG-HT of A2 (64°C).
AGR2(68:25:7)100D	Low concentration of guayule (25% by wt. of blend). High concentration of asphalt. Intermediate concentration of CRM. Accomplishing a PG-HT of 69°C, surpassing the critical PG-HT of A2 (67°C).
AGR2(62:25:13)100E	Low concentration of guayule (25% by wt. of blend). High concentration of asphalt. High concentration of CRM. Accomplishing a PG-HT of 73°C, remarkably surpassing the critical PG-HT of A2 (67°C).

5.1. CRM DISSOLUTION: AGR VS. AR

To investigate the interaction effect vs. CRM residue effect on the binder's performance, the CRM was extracted from the whole matrix as interpreted in Subsection 3.3.1.3. Accordingly, Figure 5.1 depicts the dissolved CRM% in comparing the AGR2s and their corresponding AR2s. There was no clear evidence whether CRM was more dissolved in the AR2s or AGR2s. It could be declared that there was no significant difference between AGR2s and their corresponding AR2s regarding their CRM dissolution averages, 29% and 30%, respectively. Nevertheless, the standard deviation of the AGR2s was higher than that of corresponding AR2s, 8.9 and 3.4, respectively, indicating the variable influence of different proportions of guayule in the AGR2s.
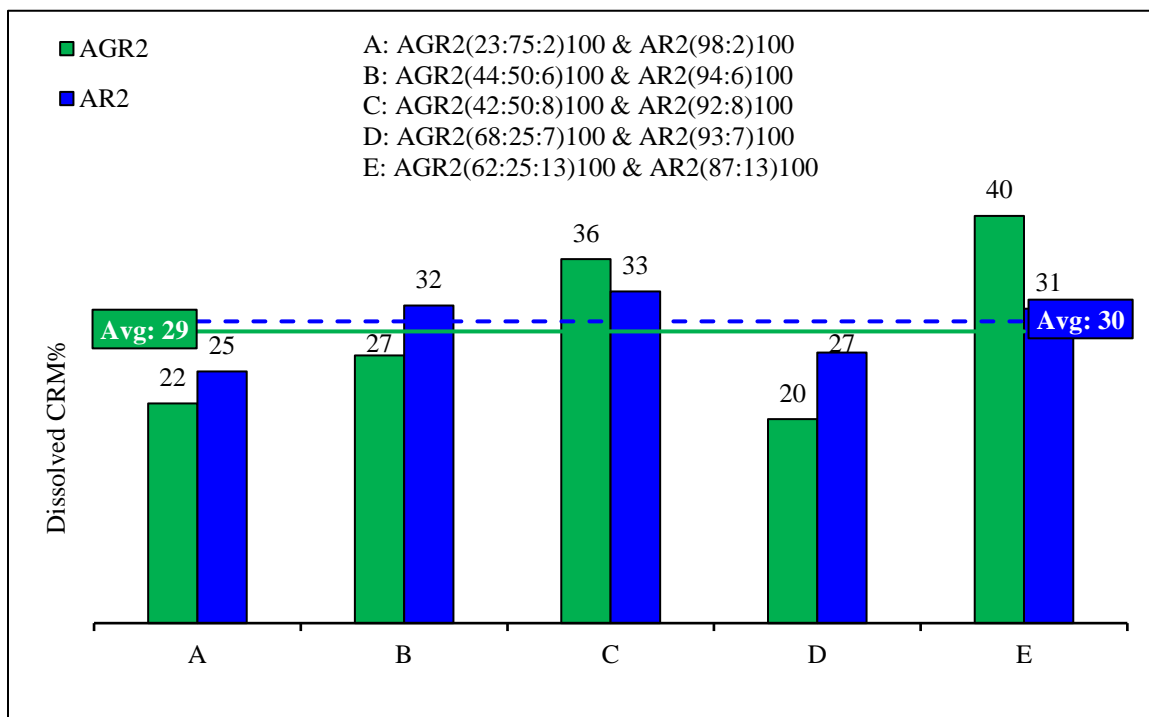
Figure 5.1 CRM Dissolution: AGR2s vs. AR2s [26].

5.2. WHOLE MATRIX VS. LIQUID PHASE GRADE SUSCEPTIBILITY

A term called the liquid phase percentage (LP%) defines the portion of the liquid phase (LP) critical high temperature relative to the whole-matrix (WM) critical high temperature of a particular binder as a percentage and is defined in Equation (12).

$$LP\% = \frac{\text{liquid phase critical high temperature}}{\text{whole matrix critical high temperature}} \text{ x } 100 \qquad (2)$$

The LP% was determined to show the interaction effect on the binder's liquid phase performance as a function of the critical high temperature. As shown in Table 5.2, the variation between the whole-matrix performance grade (PG) and the liquid-phase PG was not significant at the high temperature, indicating a high contribution of dissolved CRM. Furthermore, the LP% of AGR2(23:75:2)100A showed almost identical PG for both whole matrix and liquid phase at the high temperature (99.6%), which is justified by the low CRM concentration (2.3% by wt. of blend). However, it was lower for AGR2(44:50:6)100B, AGR2(42:50:8)100C, and AGR2(68:25:7)100D, which were all in the range of 96-97% relative to the intermediate CRM concentrations of 6.5%, 8.3%, and 6.8%, respectively. On the other hand, when raising the CRM concentration to 12.5% in AGR2(62:25:13)100E, the LP% decreased to 93.6%. The LP% of the corresponding ARs was relatively lower, indicating a lower performance when the AR binder performed as a liquid phase. For example, the LP% of AGR2(23:75:2)100A was 99.6% against 98.7% for AR2(98:2)100A.

Table 5.2 Whole Matrix vs. Liquid Phase Grade Susceptibility [26].

Binder Code	CRM% by wt. of blend	Whole Matrix		Liquid Phase		LP%[10]
		Critical high Temp [°C]	PG	Critical high Temp [°C]	PG	
AGR2(23:75:2)100A	2.3	59	58	59	58	99.6
AR2(98:2)100A	2.3	68	64	67	64	98.7
AGR2(44:50:6)100B	6.5	64	64	62	58	96.5
AR2(94:6)100B	6.5	72	70	69	64	95.7
AGR2(42:50:8)100C	8.3	65	64	62	58	96.2
AR2(92:8)100C	8.3	74	70	70	70	94.3
AGR2(68:25:7)100D	6.8	67	64	65	64	96.6
AR2(93:7)100D	6.8	73	70	70	64	95.3
AGR2(62:25:13)100E	12.5	72	70	68	64	93.6
AR2(87:13)100E	12.5	80	76	74	70	91.3

5.3. RUTTING PARAMETERS: AGR VS. AR

Figure 5.2a,b compares the rutting parameters of AGR2s to the corresponding ARs and A2 at 64°C at the two scales (liquid phase and whole matrix). The dissolved CRM improved the AGR2 physical properties on the liquid phase scale. For instance, the liquid phase of AGR2(62:25:13)100E [labeled AGR2(62:25:13)100E(LP)] had a |G*|/sinδ of 1.6 kPa, while AGR2(68:25:7)100D(LP) achieved 1.1 kPa. It is known that CRM significantly improves the AR binder's physical properties, as shown in Figure 5.2a,b on the liquid phase and whole matrix scales, respectively. According to the study limitations, the so-called AGR/AR ratio, as a function of |G*|/sinδ, was from 0.4 to 0.6 on the liquid phase scale (derived from Figure 5.2a). On the whole matrix scale, this latter ratio was 0.3-0.5 (derived from Figure 5.2b). This meant that the CRM residual particle effect on the AR binder was relatively better than the AGR2. On the other hand, the whole matrices of AGR2s (except

---

[10] Applied at a 64°C high grade temperature based on the unaged (original) binders.

AGR2(23:75:2)100A) performed well against the control asphalt, with higher performances occurring with higher asphalt and CRM concentrations. However, regarding the liquid phases' investigation, the AGR2(68:25:7)100D(LP) and AGR2(62:25:13)100E(LP) had performances of 1.1 kPa and 1.6 kPa, respectively, which could be compared to the control asphalt (A2).

For more clarification, Figure 5.2c depicts the percentage of the binder's liquid phase out of the binder's matrix as a function of $|G^*|/\sin\delta$ (coded LP/WM%). It was noticed that removing the residual CRM particles from the binder matrix was relatively better for the AGR2 than the AR2, as was also verified by LP%, as shown in Table 5.2.

5.4. MASTER CURVES

Master curves of the designated whole matrices (AGR2(23:75:2)100A, AGR2(44:50:6)100B, AGR2(42:50:8)100C, AGR2(68:25:7)100D, and AGR2(62:25:13)100E) as well as G2, and A2 are illustrated in Figure 5.3 with a selection of a 50℃ reference temperature. These master curves showed the effects of the frequency sweep along with temperature sweep on the material rheology represented by G', G'', and δ. In the AGR2s, a higher guayule concentration significantly affected the master-curve trends due to the different behavior associated with guayule compared to control asphalt. This different behavior led to an observed thermo-complexity shown by some master curves (Figure 5.3c) being interpreted hereafter. Overall, guayule provided a better trend at low frequencies. However, the control asphalt provided a better trend at high frequencies.
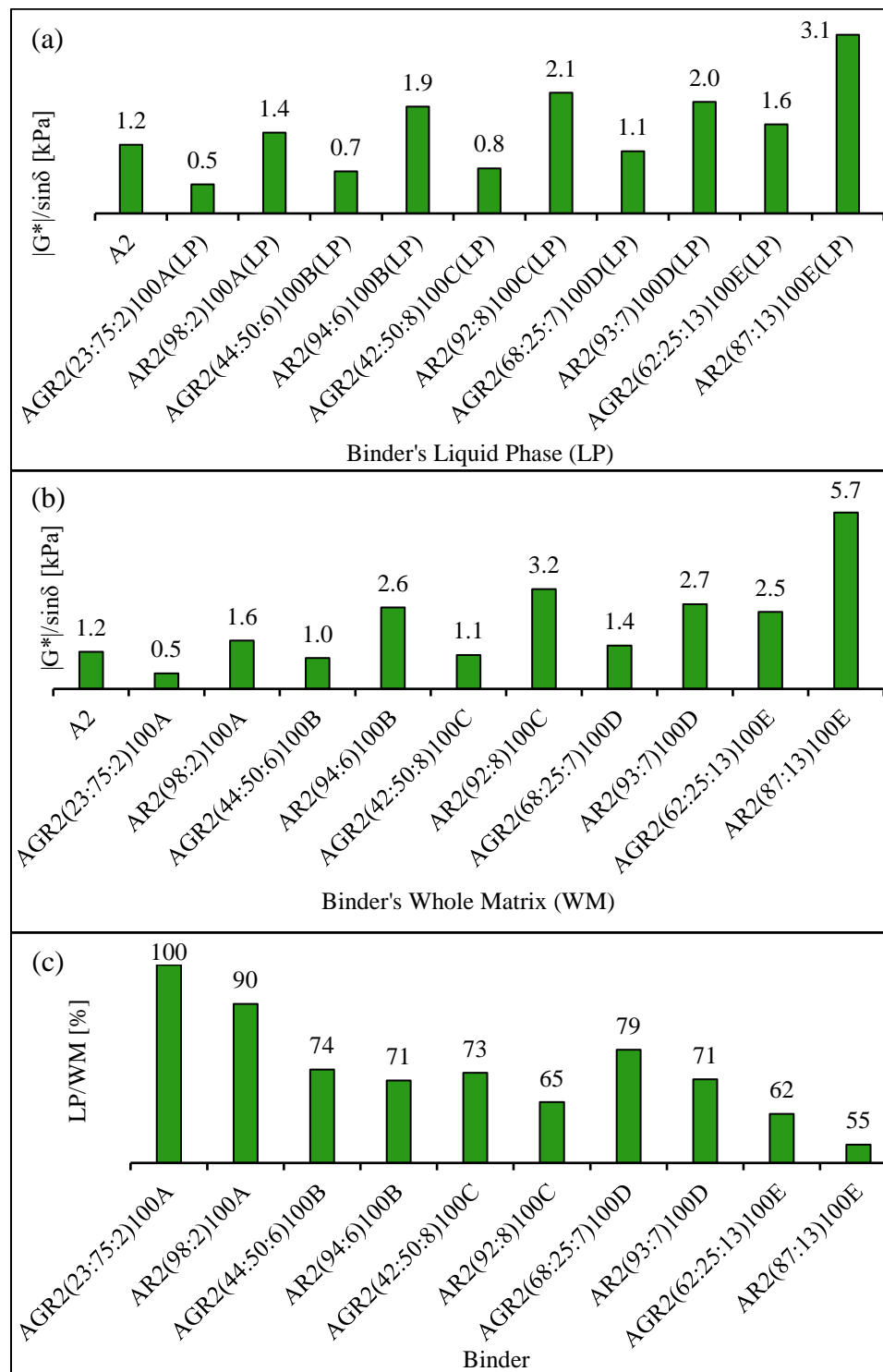
Figure 5.2 Comparing the Unaged-binders' Rutting Parameters of the Five AGR2s to the Corresponding AR2s at 64°C: (A) Liquid Phase; (B) Whole Matrix; (C) LP/WM, as a Function of |G*|/sinδ [26].
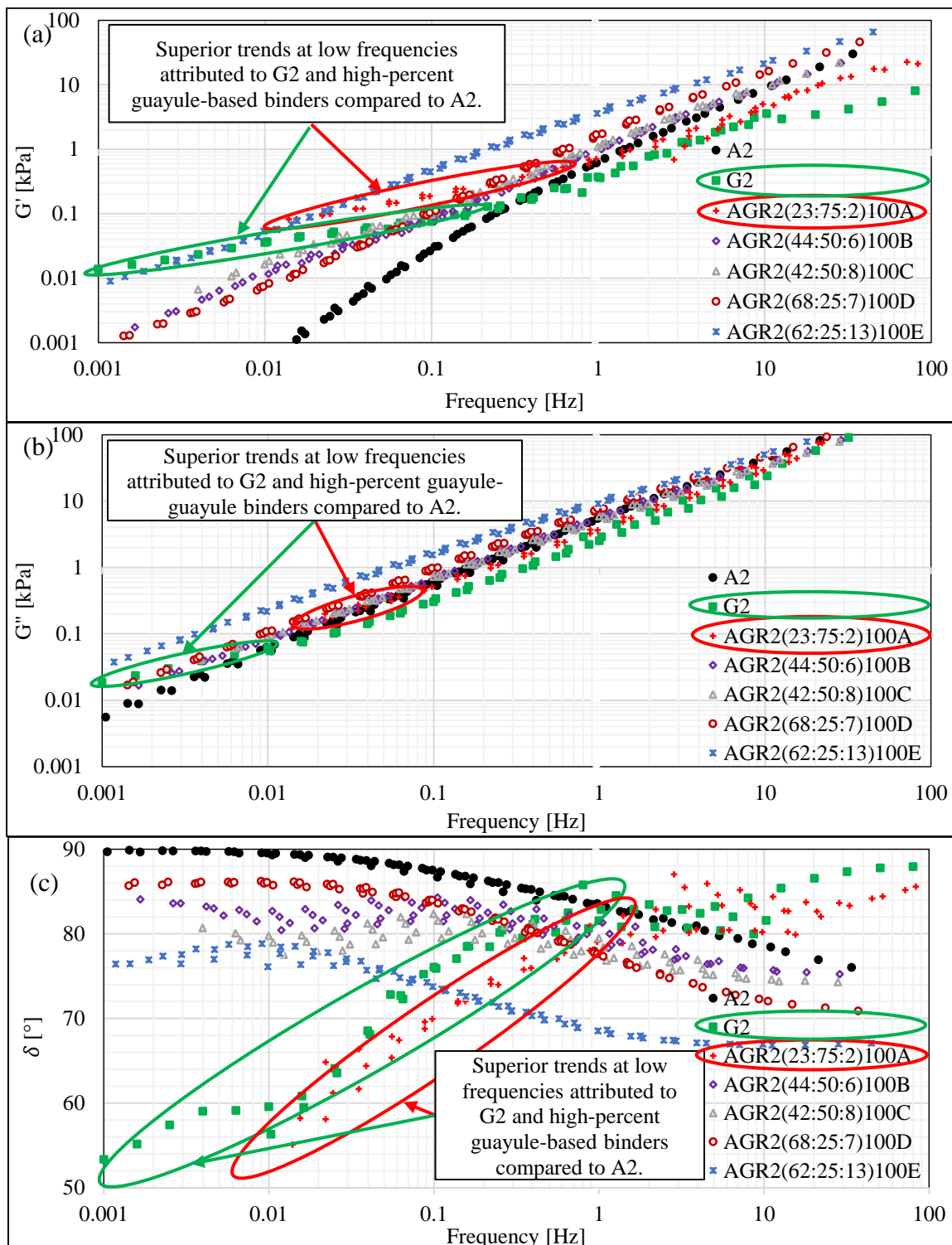
Figure 5.3 Master Curves of designated AGR2s' Whole Matrices Compared to A2 and G2 at a 50℃ Reference Temperature: (a) G', (b) G'', and (c) δ [26].

In terms of G′ and G″, it was observed that the high-percent guayule-based binders (mentioned here to denote the G2 and AGR2(23:75:2)100A binders) indicated a higher stiffness at low frequencies, as shown in Figure 5.3a,b, which developed a plateau investigated in depth in Subsection 5.5. The higher the asphalt and/or CRM concentrations, the higher the behavior except for the high-percent guayule-based binders at low frequencies. For instance, AGR2(62:25:13)100E presented the best trends except for the distinct G2 and AGR2(23:75:2)100A at low frequencies. On average, A2 showed a lower susceptibility to frequency and temperature. The AGR2(23:75:2)100A provided a guayule-like trend represented by the G2 trend. As mentioned above, both G2 and AGR2(23:75:2)100A had lower behaviors at high frequencies and higher behaviors at low frequencies than A2. Overall, what was distinct for the designated AGR2s except AGR2(23:75:2)100A was the high behavior at low frequencies and gradually increasing with higher frequencies to be close to the control asphalt behavior.

As shown in Figure 5.3c, G2 and AGR2(23:75:2)100A offered contrary δ trends to A2. In other words, A2 provided a high-to-low δ trend from low-to-high frequencies, which was contrary to the offered δ trend of the high-percent guayule-based binders. Accordingly, the other AGR2s showed a thermo-complexity via their δ trends due to the viscoelastic properties of each one. For instance, the δ trend of AGR2(62:25:13)100E started low at 0.001 Hz, reaching its peak at about 0.01 Hz, thus gradually decreased until 10 Hz, and ended up with a horizontal trend. This fluctuation could be analyzed by the dispersion of the loss (dissipation) factor (tanδ), which is defined by G″ per G′, of guayule vs. asphalt. Other AGRs such as AGR2(44:50:6)100B and AGR2(42:50:8)100C presented

significantly scattered regimes. Nevertheless, their average trends showed the lowest sensitivity to temperature and frequency than the control asphalt. This could be analyzed by balancing the AR and G concentrations in the blend.

5.5. GUAYULE RESIN PRIVILEGE

One of the significant problems facing asphalt binder behavior at high temperatures is the undesired δ behavior with traffic speed tolerance. The δ is desired to be lower at lower speeds (frequencies). Not only that but a higher stiffness is also desired at lower frequencies. Briefly, the lower the traffic speed, the more elasticity and stiffness are desired. At this point, the stiffness resists the traffic load, and the elasticity helps the binder recover. Guayule had potential of being attracted for the entirely desired δ behavior (Figure 5.3c) and desired G' and G'' behaviors at low frequencies (Figure 5.3a,b).

At low frequencies, the master curves of guayule offered an unconventional behavior. Guayule presented the best behavior compared to others at low frequencies for the three major rheological parameters G', G'', and resultant δ (Figure 5.3). That's why it showed better performance ($|G^*|/\sin\delta$) than that of the control asphalt at low frequencies, as shown in Figure 5.4. For G' trends, guayule presented a behavior much better than the control asphalt while the frequency was lower than 0.3 Hz (e.g., 0.01 kPa and 0.00001 kPa, respectively, at 0.001 Hz). For G'' trends, a similar scenario was observed in which guayule presented better behavior than asphalt while the frequency was lower than 0.01 Hz (e.g., 0.011 kPa and 0.002 kPa, respectively, at 0.001 Hz). As mentioned above, guayule presented an unconventional δ trend contrary to the control asphalt (Figure 5.3c). This trend

is desirable in terms of frequency sweep as it yields a higher elastic behavior at low frequencies, unlike the traditional behavior attributed to the control asphalt. Consecutively, guayule presented desirable characteristics at low frequencies since it presented higher G′ and G″, and lower δ. This distinction could be beneficial when vehicles stop since the pavement is desired to be stiffer (to resist the loads at low frequencies) and more elastic (to recover when deformed).
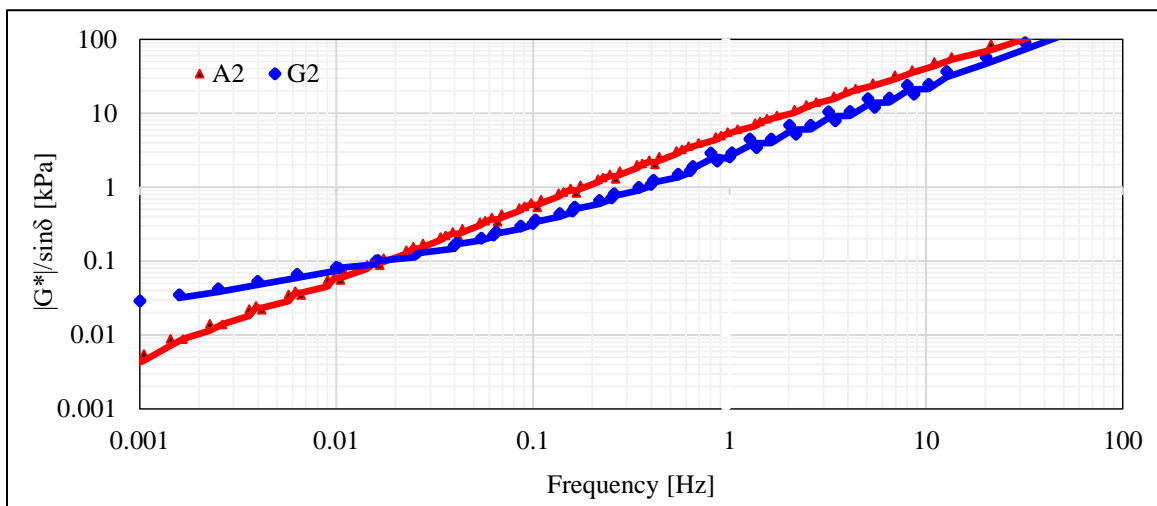
Figure 5.4 |G*|/sinδ Master Curves of Guayule (G2) vs. Control Asphalt (A2) [26].

5.6. INTERRUPTED SHEAR FLOW

Figure 5.5a-f shows the stress growth upon the interrupted shear flow of: (a) A2, (b) AGR2(23:75:2)100A(LP), (c) AGR2(44:50:6)100B(LP), (d) AGR2(42:50:8)100C(LP), (e) AGR2(68:25:7)100D(LP), and (f) AGR2(62:25:13)100E(LP) (T = 64°C, rest times of 5, 10, 20, 30, 40, and 50 s, and a shear rate of 2 s^{-1}).
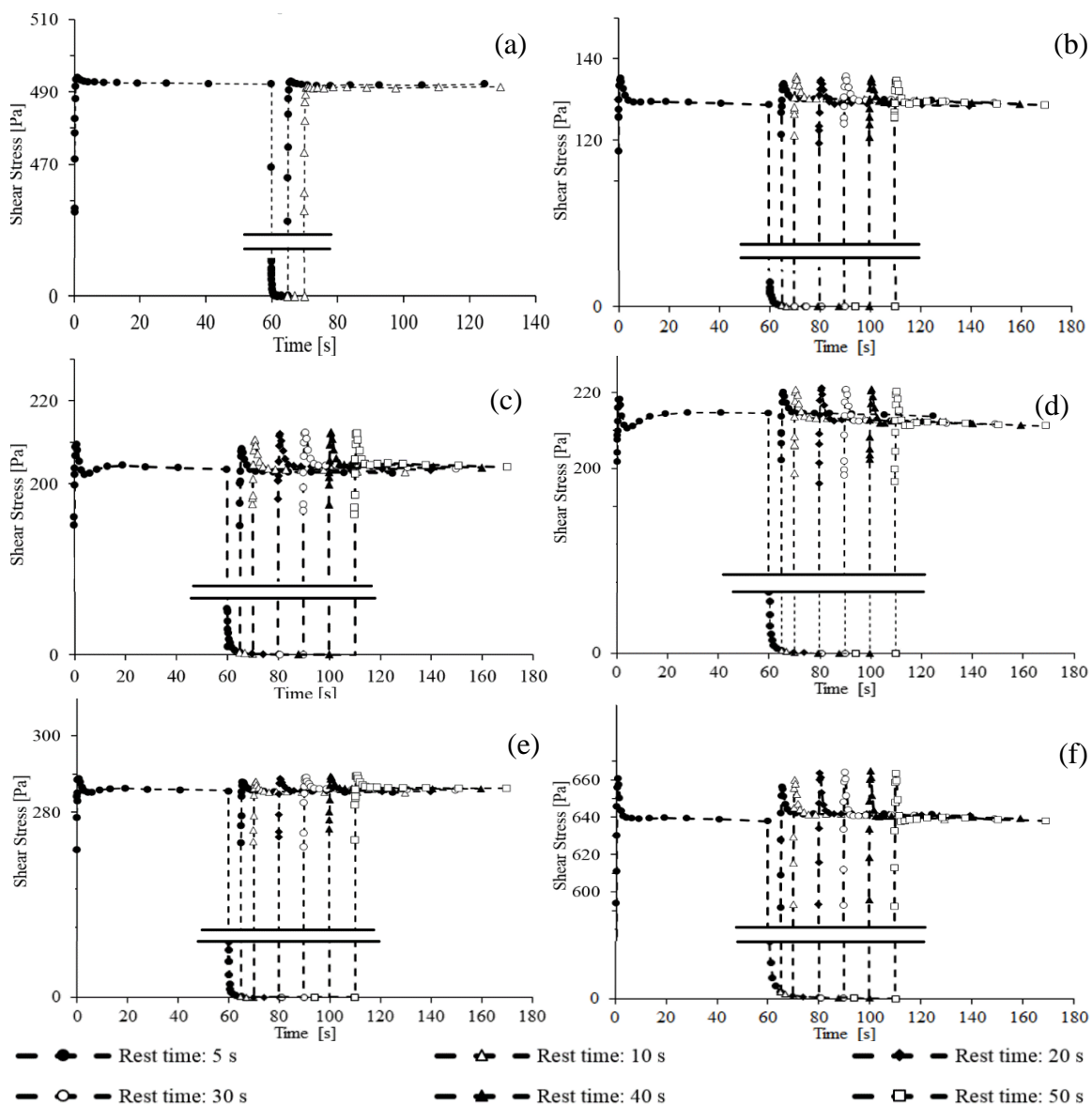
Figure 5.5 Stress Growth in the Interrupted Shear Flow of (a) A2, (b) AGR2(23:75:2)100A(LP), (c) AGR2(44:50:6)100B(LP), (d) AGR2(42:50:8)100C(LP), (e) AGR2(68:25:7)100D(LP), and (f) AGR2(62:25:13)100E(LP). T = 64℃, and Shear Rate of 2 s^{-1} [26].

Literature reported that the conventional asphalt had no peak overshoot of shear stress, just a steady-state shear flow and rapid stress relaxation as complied with the control asphalt, as shown in Figure 5.5a [100]. Wekumbura et al. reported, "This type of behavior

must be due to the weak associations, e.g., bipolar attractions, hydrogen bonding etc., which are easily destroyed by stressing or temperature variations [100]." This differs with binders modified with polymer components associated with peak overshoots [99, 100].

Overall, AGRs had potential to get back to their original peak overshoot very fast through the first 50 s, maximum after releasing the original shear growth, both initial and second overshoots followed by steady-state shear stress. The effect of asphalt, rubber, and guayule concentrations appeared here on the resultant stress growth of each AGR2. For instance, AGR2(62:25:13)100E(LP) had an initial overshoot of about 660 Pa. Even though a 5 s period was sufficient for flow relaxation, the second stress growth (655 Pa) did not reach the initial value. However, a 10 s rest time was sufficient to yield a fully recovered overshoot. This binder achieved about 1.34 times the control asphalt according to its original overshoot and about 1.3 times according to the steady-state value. This reflects a better performance of AGR2(62:25:13)100E(LP) in this regard. On the other hand, all other designated AGR2s here resulted in observed peak overshoots, as shown in Figure 5.5b-e, but their stress growth patterns were lower than the one attributed to the control asphalt.

The concept of the interrupted shear flow test applied in this study complied with the literature [78, 84, 99, 100]. Results showed a positive impact of polymeric components dissolved in the liquid AGR2 as they were attributed to a peak overshoot of shear stress in addition to their distinct rapid recovery time when applying the second stress growth. Ultimately, one could proclaim that the polymeric components dissolved from CRM in the AGR2 binder resulted in a 3D network structure that indicates a performance improvement against the conventional asphalt binder.

5.7. SUMMARY

An advanced level physical and rheological analysis was investigated in this subsection for designated AGR2s and their corresponding AR2s including CRM dissolution (CRM particle residue effect vs. interaction effect), master curves, and interrupted shear flow argumentation for unaged binders at high temperatures. Since asphalt might not perform as a whole matrix, the binder liquid phase (worst case scenario) was investigated for designated binders. It was found that the blend of 62.5% A2, 25% G2, and 12.5% CRM provided better performance than that of the control asphalt in all studied scales at high temperatures, whether as a whole matrix or a liquid phase. However, as expected, the corresponding asphalt-rubber binder resulted in relatively higher performance.

Pure guayule resin presented unconventional master-curve trends, which provided better behavior than the control asphalt at low frequencies in terms of G', G'', and δ. Accordingly, this might be beneficial in low-speed applications. It also presented an unconventional δ trend with the frequency sweep contrary to the control asphalt trend. This δ trend was desired in the asphalt industry as it provided higher elastic behavior at lower traffic speeds. Consecutively, one may notice that the AGR2 binders provided better master-curve trends at low frequencies. In agreement with the literature, a 3D network structure was associated with the AGR2 binders, reflecting the release of the CRM polymeric components in the binder liquid phase as verified by the component analysis interpreted in Section 6, and is proven to yield better performance.

6. UNDERSTANDING COMPOSITIONAL CHANGES OF THE GUAYULE-BASED BINDER COMPONENTS

The rheological performance discussed earlier can be understood by investigating compositional changes [2]. The following discussion addressed the component analysis to explain the reasons that could lead to enhancements of the binder performance concerning guayule applications in the future of the asphalt industry [2]. This section implies a reproduction of results published in [18, 26]. The component analysis was studied for designated stiff binders as representative samples to reveal the role of guayule in partial/full asphalt replacement, for privity. In compliance, the discussion presented in this section was found in agreement with the soft binders' component analysis argumentation published in [2].

6.1. FTIR ANALYSIS

6.1.1. Chemical Bonding of Guayule. The FTIR spectrum of guayule was obtained. Guayule had several identical peaks similar to the conventional asphalt. Figure 6.1 illustrates the potential functional groups associated with G2 compared to A2. Guayule involved peaks located at 2957 and 2868 cm^{-1} (CH$_3$ stretch), 2923 and 2852 cm^{-1} (CH$_2$ stretch) [56], 3035 cm^{-1} (C$-$H stretch), and 1451 and 1376 cm^{-1} (CH$_3$ bend) [62, 63]. These peaks could clarify the distinct carbon and hydrogen compositional elements attributed to guayule [20, 51]. Other distinct peaks were observed at 1706 cm^{-1} and 1031 cm^{-1}, attributed to carbonyl (C=O) and sulfoxide (S=O). The carbonyl and sulfoxide structures were reported in the literature to assess the asphalt binder's oxidative aging [17, 132, 133]. The

C–O, C=O, and O–H stretches were also reported to indicate a formation of strong oxidation bonding chains in the bio-binders [17], as discussed later. A peak was located around 1606 cm^{-1} in guayule and asphalt that could indicate C=C stretch [56]. A peak formed at 1512 cm^{-1} (C−C, lignin) for guayule [25]. Between 850 and 650 cm^{-1}, some peaks appeared such as 837, 770, 720, and 698 cm^{-1} (C−H bend), aromatic structures [8, 12, 16, 17, 60, 133, 168]. Moreover, peaks were located at 3402 cm^{-1} (O−H stretch, cellulose) [25], 1638 cm^{-1} (NH$_2$ stretch) [56], 1311, 1254, and 1203 cm^{-1} (C−O stretch) [63], 1167, 1112, and 1056 cm^{-1} (O−H bend). Peaks from 956 to 891 cm^{-1} might also indicate O−H deformation in this region [25, 169].
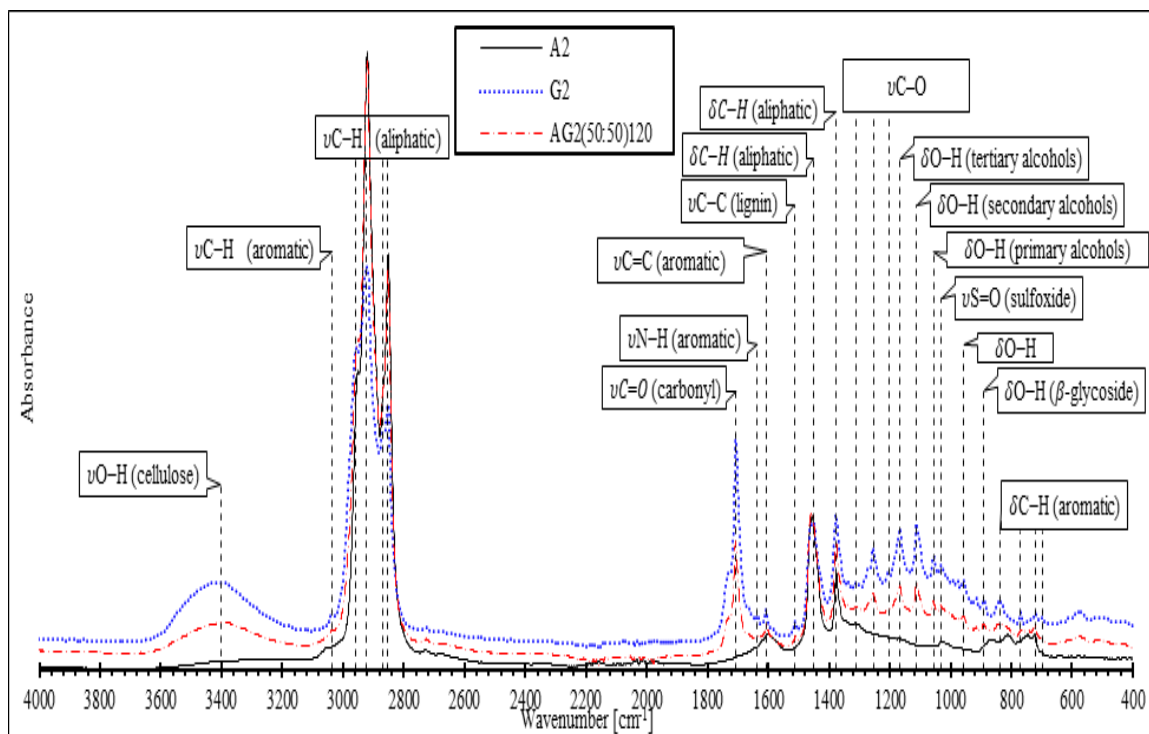
Figure 6.1 Comparative FTIR Spectra: Potential Functional Groups of Guayule (G2) against Control Asphalt (A2), in addition to Their Combination (AG2(50:50)120). (δ: bending; υ: stretching) [18].

6.1.2. Asphalt-Guayule Interaction. To investigate the interaction between asphalt and guayule, the FTIR spectrum was obtained for an asphalt-guayule (AG2) blend. The AG2 blend was 50% A2 and 50% G2 (the so-called AG2(50:50)120), mixed at 3000 rpm and 190°C for 120 min. As shown in Figure 6.1, no new peak or peak shift occurred. However, almost all asphalt and guayule peaks were formed in the blend. This pattern could indicate a physical blending (i.e., no chemical reaction between asphalt and guayule), which was in agreement with bio-based binders mentioned in the literature [10, 41]. Furthermore, Hemida and Abdelrahman (2020) [27] proved no liquid phase separation between asphalt and guayule after lab-simulated storage, as discussed in Section 7.

6.1.3. AGR vs. AR Spectra. Compared to each other, similar spectra of the AR2(98:2)100A, AR2(94:6)100B, AR2(92:8)100C, AR2(93:7)100D, and AR2(87-13)100E binders indicated no significant change in the component composition of AR2 blends regardless of material concentrations, as shown in Figure 6.2. Like AR2 spectra, no distinct peak differences among the AGR2 blends were observed. The AGR2s had multiple peaks, which did not appear in the corresponding AR2 spectra such as the very polar O−H group at 3402 cm^{-1} and C−C at 1511 cm^{-1}. These peaks belonged to the pure guayule, as discussed in Subsection 6.1.1. Due to the high C=O (carbonyl) concentration around 1706 cm^{-1} in guayule, such a peak was one of the most distinct formed peaks in the AGR2s. The significant carbonyl intensity attributed to the guayule-based binders played a crucial role in the unaged binder behavior (besides other oxidative bonds). New little peaks were formed in either AR2 or AGR2 blend, indicating the attaining chemical reaction between CRM and liquid binder (either asphalt or asphalt guayule), as discussed in Subsection 6.1.4.
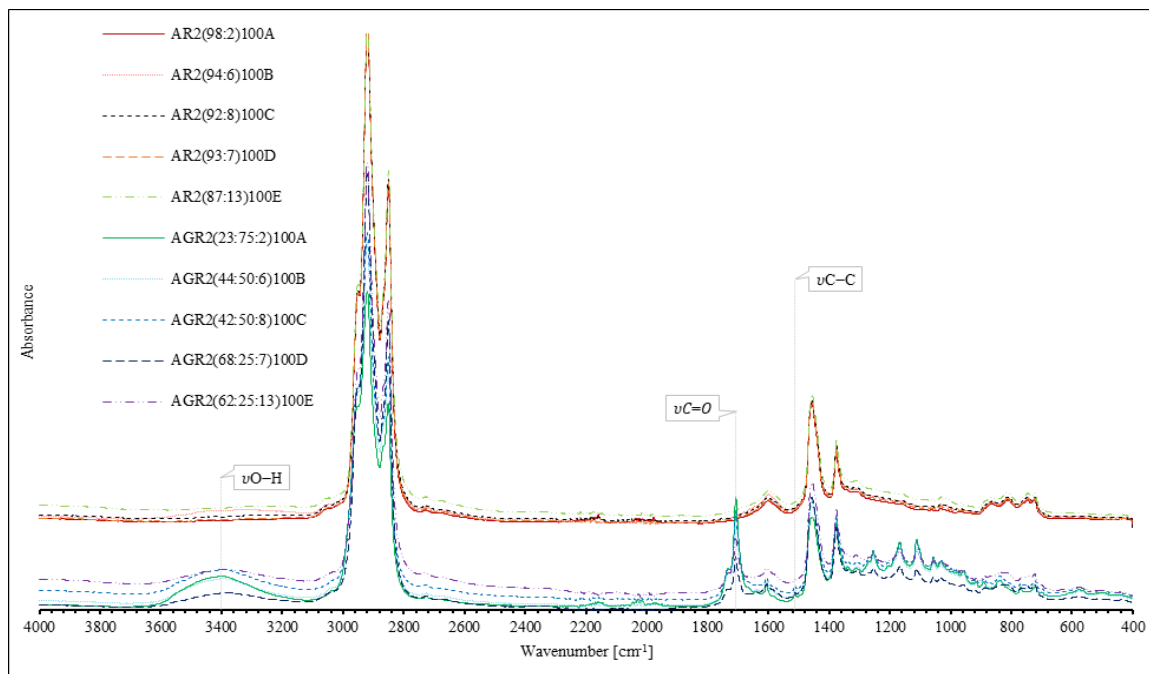
Figure 6.2 Comparative FTIR Spectra of the Liquid AGR2 and AR2 Blends [18].

6.1.4. Released Component Verification by CRM Residue Spectra. FTIR was employed to obtain the CRM residue spectra to verify the liquid binder's component analysis. The CRM spectra were initially formed with steep baselines due to carbon black's impact on the ATR technique. Therefore, the baselines of the designated CRM spectra were corrected. The CRM residue of the designated AGR2s had similar spectra. However, a significant difference between the CRM peak intensities before and after interaction (i.e., as-received vs. residue) was noticed, as shown in Figure 6.3. Likewise, the same situation was associated with AR2s. It was observed that the CRM residue peak intensities of either AGR2(62:25:13)100E or AR2(87:13)100E remarkably decreased, representing a high dissolution of CRM particles into the liquid binder, as verified by the TGA analysis in Subsection 6.2.2.
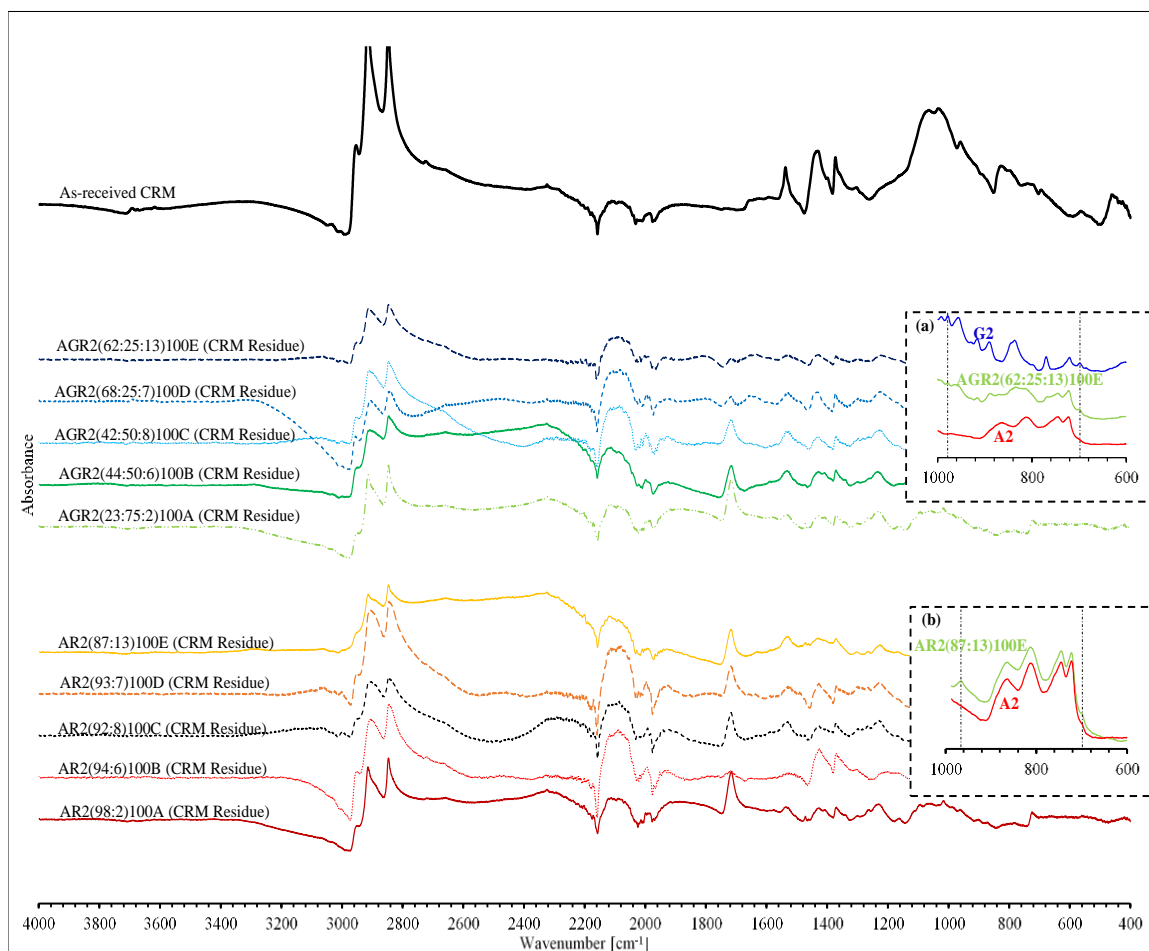
Figure 6.3 Comparative FTIR Spectra of CRM Residue in AGR2s And AR2s and the As-Received CRM. CRM Polymeric Components Release into (a) the AGR2 Blend and (b) the AR2 Blend [18].

For all investigated CRM residue of AGR2s and AR2s, the peaks significantly decreased at 1398 and 1538 cm^{-1}, as shown in Figure 6.3. Such intensities' decrease likely indicated a devulcanization of S-CH$_n$ [57, 170, 171] and diffusion of C=C in carbon black [57, 172], respectively. One could notice that aliphatic hydrocarbons between 3000 and 2800 cm^{-1} were affected, and their intensities significantly decreased. On the other hand, the FTIR analysis showed a new significant peak formed around 1718 cm^{-1} in CRM residue

in variant intensities. Such peak formation might indicate that CRM's swelling was due to the absorption of light molecular weight aromatics diffused from the liquid binder into the CRM residue [57]. The aromatics swelling intensity by CRM particles could result in a stiffer or softer RTFO-aged binders compared to their unaged binders as reflected in the contrary of RTFO aging susceptibility discussed for the AR1 binders (Subsection 4.1.3) against the AR2 binders (Subsection 4.2.3).

Distinct peaks in AGR2(62:25:13)100E were magnified, as shown in Figure 6.3a. Both guayule and as-received CRM had peak intensities around 966 and 700 cm^{-1}. The peak formations around 966 and 700 cm^{-1} in the AGR2 blend made it not clear whether these peaks were related to only guayule or CRM-component release besides guayule. Similarly, the AR2(87:13)100E spectrum had small peak intensities around 966 and 694 cm^{-1}, as shown in Figure 6.3b. These peaks depict a release of out-of-plane C−H bends of monoalkylated aromatics of polystyrene and trans-alkane of polybutadiene (polymeric components) diffused from CRM to the liquid binder (either asphalt guayule or asphalt) [57, 64, 76].

6.1.5. Oxidative Aging Behavior. Figure 6.4 illustrates the aging behavior based on the FTIR spectra of A2, AR2(87:13)100E, and AGR2(62:25:13)100E. In general, the RTFO and PAV aging raised the three listed binders' peak intensities, as shown in Figure 6.4a(1−3). Figure 6.4b(1−3) demonstrates the quantitative analysis of the carbonyl and sulfoxide aging behavior. In agreement with the literature, the evolution of carbonyl and sulfoxide bonds in the control asphalt was observed, as shown in Figure 6.4b(1) [17]. Compared to the control asphalt, the CRM did not influence the carbonyl and sulfoxide

indexes in the AR2(87:13)100E blend, as shown in Figure 6.4b(2). No observed change in the sulfoxide index of the AGR2(62:25:13)100E blend with RTFO aging, and PAV aging occurred, as shown in Figure 6.4b(3). However, the carbonyl index was dramatically influenced. This negative influence complies with the rheological properties at intermediate and low temperatures, as investigated in a study by [30]. Bio-based materials were generally proven to initiate strong oxidation bonding chains [16, 17]. The investigated oxidative aging is compatible with the rheological behavior provided in this study. The results showed that the investigated guayule-based binder (AGR2(62:25:13)100E) had significant oxidative aging behavior recognized by the carbonyl bond index, reflecting the relatively high critical intermediate temperature of the guayule-based binders compared to the AR2 binders. The strong oxidation bonding chains of the unaged guayule-based binders (compared to A2 and AR blends) explain the dramatic influence on the aged binder performance as offered by rheological analysis in this study and a previous study [30].

6.2. TGA ANALYSIS

6.2.1. TGA Analysis of Guayule. Guayule (G2) was exposed to composition analysis via TGA to indicate its multi-components. Figure 6.5 shows the complexity of guayule multi-components that contained constituents that decomposed at 233℃, 262℃, 286℃, 313℃, 339℃, 341℃, 366℃, 391℃, and 418℃, upon the decomposition temperature range from the ambient temperature to 450℃, which corresponded to almost no residue. The 450℃ terminal temperature was first determined by the ramp method as a rapid approach to recognize a 100% decomposition of the guayule material. Nevertheless, SITG was utilized to define the decomposition temperatures of guayule constituents as it

prevents the overlapping of the decomposition temperatures of components and renders a

high accuracy compared to the ramp method [81].
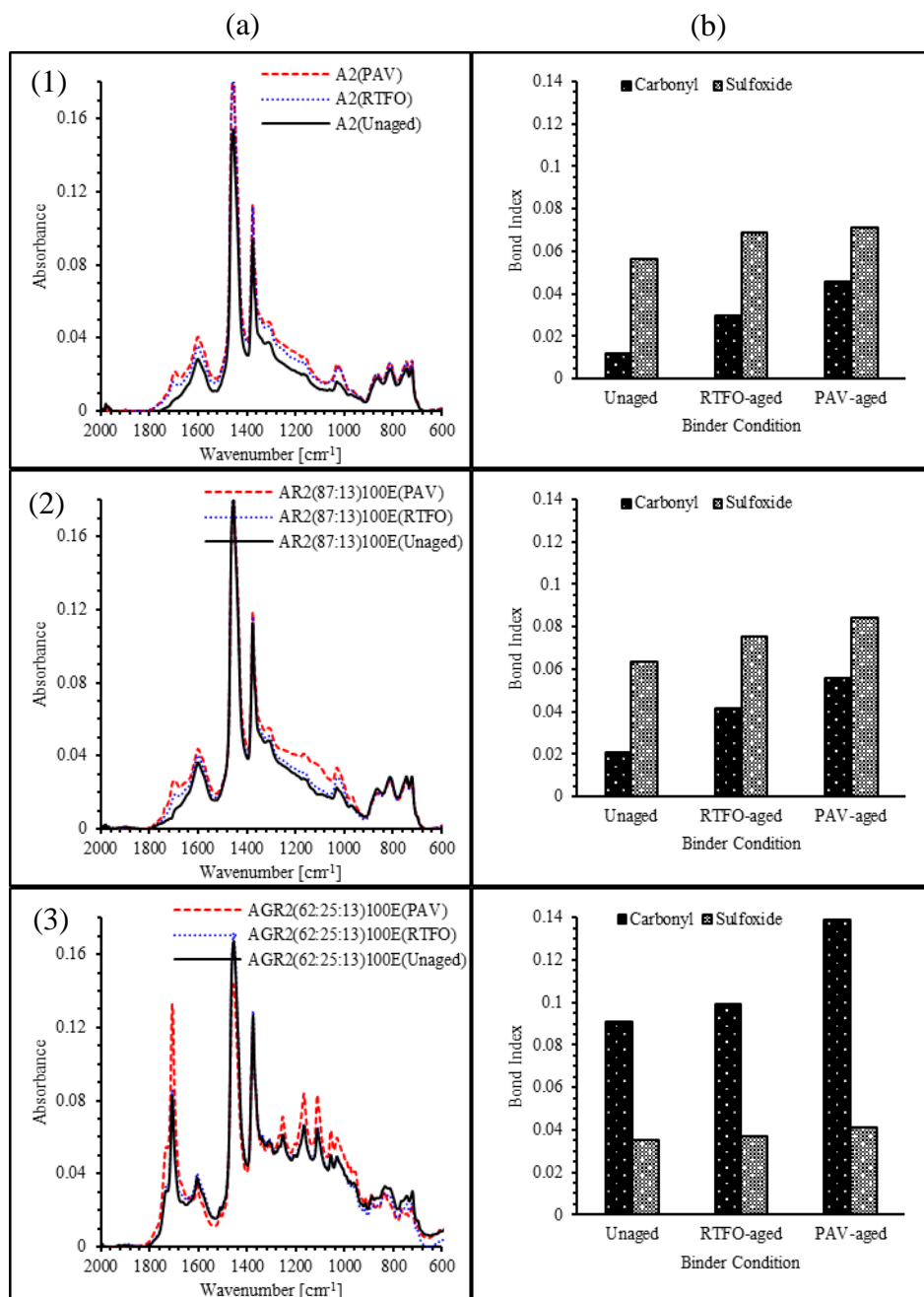
Figure 6.4 Aging Behavior Based on FTIR Spectra: (a) FTIR Spectra and (b) Bond
Indexes of (1) A2, (2) AR2(87:13)100E, and (3) AGR2(62:25:13)100E [18].
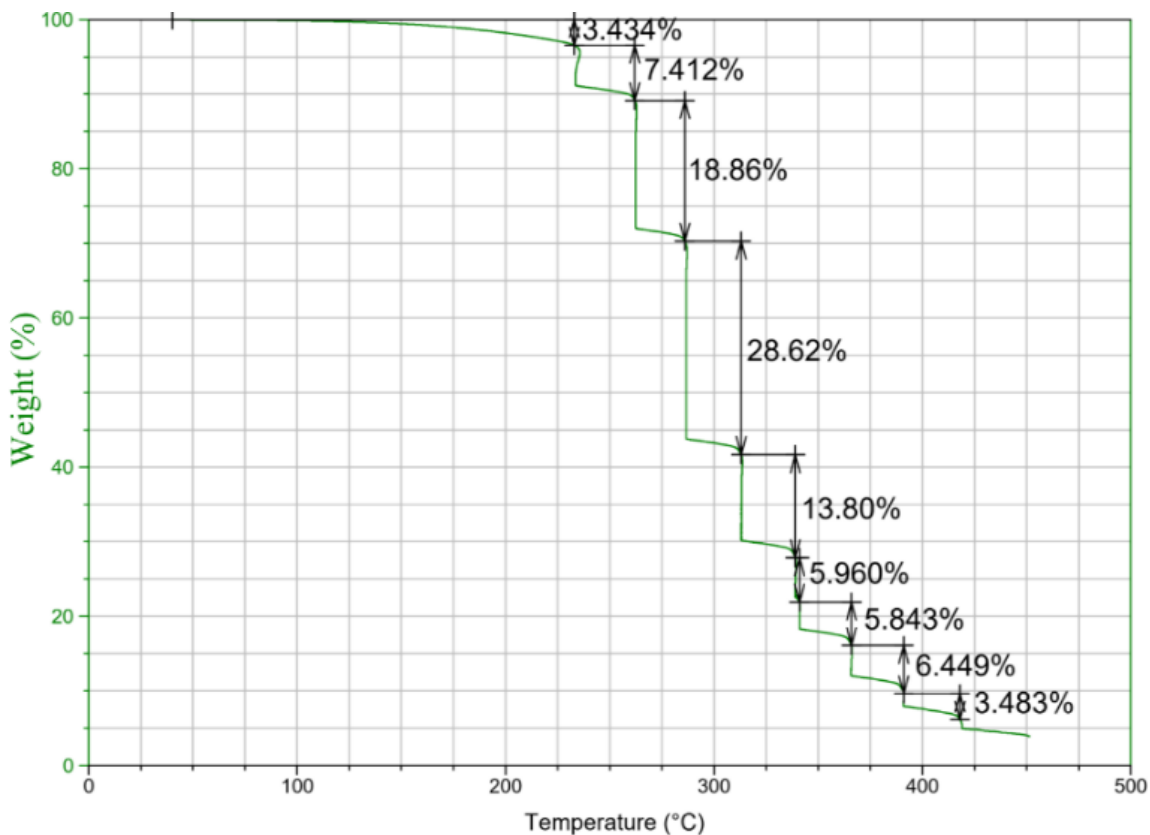
Figure 6.5 TGA Chart of Heat-Treated Guayule Resin (G2), SITG Method − from Ambient Temperature to 450°C [26].

As shown in Figure 6.6a, the minimum point at 100°C on DTG corresponds to about a 0.82% moisture mass loss, indicating a small amount of moisture with also considering loss of light molecular weight components. However, when guayule was heat-treated, the DTG did not show the minimum point at 100℃, indicating no moisture at this condition. Also, the mass loss was determined to be 0.14% at 100°C, as shown in Figure 6.6b, which may represent a loss of light molecular weight components of guayule.

6.2.2. TGA Analysis of CRM. This subsection implies thermogravimetric analysis of the as-received CRM and the extracted CRM from designated liquid binders.

decomposition was represented by the mass loss, which was 6% for oily components, 37% for natural rubber, 17% for synthetic rubber, and 40% for filler components.
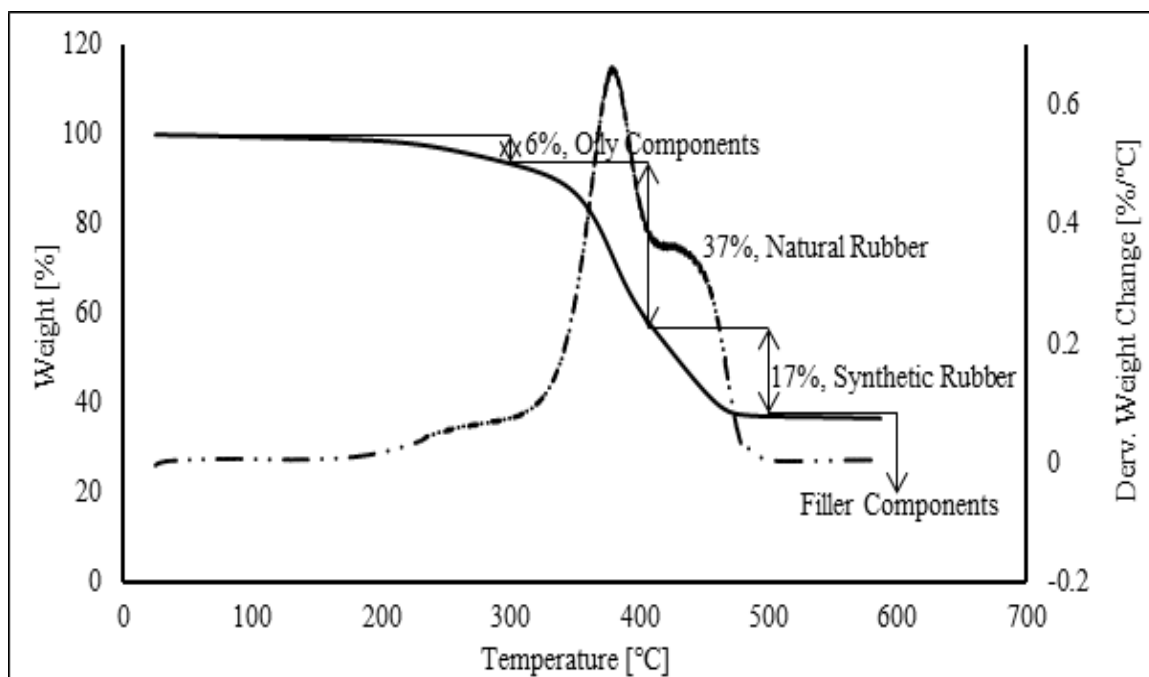
Figure 6.7 TGA Chart and DTG of As-Received CRM [18].

6.2.2.2. Extracted CRM. The CRM was released from the binder liquid phase. Consecutively, the dissolved CRM was calculated for the binder's whole matrix. In this regard, the aim of the TGA analysis was to investigate whether CRM components migrated to asphalt guayule compared to asphalt. Figure 6.8a,b illustrates the CRM-component migration to liquid binders of AGR2s and corresponding AR2s, respectively, regardless of the dissolved CRM portion. Overall, the results show that the oily component decreased,

and filler components increased in the extracted CRM. This behavior could indicate the migration of oily components to the liquid binder.
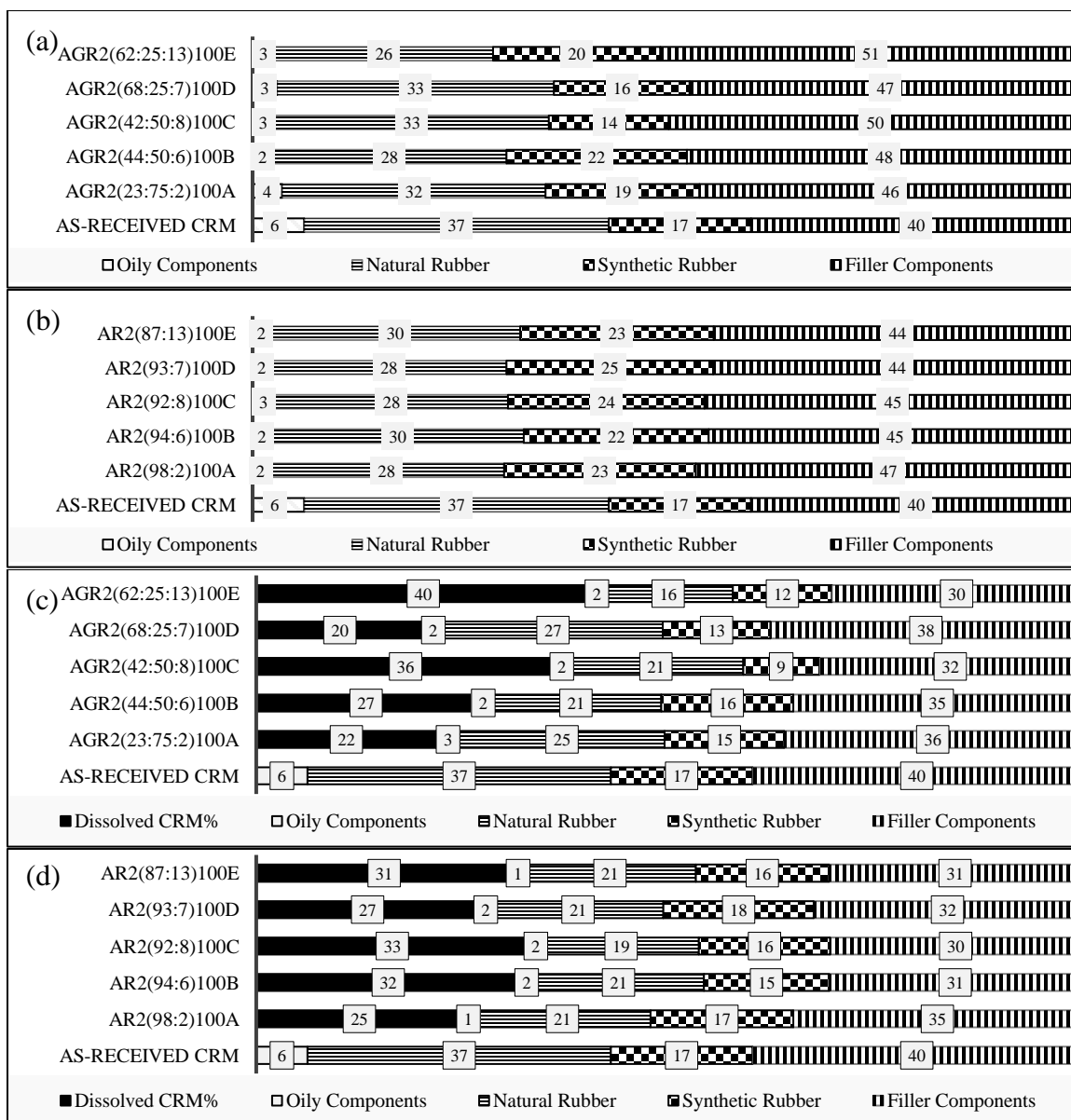
Figure 6.8 TGA Analysis: Proportional Changes in CRM Components Extracted from AGR2s (a) and AR2s (b), and Proportional Changes of CRM Components Considering the Dissolved Portion of CRM for AGR2s (C) and AR2s (D) [18].

As shown in Figure 6.8c,d, the TGA outcomes were translated as concentrations of CRM constituents, including the dissolved and extracted portions in the liquid AGR2s and AR2s. In Figure 6.8c, the higher CRM concentration resulted in a higher CRM dissolution such as 40% and 36% for AGR2(62:25:13)100E and AGR2(42:50:8)100C, respectively. Nevertheless, this went lower with lower CRM concentrations such as in the case of AGR2(44:50:6)100B and AGR2(68:25:7)100D that resulted in a dissolved CRM percentage of 27% and 20%, respectively. Furthermore, AGR2(23:75:2)100A yielded a 22% dissolved CRM. The CRM dissolution analysis indicated a maximum of about 40% of dissolved CRM that could not justify the close critical temperatures of the liquid phase vs. the whole matrix, as shown in Table 5.2.

Likewise, from Figure 6.8c, the extracted CRM constituents indicate relatively a minor dissolution of fillers (about 14% release on average). Dissolution of the polymeric components (natural rubber and synthetic rubber) was about 41% and 25% release on average, respectively. However, a significant dissolution took place to the oily components, about 67% on average.

To clarify the change in the polymeric components (natural rubber and synthetic rubber), for example, the 37% natural rubber in the as-received CRM became 16% in AGR2(62:25:13)100E and became 21% in AR2(87:13)100E. The synthetic rubber migrated to the liquid binder with lower concentrations than the natural rubber migration. For instance, the 17% synthetic rubber in the as-received CRM became 12% in AGR2(62:25:13)100E and became 16% in AR2(87:13)100E. It was not evident whether CRM was highly dissolved in asphalt guayule or control asphalt. Based on the investigated

AGR2 and AR2 blends, the CRM dissolution fluctuated up and down among AGR2 and AR2 blends. However, it was noticed that the more the CRM concentration, the more the CRM dissolution in the liquid binder in both AGR2 and AR2 blends. Accordingly, guayule likely does not affect the CRM dissolution in the asphalt-guayule blend.

Relating the TGA analysis to the rheological analysis discussed in Section 4 explains that the release of polymeric components in the liquid binder could be the reason behind the binder enhancement at high temperatures. The literature reported that such a release might be related to forming a 3D entangled network structure [57].

Relating part of released CRM components illustrated by TGA analysis to the FTIR analysis discussed in Subsection 6.1.4 emphasizes the apparent peaks of the polymeric components (e.g., polystyrene and polybutadiene) in the liquid binders of both asphalt guayule and control asphalt.

6.3. SUMMARY

This subsection provided the component analysis of designated guayule-based binders compared to their corresponding ARs and the control asphalt. The following observations conclude the outcomes. The investigation confirmed the distinct carbon and hydrogen compositional elements of guayule as an asphalt-like material. Asphalt and guayule had similarities in component composition and rheological behavior with temperature susceptibility. No new peak or peak shift was observed for the asphalt-guayule blend. This kind of blending indicated a physical interaction (with no chemical reaction). The polymeric components' migrations from CRM were more harmonious with asphalt than guayule at the same interaction parameters [2]. This might contribute to the

remarkable enhancement of the asphalts' rheological properties compared to guayule [2].

Conversely, CRM was similarly released in either AGR2 or AR2 blends. In other words,

the guayule addition did not affect the CRM component dissolution through the AGR's

liquid binder. However, since the conventional asphalt did not have the exact chemical

structure of guayule, the rheological behavior of AGR2 was not the same as AR2, which

was better for AR2. The distinct decrease in peak intensities was associated with the highest

CRM concentration as in AGR2(62:25:13)100E and AR2(87:13)100E blends, verified by

the highest CRM dissolution illustrated by the TGA analysis. A new peak formed at 1718

cm^{-1} in CRM residue for all investigated binders in variant intensities. Such a peak

formation could indicate CRM swelling due to liquid binder constituents (asphalt/guayule)

diffusion into the CRM residue. Depolymerization occurred, resulting in a partial migration

of CRM polymeric components (e.g., polystyrene and polybutadiene) to the liquid binder

of either AGR2 or AR2. This was reflected in the enhanced performance of AGR2 at high

temperatures. Due to the strong oxidation bonding chains attributed to guayule (e.g.,

carbonyl, sulfoxide, and hydroxyl) [2], it was reflected in the low intermediate- and low-

temperature performances compared to the conventional asphalt [2].

7. SEPARATION TENDENCY

This section implies a reproduction of results published in [27]. It involves results interpreting the effect of adding guayule (G2) to asphalt-rubber blend (AR2) on the CRM dissolution, viscosity, density, and separation tendency. In addition, extra results were acquired to verify the liquid phase separation, if any, which included investigations by master curves, TGA, and FTIR analysis. Statistical analysis was also implied for SI and master curve results to show the significance of difference using the single factor analysis of variance (ANOVA). Regarding SIs, the significance of difference was studied to compare each designated binder to the control binder (A2). Regarding master curves, the statistical analysis was implemented to show the significance of difference among binder fractions: tops (T) and bottoms (B).

7.1. CRM DISSOLUTION: AGR VS. AR

As interpreted in Subsection 5.1, Figure 7.1 depicts the dissolved CRM% of designated AGR2s in comparison with their corresponding AR2s. As shown, it is not clear whether asphalt or asphalt guayule had higher CRM dissolution. One could declare no significant difference between both AGR2s and AR2s regarding their dissolved CRM averages (29% for the AGR2s and 30% for the AR2s). Subsequently, this dissolution could be translated to the dispersed CRM residue. The higher the dissolution, the lower the residue radius, which would be reflected in the sedimentation velocity of dispersed particles, as discussed later.
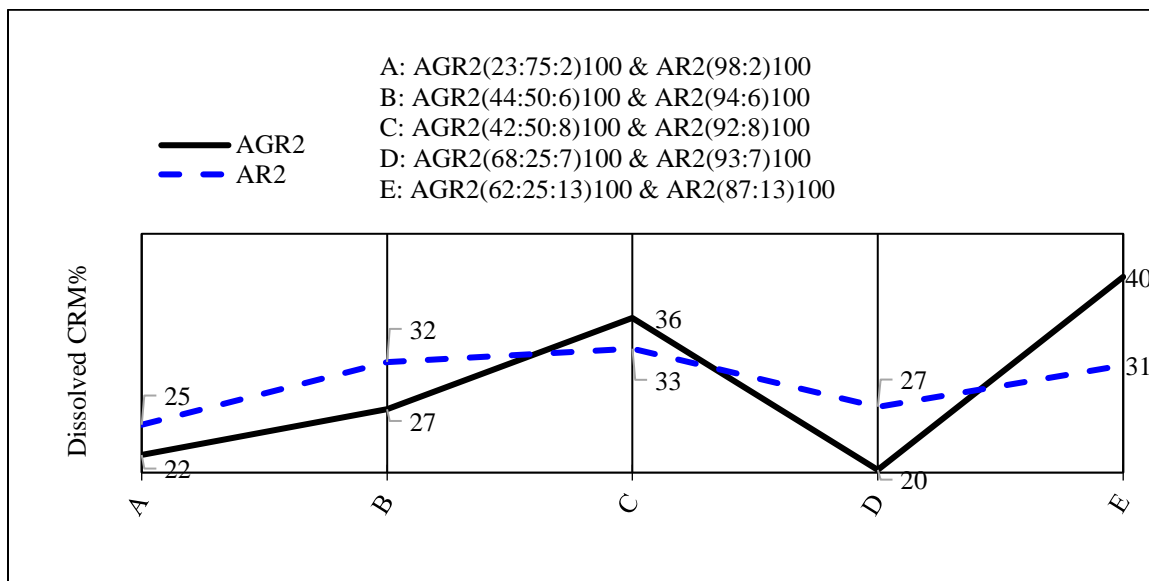
Figure 7.1 CRM Dissolution: AGR2s vs. AR2s [27].

7.2. VISCOSITY, DENSITY, AND SEPARATION TENDENCY

The viscosity was measured for the LPs of the designated AGR2s and their corresponding AR2s (Figure 7.2) at 163℃ (the same temperature as the lab-simulated storage) [81]. However, to assess the viscosity of these binders' LPs, the original binder (A2 and G2) viscosities were measured, 127 cP and 82 cP, respectively, indicating a lower viscosity for G2 than that of A2. Subsequently, increasing the CRM and A2 concentrations yielded a relatively higher viscosity. Increasing CRM concentration increased the LP viscosity by further releasing CRM components. In addition, a higher A2 concentration raised the viscosity, as it had a viscosity higher than that of G2. The average viscosity of the AGR2s and the AR2s resulted in 135 and 175 cP, respectively. This difference would affect the storage instability to a great extent, as discussed hereafter.
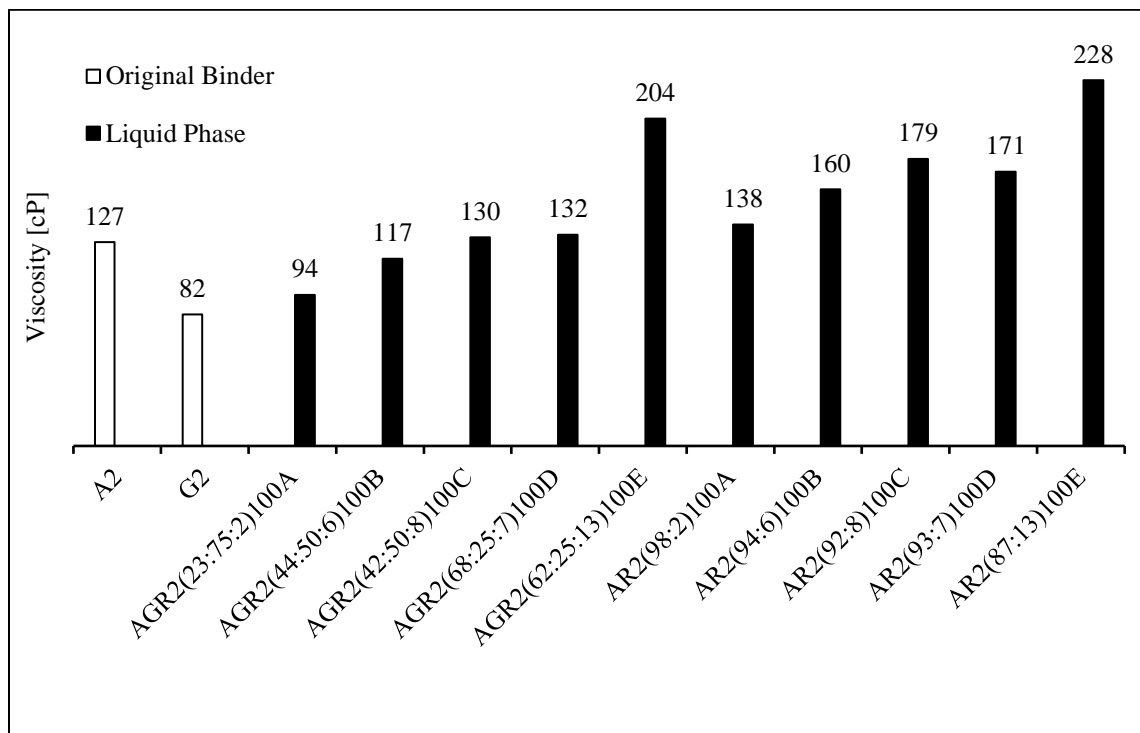
Figure 7.2 Binder Viscosities (at 163℃) [27].

The densities of the original binders (A2, G2(As-Received), and G2) and the LPs and WMs of AGR2s and AR2s were measured, as shown in Figure 7.3. The G2(As-Received) had a density of 1036 g/dm^3. The G2 had a little higher density (1038 g/dm^3). The A2 had a relatively lower density (1028 g/dm^3). The density of the LPs was measured because it affected the particle sedimentation velocity. Additionally, the density of the WMs was measured to see the effect of CRM residue.

As expected, the AGR2 LPs resulted in a lower density than their WMs. The same scenario was observed for the AR2s. Overall, the AR2s had densities lower than the AGR2s by the low A2 density. The LP and WM densities indicated a higher density of CRM residue than A2 and G2, which was compatible with the literature, whereas CRM density

was previously determined (about 1150 g/dm^3) [15, 173]. Not only that, but the CRM residue also involved filler components such as carbon black. Carbon black had a much higher density (1800–2100 g/dm^3) [15, 173], which was not easy to dissolve, as interpreted by the TGA analysis. Overall, Δρ of AGR2 was lower than that of AR2. Likewise, a higher CRM concentration resulted in a higher density of the binder's LP, which emphasized a relatively higher density of CRM components released. Nevertheless, this closeness of AGR2 and AR2 densities made it an insignificant parameter for rapid residue sedimentation velocity.

The investigation showed poor storage stability for the designated AGR2 WMs, which resulted in SIs of 17%, 57%, 59%, 60%, and 52%, respectively (Figure 7.4). However, their corresponding AR2s resulted in relatively better SIs, which were 4%, 29%, 26%, 31%, and 30%, respectively. The LPs of both AGR2s and AR2s yielded much better SIs, which were in a range of 0.9–4.3% for AGR2s and 0.3–1.6% for AR2s, indicating almost no liquid phase separation. Even though the AGR2 LP showed almost no liquid phase separation, the poor storage stability associated with the WM is still an issue. Seeking how to improve the storage stability of AGR2 WM is out of the scope of this study. Overall, there is a belief that manipulating the interaction parameters (speed, time, and temperature) is the key to overcoming the storage instability problem. The literature showed that the AR could result in perfect storage stability by selecting the proper interaction parameters. For instance, the literature reported that the SI of AR as a WM significantly decreased up to 2% when interacting at 190℃ and 3000 rpm for 480 min, whereas the corresponding SI of its liquid phase reached 1% [84].
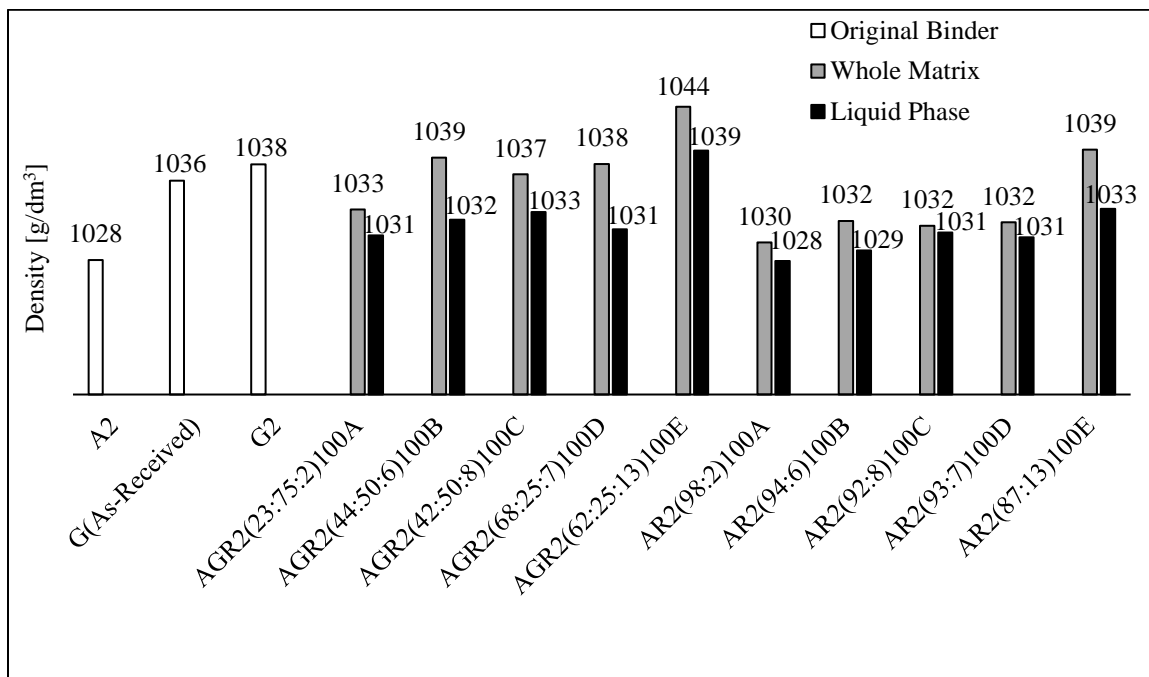
Figure 7.3 Binder Densities (at 25°C) [27].
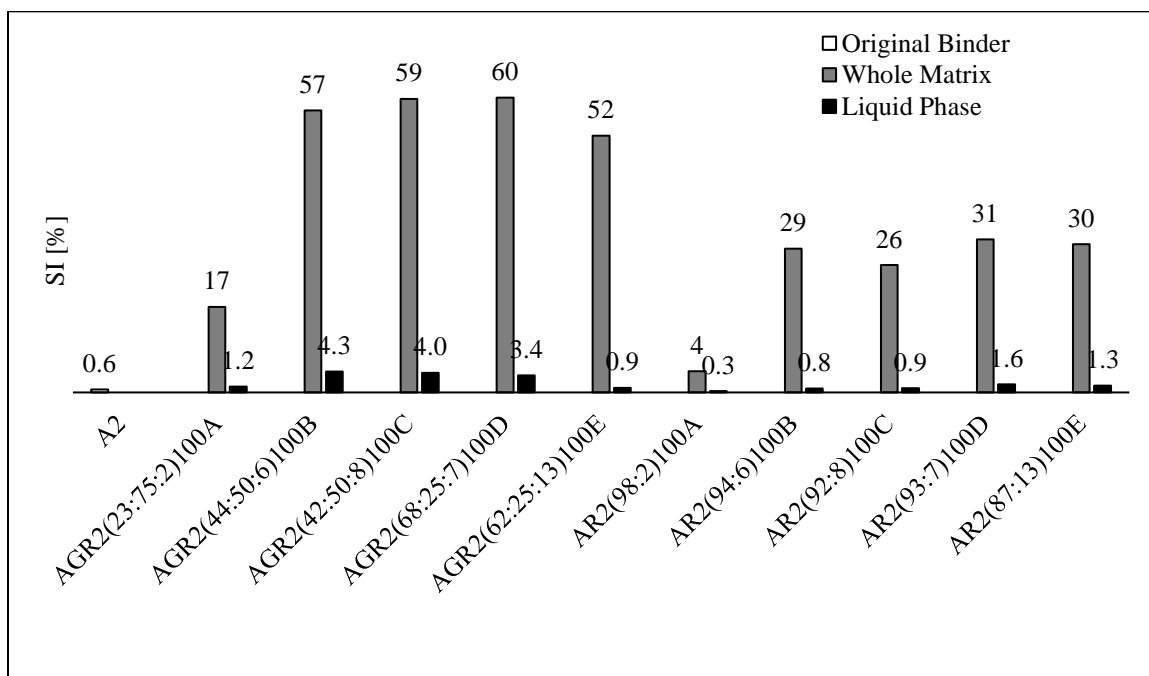
Figure 7.4 Separation Indexes [27].

Table 7.1 presents the single factor ANOVA results to show the statistical significance of the difference between the control asphalt (A2) and each designated binder. The F-statistic results showed a significant difference between the control binder and each designated binder in terms of the whole matrix analysis, either the AGR2 binder or AR2 binder. However, the situation was different in terms of the liquid phase analysis. The AGR2(62:25:13)100E did not provide a significant difference with the control asphalt compared to the other AGR2s (F = 1.034), followed by AGR2(23:75:2)100A (F = 2.710). However, the other three AGR2s showed a relatively higher significant difference, compatible with the fluctuated SI values. On the other hand, a relatively better indication was associated with the AR2s. Each AGR2 binder was statistically compared to its corresponding AR2. The SI statistical analysis showed a significant difference, indicating the negative effect of replacing asphalt by guayule in the AR2 binder in terms of storage stability comparison.

Table 7.1 Single-Factor ANOVA for Control Binder vs. Designated Binders [27].[11]

Control Asphalt (A2) vs.	WM	LP	Control Asphalt (A2) vs.	WM	LP
	F	F		F	F
AGR2(23:75:2)100A	*	2.710	AR2(98:2)100A	*	0.696
AGR2(44:50:6)100B	*	99.846	AR2(94:6)100B	*	0.992
AGR2(42:50:8)100C	*	82.050	AR2(92:8)100C	*	0.563
AGR2(68:25:7)100D	*	60.221	AR2(93:7)100D	*	6.477
AGR2(62:25:13)100E	*	1.034	AR2(87:13)100E	*	6.196

[11] *The F-statistic was relatively higher than the presented values (> 100).

The compatibility of the viscosity and density with the separation tendency was apparent when comparing AGR2(68:25:7)100D to AGR2(62:25:13)100E. The AGR2(68:25:7)100D(LP) and AGR2(62:25:13)100E(LP) viscosities were 132 and 204 cP, respectively (Figure 7.2). Their densities were 1031 and 1039 g/dm^3 (Figure 7.3). These viscosity and density values were compatible with Stoke's law to result in a lower SI for AGR2(62:25:13)100E (52%) compared to 60% for AGR2(68:25:7)100D, as shown in Figure 7.4. Consecutively, a relatively higher CRM concentration caused better storage stability at this level of interactions, which complied with previous research [81, 174]. Furthermore, lower CRM concentration led to lower viscosity of AGR2(44:50:6)100B(LP) compared to AGR2(42:50:8)100C(LP) (117 and 130 cP, respectively). Their density variation was minimal at 1032 and 1033 g/dm^3, respectively. Hence, the SI variation between binder's WMs was slight (57% and 59%, respectively). The AGR2(23:75:2)100A could not be located in this kind of comparison since it contained the lowest CRM concentration (2.3% by wt. of blend). This minimal concentration resulted in relatively better storage stability of the WM (lower SI, 17%) since the mechanical property variation between the top and bottom fractions was not high. More analyses by master curve, TGA, and FTIR tools were provided in the following subsections to support the resultant storage stabilities.

7.3. MASTER CURVES

Figure 7.5 shows that the "almost identical" label was attributed to the top and bottom portions of liquid phases in addition to the top portion of the whole matrix. Consecutively, two outputs could be derived: (1) almost no CRM residue in (WM)T, which

was compatible with the literature [173], and (2) no liquid phase separation. It might be observed that the bottom portion of the whole matrix significantly had a higher master curve trend due to the high saturation of CRM residue that settled down during the separation tendency test duration, as verified by the statistical analysis hereafter. Consecutively, one may observe that the SI of the liquid phase was very small complied with the closeness of master curves of liquid-phase top and bottom portions. On the other hand, the significantly different SI values were only associated with the whole-matrix top and bottom portions, verified by the high variation of their master curves. Most AGR2 WM bottoms provided the so-called ascending sag curve that was distinguished with better performance than others at low frequencies [26]. This curve could be described by the left-portion trend, whereas the AGR2 WM bottoms were divided into two trends (Left-Portion Trend and Right-Portion Trend, illustrated in Figure 7.5c). This distinct trend was initially attributed to guayule, as discussed in Subsection 5.4 [102]. Nevertheless, the right-portion trend of AGR2 WM bottoms provided an asphalt-like (parallel) trend (Figure 7.5a-e). Figure 7.5e was unique in its trends of AGR2(23:75:2)100A fractions. All trends were close to each other, as the overall CRM% was 2.3%. Despite the almost identical trends of AGR2(23:75:2)100A [(LP)T, (LP)B, and (WM)T], the corresponding AR2 – AR(98:2)100A – was not the same. The AGR2(23:75:2)100A [(LP)T and (LP)B] provided identical trends, but the AGR2(23:75:2)100A(WM)T was close to the AGR2(23:75:2)100A(WM)B, again due to little CRM concentration. Overall, the investigation revealed a potential of no liquid phase separation but a significant storage instability, as CRM residue was mainly concentrated at the bottom.
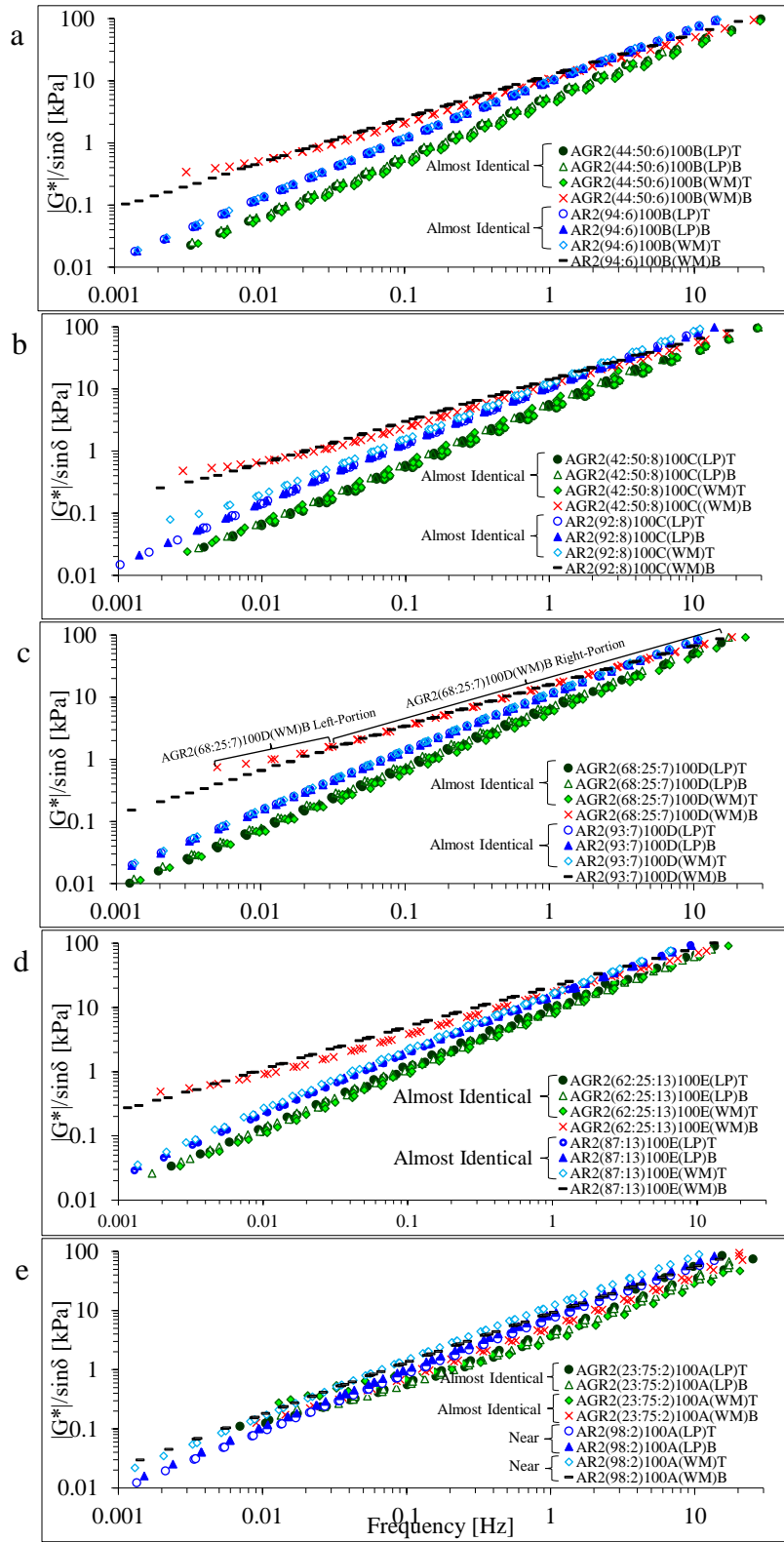
Figure 7.5 |G*|/sinδ Master Curves of Designated AGR2s vs. AR2s (a–e) [27].

The statistical analysis of master curves was established based on the logarithmic transformation of $|G^*|/\sin\delta$ values to minimize the significant variation between small and large values at different frequencies. As shown in Table 7.2, the F-statistic was evaluated for master curves of (LP)T, (LP)B, and (WM)T of each designated binder, and also for (WM)T and (WM)B. The F-statistic verified no significant difference among (LP)T, (LP)B, and (WM)T. However, the F-statistic showed a significant difference between (WM)T and (WM)B, particularly for AGR2s against AR2s. It was also observed the no-significant difference for (LP)T and (LP)B of AGR2(23:75:2)100A and AR2(98:2)100A (0.016 and 0.217, respectively).

Table 7.2 Single-Factor ANOVA for Master Curve Statistical Analysis [27].[12]

Binder	Compared Fractions	F	Compared Fractions	F
AGR2(23:75:2)100A*	(LP)T; (LP)B; (WM)T	0.056	(WM)T; (WM)B	0.053
AR2(98:2)100A**	(LP)T; (LP)B;(WM)T	0.900	(WM)T; (WM)B	0.207
AGR2(44:50:6)100B	(LP)T; (LP)B; (WM)T	0.069	(WM)T; (WM)B	12.693
AR2(94:6)100B	(LP)T; (LP)B; (WM)T	0.004	(WM)T; (WM)B	2.117
AGR2(42:50:8)100C	(LP)T; (LP)B; (WM)T	0.018	(WM)T; (WM)B	12.982
AR2(92:8)100C	(LP)T; (LP)B; (WM)T	0.184	(WM)T; (WM)B	1.549
AGR2(68:25:7)100D	(LP)T; (LP)B; (WM)T	0.109	(WM)T; (WM)B	17.741
AR2(93:7)100D	(LP)T; (LP)B; (WM)T	0.008	(WM)T; (WM)B	3.404
AGR2(62:25:13)100E	(LP)T; (LP)B; (WM)T	0.064	(WM)T; (WM)B	10.411
AR2(87:13)100E	(LP)T; (LP)B; (WM)T	0.035	(WM)T; (WM)B	3.361

7.4. TGA ANALYSIS

The ramp method was used to study the composition analysis of the as-received and extracted CRMs from AGR2s, as discussed in Subsection 6.2.2. The analysis for the

[12] *F-statistic of AGR2(23:75:2)100A [(LP)T, (LP)B] was found to be 0.016.
**F-statistic of AR2(98:2)100A [(LP)T, (LP)B] was found to be 0.217.

as-received CRM showed 6% oily components, 37% natural rubber, 17% synthetic rubber, and 40% fillers, as shown in Figure 7.6. As shown in Figure 7.6a, the high CRM dissolution of the AGR2(62:25:13)100E binder (40%) verified its introduction of lower SI among the designated AGR2s. It indicated a relatively small radius of the dispersed CRM particle that decreased the sedimentation velocity (i.e., increased storage stability or decreased SI). Furthermore, it provided the lowest concentration of extracted carbon black (reached 30%), which had the highest density among CRM components (1800-2100 g/dm^3) [84]. The binders with high-percent CRM proportions resulted in a higher dissolution such as the AGR2(62:25:13)100E and AGR2(42:50:8)100C binders at 40% 36%, respectively. Decreasing the CRM concentration for the AGR2(44:50:6)100B and AGR2(68:25:7)100D binders yielded 27% and 20%, respectively. As a result, a higher CRM concentration might lead to a higher dissolved portion of CRM in the liquid binder.
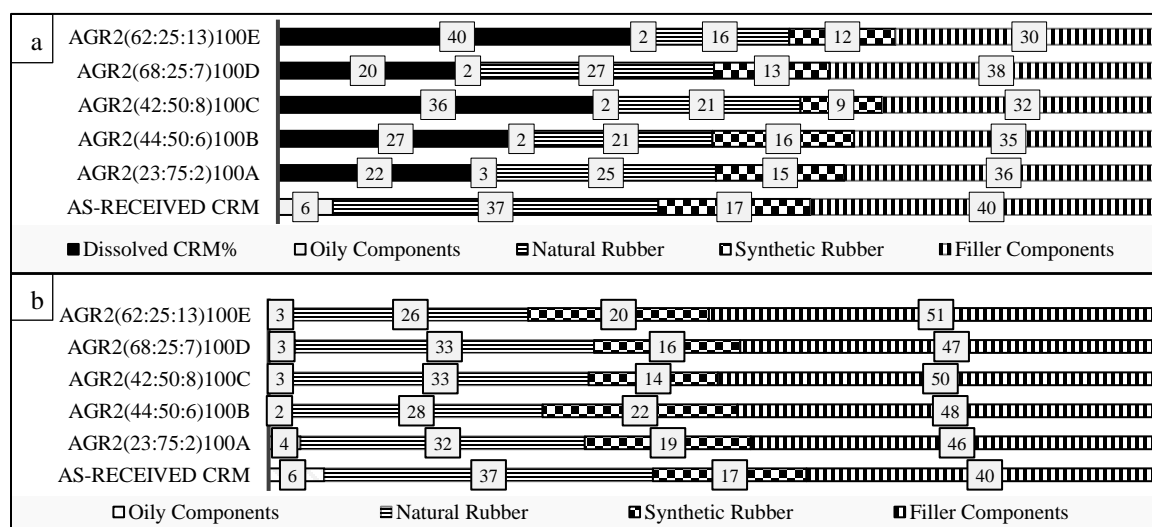
Figure 7.6 As-Received and Extracted CRM Component Proportions by TGA: (a) Four-CRM-Component Plus Dissolved CRM Proportions, and (b) Four CRM Component Proportions [27].

Figure 7.6b depicts the remaining components in the dispersed CRM residue. The remaining components (on average) were as follows: considerable existence of fillers (48%; initially 40%), a significant amount of natural rubber (31%; initially 37%) and synthetic rubber (18%; initially 17%), unlike the oily components that were significantly released (3%; initially 6%). This could justify the overall poor storage stability (high SI) in the case of the WMs that carried this high-density dispersed CRM residue.

On the other hand, TGA was utilized to verify the liquid phase separation analysis of the AGR2(62:25:13)100E binder using the SITG method. The TGA analysis provided a very close decomposition of both top and bottom fractions of the AGR2(62:25:13)100E liquid phases, as shown in Figure 7.7. Such thermal analysis verified almost no liquid phase separation.
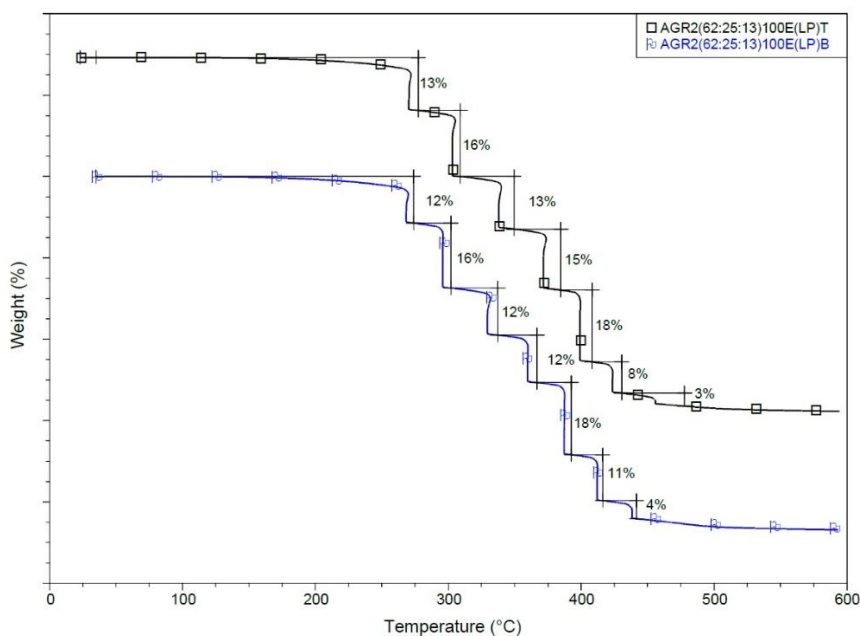
Figure 7.7 SITG Curves of AGR2(62:25:13)100E [(LP)T and (LP)B] in a Temperature Range of the Ambient Temperature through 600℃ and a Heating Rate of 20℃/min [27].

7.5. FTIR ANALYSIS

By comparing the individual blend components (A2, G2, and CRM) spectra (Figure 7.8a-c) to the blend AGR2(62:25:13)100E spectra, no peak shifts or new-formed peaks in AGR2(62:25:13)100E were noticed to recognize a chemical reaction. In other words, with the study limitations, the results show that the A2, G2, and CRM interaction was physical, the same as the AR interaction at specific conditions [77].
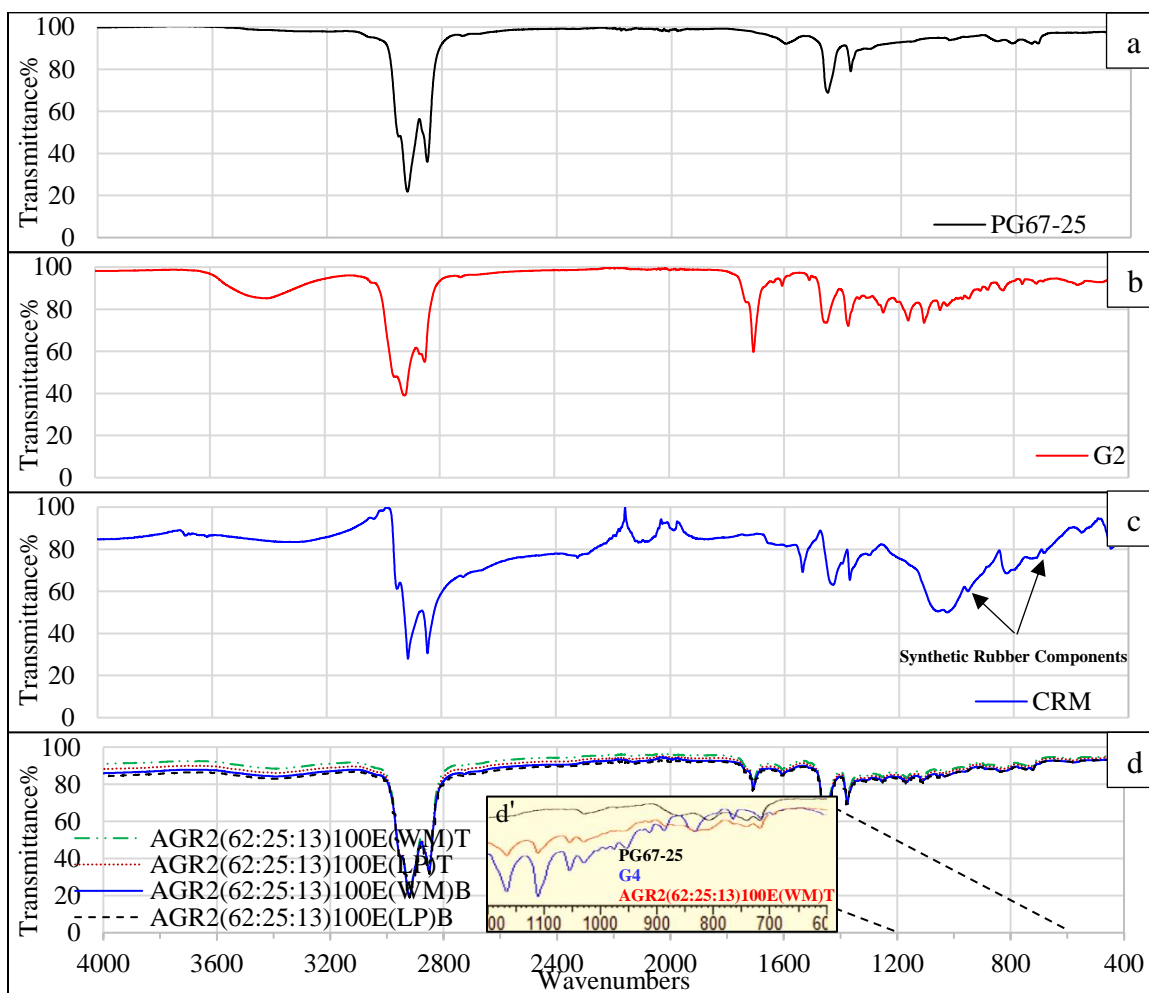
Figure 7.8 FTIR Spectra: (a) A2, (b) G2, (c) CRM, and (d) the Four Fractions of AGR2(62:25:13)100E [(WM)T, (WM)B, (LP)T, and (LP)B] [27].

The comparison among the four AGR2(62:25:13)100E fractions [(WM)T, (WM)B, (LP)T, and (LP)B] depicted no differences in chemical composition. Such comparison showed similar constituents and verified that almost no liquid phase separation occurred to AGR2(62:25:13)100E according to their almost identical spectra, as shown in Figure 7.8d.

The AR FTIR spectra investigation in the literature has indicated a release of dissolved CRM components (e.g., synthetic rubber components) in liquid asphalt [57, 64, 77]. This dissolution was observed at wavenumbers around 696 and 966 cm^{-1}, which denoted the carbon-hydrogen out-of-plane bending of monoalkylated aromatics in polystyrene and trans-alkene in polybutadiene, respectively [64, 77]. These two peaks were formed in the AGR2(62:25:13)100E fractions. However, these peaks were also noticed in the G2 spectrum (Figure 7.8b). These peaks might indicate rubber components of low-molecular weight in guayule, but the potential of CRM components release also exists since the TGA analysis verified CRM dissolution.

For brevity, one can observe in Figure 7.8d' that the intensity of the peaks in AGR2(62:25:13)100E(WM)T was remarkably lower than the corresponding ones in G2 between wavenumbers 890–1150 cm^{-1}. This intensity was due to the low concentration of guayule in the AGR2 blend. Nevertheless, some peaks in this wavenumber range seemed to be disappeared. As mentioned in the literature, this disappearance may occur due to the lightweight components resulting in the CRM swelling [14, 175].

7.6. SUMMARY

The argumentation presented in this subsection aimed to investigate the influence of guayule on the novel binder's separation tendency (whole matrix storage stability and

liquid phase separation). Five designated AGR2s vs. their corresponding AR2s (same CRM concentration and same scenario of interactions) were investigated as whole matrices and liquid phases. The AGR2s presented poor storage stability compared to the AR2s on the whole matrix scale. However, the liquid phase scale showed a low separation tendency for both AGR2s and AR2s, reflecting almost no liquid phase separation as proven by identical master curve trends of top and bottom fractions (acquired by the lab-simulated storage). Likewise, the SITG analysis showed similar thermal stability between the top and bottom fractions of the liquid binder. The FTIR analysis also showed identical spectra of the top and bottom fractions, verifying almost no liquid phase separation. According to Stoke's law, the poor storage stability attributed to the whole-matrix AGR2s were analyzed by (1) liquid-medium viscosity (η), (2) density difference between liquid medium and dispersed particles ($\Delta\rho$), and (3) dispersed CRM particle residue radius (a). The crucial parameter that affected storage stability was the viscosity variance between control asphalt and guayule (i.e., a little-to-no influence of $\Delta\rho$ or dissolved CRM).

8. MIXTURE PERFORMANCE ASSESSMENT: VALIDATION

This section implies a reproduction of results published in [90].[13] Based on the literature, the guayule-based binder could not be fully assessed without investigating its behavior in the binder-aggregate mixture. Therefore, this section aimed to evaluate the behavior of previously established guayule-based binders in the mixture by carrying out commonly used asphalt mixture tests. Five mixtures were designated. As interpreted in Subsection 3.4.2, the tests involved assessments of the major distresses encountering flexible pavement as follows: moisture susceptibility, rutting resistance, fatigue cracking resistance, and thermal cracking resistance. The modified Lottman test was used to evaluate moisture susceptibility. The rut test using APA was employed to assess rutting resistance. Additionally, the HWT test was used to evaluate both moisture susceptibility and rutting potential simultaneously. Fatigue cracking and thermal cracking resistances were evaluated by the fracture energy mechanism employing the SCB and DCT tests, respectively. Therefore, the applicability of guayule in the flexible pavement mixture could be initiated. Hence, guayule-based mixtures' enhancements could be founded in the future.

8.1. MOISTURE SUSCEPTIBILITY

Figure 8.1 illustrates the TSR results. The G2-Mix resulted in a dramatically low TSR (40%). Conversely, A2-Mix resulted in an 82% TSR at the same mixture parameters,

---

[13] Submitted paper to Journal of Materials in Civil Engineering, Ahmed Hemida, Magdy Abdelrahman, Performance Assessment of Bio-Asphalt Mixtures Containing Guayule Resin as an Innovative Bio-Based Asphalt Alternative, With permission from ASCE (2022).

indicating potentially significant moisture damage to the G2-Mix at a 7% V_a level. Using guayule as a 100% asphalt alternative in the mixture would require mix parameter changes according to the standard (TSR) test criteria such as P_b, anti-stripping agent addition parameters (out of the scope) and/or V_a. For instance, changing V_a to 3.5% changed the TSR of G2-Mix to 71%, indicating a significant moisture-resisting enhancement to the pure guayule mix. Additionally, the CRM concentration gradually increased the moisture damage resistance. For instance, adding 25% CRM to guayule in GR2(75:25)100-Mix changed the TSR from 40% to 73% at the same V_a (7%). The AGR2(62:25:13)100E-Mix provided enhanced TSR values at 7% V_a and 3.5% V_a (86% and 96%, respectively).
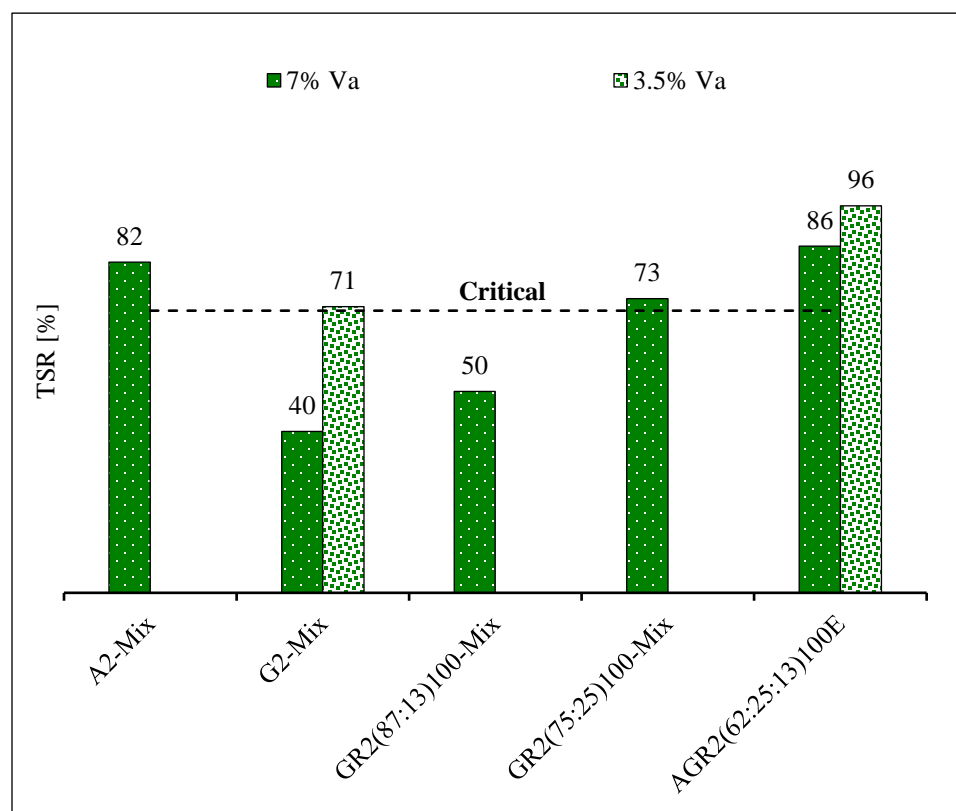
Figure 8.1 Moisture Susceptibility (TSR) Results from the Modified Lottman Test [90].

8.2. RUTTING SUSCEPTIBILITY

The standard PG-HTs of A2-Mix, AGR2(62:25:13)100E-Mix, and GR2(75:25)100-Mix were 64℃, 70℃, and 64℃, respectively. Nevertheless, to compare the novel binders' behaviors in the mixture to the A2-Mix, rut depths were addressed at a 64℃ test temperature. On the other hand, G2-Mix and GR2(87:13)100-Mix were compared at a 58℃ test temperature because they had the same standard PG-HT (58℃).

As shown in Figure 8.2a, the results showed that the rut depth trend was minor with GR2(75:25)100-Mix, followed by AGR2(62:25:13)100E-Mix, then A2-Mix. Compared to the measured binder performance at high temperatures, the rut test revealed that the GR2(75:25)100-Mix had a significantly lower rut depth (0.4 mm), thereby indicating that the GR2(75:25)100-Mix could provide a high enhancement to the rutting resistance more than what was expected according to the binder performance Superpave criteria. As expected, AGR2(62:25:13)100E-Mix presented a better performance than A2-Mix because AGR2(62:25:13)100E had a 70℃ standard PG-HT, whereas A2-Mix had a 64℃ standard PG-HT. Ultimately, the three mixtures provided undoubtedly excellent resistance to rutting.

As shown in Figure 8.2b, G2-Mix provided an acceptable rut depth at a 58℃ test temperature, which was compatible with the binder's rheological performance. The maximum rut depth associated reached 6.4 mm. At the same test temperature (58℃), GR2(87:13)100-Mix provided an enhanced rutting resistance (rut depth = 2.3 mm) compared to G2-Mix, indicating the enhancement associated with the CRM addition to the

pure guayule at high temperatures. In all studied cases, the rut depth went lower than the limits recommended by many DOTs [176].
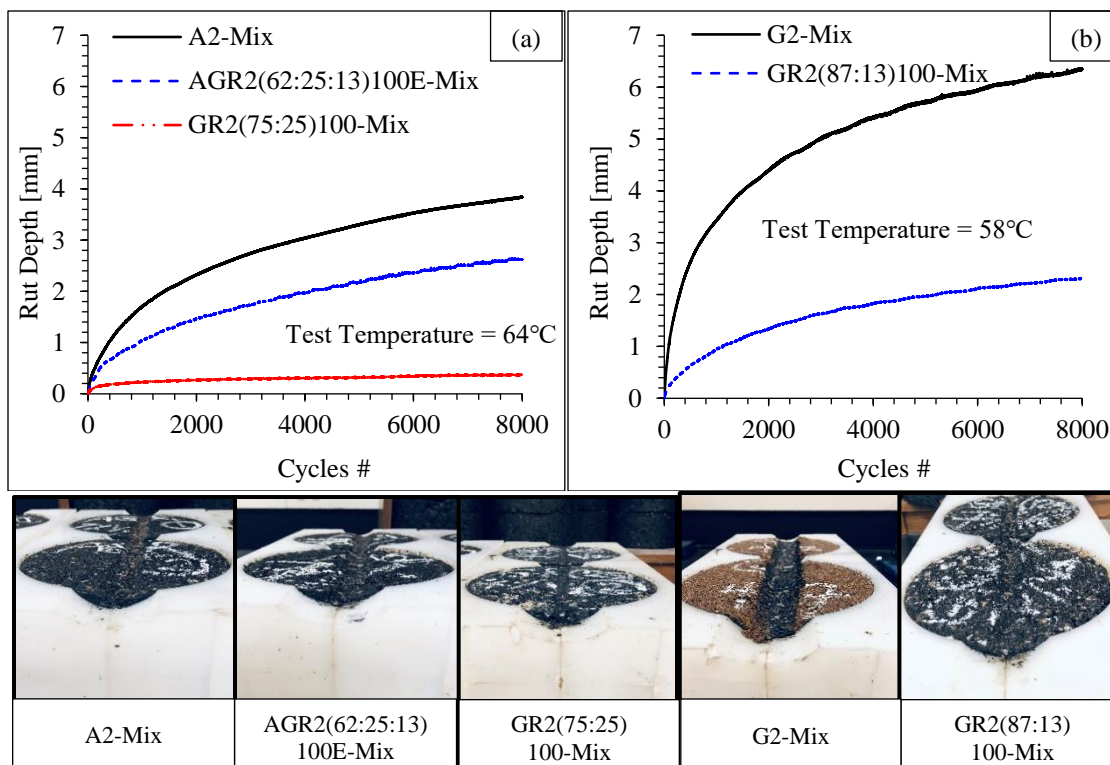
Figure 8.2 Rut Test Results: (a) A2-Mix, AGR2(62:25:13)100E-Mix, and GR2(75:25)100-Mix at a 64℃ Test Temperature, and (b) G2-Mix and GR2(87:13)100-Mix at a 58℃ Test Temperature; Associated with the Specimens' Appearances after 8,000 cycles [90].

8.3. HWT

Figure 8.3 illustrates the designated mixtures' performances using the HWT test. Most mixtures were tested at two different air contents: 4% V_a and 6% V_a. Generally, the designated mixtures behaved perfectly despite their exposure to severe environmental and load parameters. In addition, the stripping inflection point was not reached for all

designated mixtures, indicating no moisture damage (stripping) potential at this level of testing. Due to the binder performance outcomes described in Subsection 3.4.1.1, G2-Mix and GR2(87:13)100-Mix were tested at 45℃ test temperature, whereas A2-Mix, AGR2(62:25:13)100E-Mix, and GR2(75:25)100-Mix were tested at 50℃ test temperature. The G2-HMA exhibited an outstanding performance after 10,000 passes (in agreement with CP-L 5112) and after the extended 20,000 passes, as shown in Figure 8.3a. The rut depth decreased when modifying guayule by CRM in GR2(87:13)100-Mix. As expected, the evolution of V_a slightly increased the rut depth, as observed from the difference between GR2(87:13)100-Mix [4%V_a] and GR2(87:13)100-Mix [6%V_a].

At 64℃ test temperature, A2-Mix, AGR2(62:25:13)100E-Mix, and GR2(75:25)100-Mix were HWT tested. These mixtures were not exposed to stripping at this level of testing as their stripping inflection points were not reached. The results revealed that all mixtures passed the HWT test with respect to all checked standards/specifications after either 10,000 or 20,000 passes, as shown in Figure 8.3b. Figure 8.3c shows the appearance of some core specimens after 20,000 passes. When comparing A2-Mix [4%V_a] to A2-Mix [6%V_a], the rut depth noticeably changed due to the V_a parameter change. The GR2(75:25)100-Mix at the two levels of air contents (4% and 6%) resulted in slight changes in rut depths at 10,000 and 20,000 passes. The AGR2(62:25:13)100E-mix presented an enhanced moisture resistance compared to A2-Mix. Therefore, the three designated mixtures' performances against moisture damage were ranked in descending order: GR2(75:25)100-Mix, AGR2(62:25:13)100E-Mix, then A2-Mix, which agree with the rut test outcomes mentioned above in Subsection 8.2.
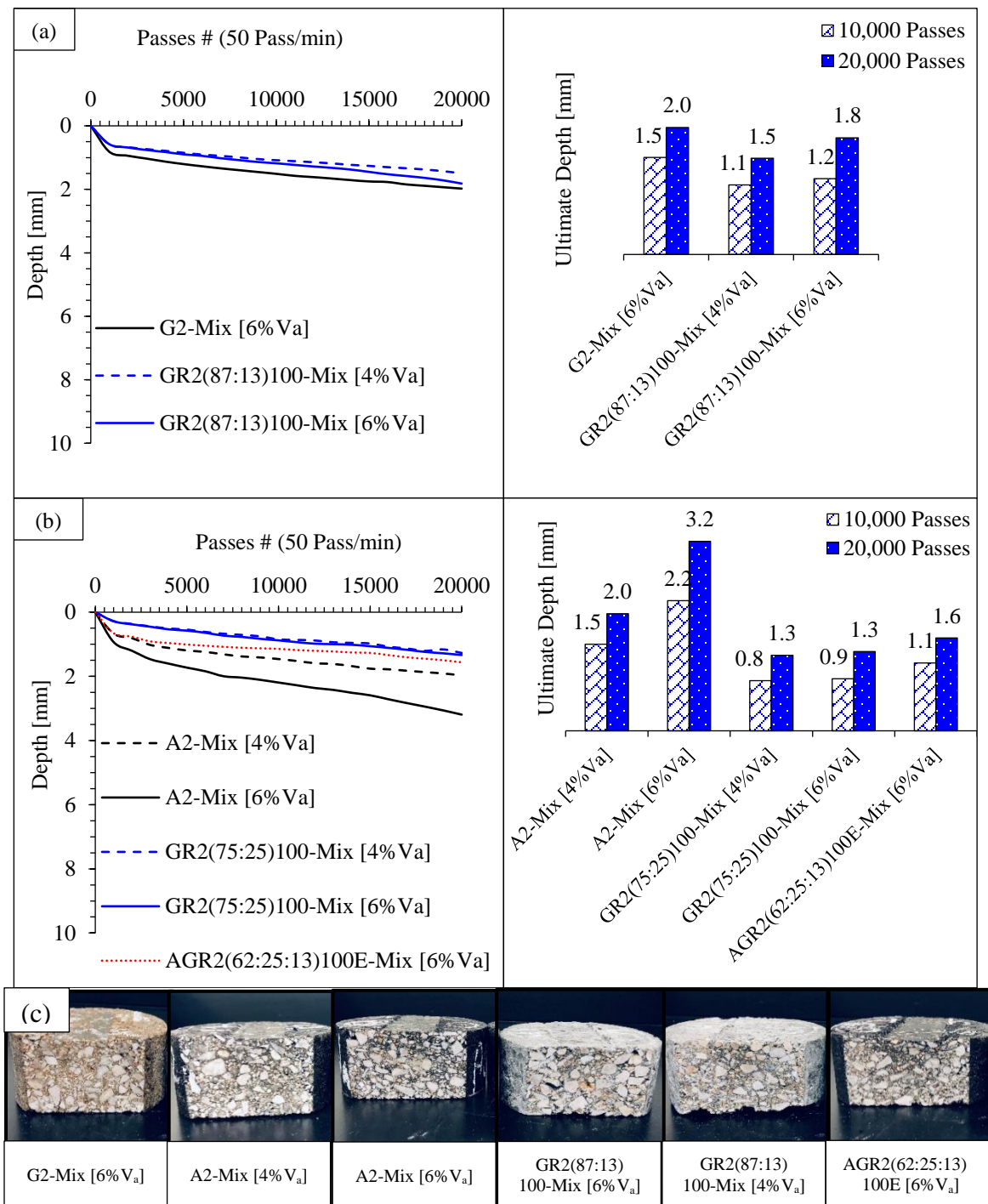
Figure 8.3 HWT Test Results: (a) G2-Mix and GR2(87:13)100-Mix at a 45℃ Test Temperature, (b) A2-Mix, GR2(75:25)100-Mix, and AGR2(62:25:13)100E-Mix at 50℃ Test Temperature, and (c) Some Specimens' Appearances after 20,000 Passes [90].

8.4. MIXTURE PERFORMANCE AT INTERMEDIATE TEMPERATURE

Figure 8.4 illustrates the strain energy vs. notch depth charts of the designated mixtures in linear regression to acquire the resultant slope (dU/da) and J_c values. The steeper the slope, the tougher the material [159]. Figure 8.4a demonstrates comparable A2-Mix and AGR2(62:25:13)100E-Mix slope values. Further, it demonstrates comparable G2-Mix, GR2(87:13)100-Mix, and GR2(75:25)100-Mix slope values. In Figure 8.4b, the J_c of A2-Mix resulted in 0.46 kJ/m^2. This value was considered the control J_c value to assess the novel guayule-based mixtures. The AGR2(62:25:13)100E-Mix yielded a 0.48 kJ/m^2 J_c. This value indicated the predicted applicability (or harmony) between asphalt, guayule, and CRM in the mixture against fatigue fracture resistance. Additionally, this application explained the excessive compensation of conventional asphalt performance by CRM and guayule at this level of testing and material parameters. The G2-Mix yielded a 0.66 kJ/m^2 J_c, which contrasted with the binder's intermediate-temperature performance assessment, but it was in agreement with the SCB testing background [156, 158, 161]. The control asphalt presented a better performance at intermediate temperatures (i.e., the control asphalt possessed a lower PG-IT) than the pure guayule. The 0.66-kJ/m^2 J_c value demonstrated the G2-Mix's high fatigue fracture resistance compared to the A2-Mix, which was better than expected. The GR2 mixtures produced comparable mix performances to the G2-Mix against fatigue fracture, 0.65 kJ/m^2 for GR2(87:13)100-Mix and 0.69 kJ/m^2 for GR2(75:25)100-Mix. This could be an initial indication of the effect of CRM concentration increase/decrease on the fatigue fracture resistance of GR2 mixtures. This exact point is in compliance with the rheological analysis presented in Section 4,

which revealed that CRM did not enhance guayule performance at intermediate temperatures.
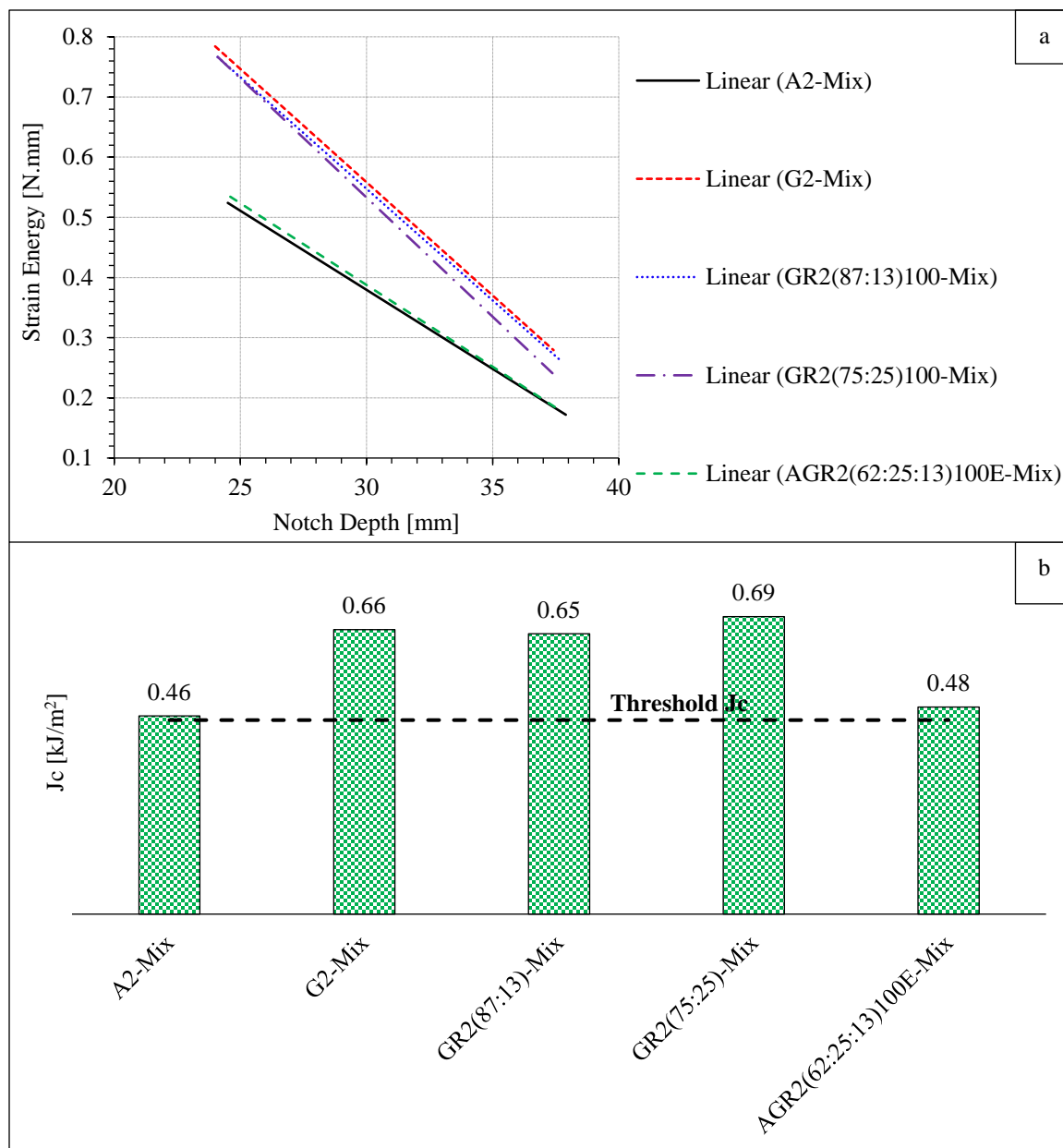
Figure 8.4 SCB Test Results: (a) Rate of Change of Strain Energy per Notch Depth, Strain Energy-Notch Depth Slope (dU/da), and (b) Critical Strain Energy Release Rate (J_c) [90].

The positive impact of the guayule-based mixtures regarding the fracture resistance reflected the great fracture toughness of partial or full asphalt replacement by guayule. Guayule presented a better performance in the mixture than the control asphalt. The reason for that might be the ignorance of fracture toughness assessment regarding binders. The guayule-based mixture offered a steeper absolute value of the slope (dU/da) (i.e., a higher rate of change of strain energy per notch depth, which indicated a tougher material at this level of testing) compared to that of the asphalt-based mixtures (A2-Mix and AGR2(62:25:13)100E-Mix) [159].

8.5. MIXTURE PERFORMANCE AT LOW TEMPERATURE

Figure 8.5a shows an example of a G2-Mix specimen before and after the DCT test. Figure 8.5b illustrates the fracture energy (G_f) of the designated mixtures at 10℃ greater than the standard PG-LT. The mixtures were exposed to other low temperatures to monitor the differences in their behaviors. Results showed that the control asphalt mixture yielded a G_f value of 429 J/m^2 at a -12℃ test temperature, which passed the threshold value established in the literature [165]. The pure guayule mixture or its modification by CRM did not improve the low-temperature cracking resistance. According to the Superpave criteria, binder investigations revealed the destructive behaviors of guayule binders at low temperatures, but not to the extent shown by the mixture outcomes. The threshold G_f value (400 J/m^2) was not reached for any of the tested designated guayule-based mixtures [G2-Mix, GR2(87:13)100-Mix, or GR2(75:25)100-Mix] at 6℃ or 0℃ test temperatures. This could indicate the difficulty of using guayule (as a 100% asphalt alternative) with or

without CRM, regarding the assigned material and interaction parameters, to resist the potential thermal cracking, indicating a worse low-temperature performance than predicted by the binder investigations presented in Section 4.
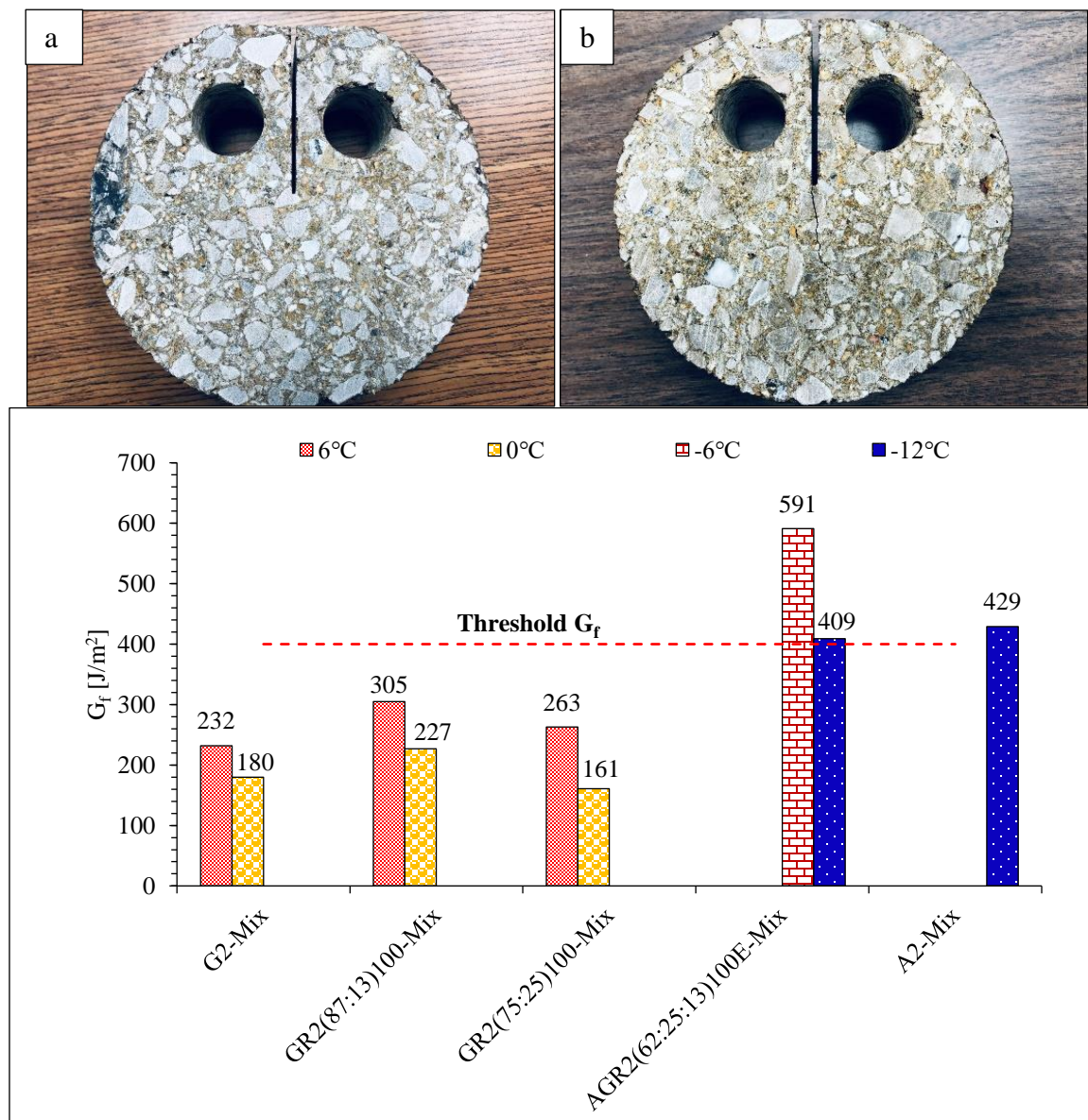
Figure 8.5 DCT Test: (a) Example of a G2-Mix before and after Fracture, and (b) Fracture Energy (G_f) Results [90].

The AGR2(62:25:13)100E-Mix, which had a standard PG-LT of -16℃, remarkably provided an excellent fracture resistance at the corresponding test temperature (-6℃), 591 J/m^2. The same mixture was also exposed to a -12℃ to monitor its performance at that low test temperature. The results of AGR2(62:25:13)100E-Mix positively ended with a G_f value of 409 J/m^2, indicating a potentially accepted mixture at a standard PG-LT of -22℃.

8.6. SUMMARY

This section provided an evaluation of designated guayule-based mixtures against major distresses: moisture damage, rutting, fatigue cracking, and thermal cracking. In Table 8.1, a summary of the major data acquired through this section is reported to summarize the input parameters (test temperature and air content) and end result parameters (TSR, rut depth (by APA), HWT rut depth, J_c, and G_f). The following observations were made. Guayule was worse than asphalt resisting moisture damage through the standard (TSR) test. By contrast, guayule-based mixtures presented a high resistance to moisture damage evaluated by the HWT test, and it was more reliable to address the field performance. The pure guayule mixture had a high resistance to rutting at its high-temperature performance grade. Guayule modification using CRM and partial asphalt replacement by guayule and CRM enhanced the rutting resistance. This was compatible with the binder performance evaluated by the Superpave criteria in Section 4. Changing parameters (e.g., CRM addition and guayule's partial replacement by asphalt and rubber) enhanced the guayule-based mixture's resistances to rutting and moisture damage resulting in acceptable performances by TSR, rut, and HWT tests. The positive impacts of

the guayule-based binders in mixtures regarding the fracture resistance at the intermediate temperature reflected the great fracture toughness of partial or full asphalt replacements by guayule. Guayule offered better performance in the mixture than the control asphalt due to the unavailability of the fracture toughness criterion in binder evaluation by the Superpave criteria. Compared to the control asphalt mixture, the guayule-based mixture presented a higher rate of change of strain energy per notch depth (slope), which indicated a tougher material. Guayule (with or without CRM modification) did not offer the desired performance at low temperatures. This could indicate the difficulty of using guayule (as a 100% asphalt substitute) to resist the potential thermal cracking, thus indicating an unexpectedly inferior low-temperature performance based on the Superpave's binder evaluation criteria. However, partial asphalt replacement by guayule and CRM resisted the thermal fracture greatly.

Table 8.1 Mixture Performance Assessment Summary Outcomes [90].

Mixture	Parameter(s)	TSR Test		Rut Test (APA)	HWT Test				SCB Test	DCT Test			
A2-Mix	T [°C]	25		64	50				25	6	0	-6	-12
	Va [%]	7±0.5%	N/A	7±0.5%	4%		6%		7±0.5%	7±0.5%			
	Outcomes	TSR: 82%	N/A	RD: 3.8 mm	10,000 Passes	20,000 Passes	10,000 Passes	20,000 Passes	Jc: 0.46 J/m2	N/A	N/A	N/A	Gf: 429 J/m2
					RD: 1.5 mm	RD: 2 mm	RD: 2.2 mm	RD: 3.2 mm					
G2-Mix	T [°C]	25		58	45				25	6	0	-6	-12
	Va [%]	7±0.5%	3.50%	7±0.5%	4%		6%		7±0.5%	7±0.5%			
	Outcomes	TSR: 40%	TSR: 71%	RD: 6.3 mm	10,000 Passes	20,000 Passes	10,000 Passes	20,000 Passes	Jc: 0.66 J/m2	Gf: 232 J/m2	Gf: 180 J/m2	N/A	N/A
					N/A	N/A	RD: 1.5 mm	RD: 2.0 mm					
AGR2(62:25:13) 100E-Mix	T [°C]	25		64	50				25	6	0	-6	-12
	Va [%]	7±0.5%	3.50%	7±0.5%	4%		6%		7±0.5%	7±0.5%			
	Outcomes	TSR: 86%	TSR: 96%	RD: 2.6 mm	10,000 Passes	20,000 Passes	10,000 Passes	20,000 Passes	Jc: 0.48 J/m2	N/A	N/A	Gf: 591 J/m2	Gf: 409 J/m2
					N/A	N/A	RD: 1.1 mm	RD: 1.6 mm					
GR2(87:13)100-Mix	T [°C]	25		58	45				25	6	0	-6	-12
	Va [%]	7±0.5%		7±0.5%	4%		6%		7±0.5%	7±0.5%			
	Outcomes	TSR: 50%	N/A	RD: 2.3 mm	10,000 Passes	20,000 Passes	10,000 Passes	20,000 Passes	Jc: 0.65 J/m2	Gf: 305 J/m2	Gf: 227 J/m2	N/A	N/A
					RD: 1.1 mm	RD: 1.5 mm	RD: 1.2 mm	RD: 1.8 mm					
GR2(75:25)100-Mix	T [°C]	25		64	50				25	6	0	-6	-12
	Va [%]	7±0.5%		7±0.5%	4%		6%		7±0.5%	7±0.5%			
	Outcomes	TSR: 73%	N/A	RD: 0.4 mm	10,000 Passes	20,000 Passes	10,000 Passes	20,000 Passes	Jc: 0.69 J/m2	Gf: 263 J/m2	Gf: 161 J/m2	N/A	N/A
					RD: 0.8 mm	RD: 1.3 mm	RD: 0.9 mm	RD: 1.3 mm					

*N/A: not available; RD: Rut Depth; T: Test Temperature; V_a: Air Content.

9. CONCLUSIONS AND RECOMMENDATIONS

This study aimed to present guayule resin (guayule) as an innovative bio-based asphalt alternative in part and in full for sustainable, flexible pavement development. The CRM was used as an asphalt modifier/enhancer. The designated binders involved control asphalts, virgin guayules, as well as asphalt-guayule, asphalt-rubber, guayule-rubber, and asphalt-guayule-rubber blends. Assessments were established according to Superpave criteria and advanced rheological tests, in addition to component analysis to link the macroscale level to the microscale level. To validate the novel binder, satisfying mix performance tests were conducted.

9.1. CONCLUSIONS

9.1.1. Viscosity. Guayule had a much lower viscosity than asphalt at the same high-temperature grade, indicating savings in plant energy consumption and environmental emissions.

9.1.2. Rutting Resistance. According to Superpave criteria at high temperatures, the heat treatment process revealed considerable growth in stiffness of guayule due to potential removal of moisture and light molecular weight components in the as-received guayules. Guayule had little-to-no change in elasticity either before vs. after RTFO aging or as-received vs. heat-treated guayules. The CRM raised guayule stiffness and elasticity, reflected in a higher rutting resistance. The CRM in the asphalt-guayule-rubber blend also enhanced the blend stiffness and elasticity compared to either individual asphalt, individual guayule, or asphalt-guayule blend. Pure guayule presented unconventional master-curve

trends, which provided better behavior than conventional asphalt at low frequencies in terms of G′, G″, and δ, thus |G*|/sinδ. Accordingly, this might be beneficial in low-speed applications. Guayule also presented an unconventional δ master-curve trend contrary to the control asphalt trend. This δ trend was desired in the asphalt industry as it provided higher elastic behavior at lower traffic speeds. A formation of a 3D network structure was attributed to asphalt-rubber-guayule binders, unlike asphalt, using the interrupted shear flow technique, which reflected the CRM polymeric components' release in the binder's liquid phase.

9.1.3. Fatigue Cracking Resistance. According to Superpave criteria at intermediate temperatures, in compliance with high-temperature analysis, guayule had lower elastic behavior than the conventional asphalt at the same intermediate temperatures. Even though control asphalts were relatively stiffer than guayules at high temperatures, guayules provided higher stiffnesses at intermediate temperatures, followed by lower resistance to fatigue cracking. The CRM slightly changed guayule stiffness and elasticity (almost no change in resisting fatigue compared to neat guayule). Nevertheless, this concept showed a contrary trend to the mix assessment argumentation. The CRM decreased asphalt stiffness and increased guayule stiffness, so its effect on the asphalt-guayule blend mainly depended on the material concentrations.

9.1.4. Thermal Cracking Resistance. According to Superpave criteria at low temperatures, CRM offered little-to-no change in the performance of guayule-rubber blends. The control asphalts had significantly lower critical temperatures than guayules;

thus, higher asphalt concentration in guayule-based binders yielded enhanced low-temperature performances.

Premature thermal cracking could take place with the wide-ranged negative ΔT_c values. Accordingly, this trend was attributed to asphalt-rubber binders. Conversely, guayule-based binders offered low-ranged negative ΔT_c values. The higher the guayule concentration in the blend, the lower-ranged negative the ΔT_c parameter, indicating the guayule's low susceptibility to premature thermal cracking at its low-temperature grade, unlike asphalt or asphalt-rubber binders.

9.1.5. Aging Susceptibility. Dependency on a high concentration of guayule in the binder blend would lead to insufficient fatigue and thermal-cracking resistances compared to control asphalts. This was due to the aging mechanism of guayule and the high oxidation bonding in virgin guayules that had negative influences on long-term distress resistances. The high oxidation bonding in the as-received guayules caused premature oxidative aging, negatively affecting the guayule-based binders' intermediate- and low-temperature grades.

The CRM dissolution mechanism was different when comparing asphalt to guayule. At the same interaction parameters, the release of polymeric components was more evident in asphalt than guayule. The laboratory aging processes did not observably change the released polymeric components' intensities from CRM to the liquid binder in the cases of asphalt-rubber and asphalt-guayule-rubber blends (asphalt-involved binders). By contrast, the influence of laboratory aging appeared in the guayule-rubber blend, particularly the release of the trans component in polybutadiene. Nevertheless, the migrations of polymeric components were more harmonious with asphalt than guayule at

the same interaction parameters. This might be the reason behind enhancing the rheological properties of asphalt compared to guayule.

9.1.6. Applicable Superpave Grades. Overall, guayule-based binders provided competitive performances to that of the control asphalts. For instance, regarding soft binders, the closest Superpave grade to the control asphalt (PG57-29) was observed using a blend of 68.2% asphalt, 22.8% guayule, and 9.1% CRM (PG60-28), and a blend of 41.65% asphalt, 41.65% guayule, and 16.7% CRM (PG61-26). On the other hand, regarding stiff binders, guayule provided binders with higher rutting resistances but lower thermal cracking resistances than that of the control asphalt (PG67-25) such as a blend of 62.5% asphalt, 25% guayule, and 12.5% CRM (PG73-16).

9.1.7. Component Analysis. According to FTIR analysis, the study confirmed the distinct carbon and hydrogen compositional elements of guayule. Asphalt and guayule had similarities in component composition and rheological behavior with temperature susceptibility. No new peak or peak shift was observed for the asphalt-guayule blend. This kind of blending indicated a physical blending with no chemical reaction. Since asphalt did not have the exact compositional structure of guayule, the rheological enhancements of the asphalt-guayule-rubber blend were not the same as the asphalt-rubber blend, which were better for the asphalt-rubber blend. The distinct decrease in peak intensities was associated with the highest CRM concentration, verified by the highest CRM dissolution. A new peak formed around 1718 cm^{-1} in CRM residue in rubber-involved binders. Such a peak formation could indicate CRM swelling due to some liquid binder constituents (asphalt/guayule) diffusion into CRM residue. Depolymerization occurred, resulting in a

partial migration of CRM polymeric components (e.g., polystyrene and polybutadiene) to the liquid binder of either asphalt-guayule-rubber or asphalt-rubber blends. This was reflected in the enhanced performance of asphalt-guayule-rubber blends at high temperatures. Due to the strong oxidation bonding chains attributed to guayule, particularly carbonyl bond, the oxidative aging negatively affected the guayule-based binder performance negatively reflected on the long-term aging distresses.

9.1.8. Separation Tendency. The study showed the asphalt-guayule homogeneity with no phase separation or guayule coagulation. Asphalt-guayule-rubber blends presented storage instability than asphalt-rubber blends on the whole-matrix scale. However, the liquid-phase scale showed a low separation index for both asphalt-guayule-rubber blends and asphalt-rubber blends, reflecting almost no liquid phase separation, as proven by identical master curve trends of top and bottom fractions. Likewise, the SITG analysis showed similar thermal stability between the top and bottom fractions of the liquid binder. The FTIR analysis also showed identical spectra of the top and bottom fractions, verifying almost no liquid phase separation. According to Stoke's law, the crucial parameter affecting storage stability of the whole-matrix asphalt-guayule-rubber blends was the viscosity variance between asphalt and guayule (i.e., a little-to-no influence of $\Delta\rho$ or dissolved CRM).

9.1.9. Mixture Performance Assessment. From the perspective of the performance assessment of binder-aggregate mixture, moisture damage, rutting, fatigue cracking, and thermal cracking were assessed. The following observations were made based on designated mixtures. Guayule was worse than asphalt resisting moisture damage

through the standard (TSR) test. By contrast, guayule-based mixtures presented a high resistance to moisture damage evaluated by the HWT test considering the HWT reliability for addressing the field performance. Pure guayule mixture had a high resistance to rutting at its high temperature grade. Guayule modification using CRM and partial guayule replacement by asphalt and CRM enhanced the rutting resistance. This was compatible with the binder performance evaluated by the Superpave criteria. Changing parameters (e.g., CRM addition and guayule's partial replacement by asphalt and CRM) enhanced the guayule-based mixture's resistance to rutting and moisture damage resulting in acceptable performances by TSR, rut, and HWT tests. The positive impacts of the guayule-based binders in mixtures regarding the fracture resistance at the intermediate temperature reflected the excellent fracture toughness of partial or full asphalt replacement by guayule. Guayule offered better performance in the mixture than the pure asphalt due to the unavailability of the fracture toughness criterion in binder evaluation by the Superpave criteria. Compared to the pure asphalt mixture, the guayule-based mixture presented a higher rate of change of strain energy per notch depth, which indicated a tougher material. Guayule (with or without CRM modification) did not offer the desired performance at low temperatures. This could indicate the difficulty of using guayule (as a 100% asphalt alternative) to resist the potential thermal cracking, thus indicating a worse low-temperature performance than expected from the Superpave's binder evaluation criteria. However, partial asphalt replacement by guayule and CRM resisted the thermal fracture greatly.

9.2. RECOMMENDATIONS

It is not recommended to store the designated guayule-based binders involving CRM. Instead, the binder-aggregate mixing process should follow the binder production avoiding the CRM residue sedimentation. Otherwise, other techniques (or new technologies), e.g., continuous agitation, must be used to overcome the CRM residue sedimentation. Thus, a homogeneous binder blend will be reached, and its efficiency as a whole matrix will be much better in the overall mix.

Future investigations to the interaction parameters (temperature, speed, and time) could optimize the guayule-based binders' performances at high, intermediate, and low temperatures.

To boost applicability in a broader range of temperature continuous performance grades, guayule requires further investigations to enhance its performance considering drawbacks such as high oxidative components and aging subsequences. This could be achieved by experiencing other modifiers such as polymers.

Future work is recommended to enhance the performance of the guayule-based mixtures at low temperatures. The rejuvenators' additions are a potential material parameter that could improve the mixture performance at low and intermediate temperatures.

BIBLIOGRAPHY

[1]   M. M. A. Aziz, M. T. Rahman, M. R. Hainin, and W. A. W. A. Bakar, "An Overview on Alternative Binders for Flexible Pavement," *Construction and Building Materials,* vol. 84, pp. 315-319, 2015.

[2]   A. Hemida and M. Abdelrahman, "Guayule Resin: An Innovative Bioresource for Asphalt Cement Replacement," *Journal of Cleaner Production,* p. 128065, 2021.

[3]   R. J. Kuhns and G. H. Shaw, "Peak Oil and Petroleum Energy Resources," in *Navigating the Energy Maze*: Springer, 2018, pp. 53-63.

[4]   A. Hemida, M. Abdelrahman, and E. Deef-Allah, "Quantitative Evaluation of Asphalt Binder Extraction from Hot Mix Asphalt Pavement Using Ashing and Centrifuge Methods," *Transportation Engineering,* vol. 3, p. 100046, 2021.

[5]   Y. Ma, P. Polaczyk, H. Park, X. Jiang, W. Hu, and B. Huang, "Performance Evaluation of Temperature Effect on Hot in-Place Recycling Asphalt Mixtures," *Journal of Cleaner Production,* vol. 277, p. 124093, 2020.

[6]   S. Zhao, B. Huang, X. Shu, and M. Woods, "Comparative Evaluation of Warm Mix Asphalt Containing High Percentages of Reclaimed Asphalt Pavement," *Construction and Building Materials,* vol. 44, pp. 92-100, 2013.

[7]   Y. Ma *et al.*, "Compatibility and Rheological Characterization of Asphalt Modified with Recycled Rubber-Plastic Blends," *Construction and Building Materials,* vol. 270, p. 121416, 2021.

[8]   Z.-j. Dong, T. Zhou, H. Wang, and H. Luan, "Performance Comparison between Different Sourced Bioasphalts and Asphalt Mixtures," *Journal of Materials in Civil Engineering,* vol. 30, no. 5, p. 04018063, 2018.

[9]   A. Hemida and M. Abdelrahman, "Review on Rheological Characterization of Bio-Oils/Bio-Binders and their Applicability in the Flexible Pavement Industry," *International Journal of Civil Engineering and Technology (IJCIET),* vol. 10, pp. 395-405, 2019.

[10]   L. P. Ingrassia, X. Lu, G. Ferrotti, and F. Canestrari, "Chemical, Morphological and Rheological Characterization of Bitumen Partially Replaced with Wood Bio-Oil: Towards More Sustainable Materials in Road Pavements," *Journal of Traffic and Transportation Engineering (English Edition),* vol. 7, no. 2, pp. 192-204, 2020.

[11]   M. Metwally, "Development of Non-Petroleum Binders Derived from Fast Pyrolysis Bio-Oils for Use in Flexible Pavement," Ph.D., Iowa State University, 11604, 2010.

[12]   J. Mills-Beale, Z. You, E. Fini, B. Zada, C. H. Lee, and Y. K. Yap, "Aging Influence on Rheology Properties of Petroleum-Based Asphalt Modified with Biobinder," *Journal of Materials in Civil Engineering,* vol. 26, no. 2, pp. 358-366, 2014.

[13]   J. Peralta, H. M. R. D. d. Silva, R. C. Williams, M. Rover, and A. Machado, "Development of an Innovative Bio-Binder Using Asphalt-Rubber Technology," *International Journal of Pavement Research and Technology,* vol. 6, no. 4, pp. 447-456, 2013.

[14]   J. Peralta, R. C. Williams, M. Rover, and H. M. R. D. d. Silva, "Development of a Rubber-Modified Fractionated Bio-Oil for Use as Noncrude Petroleum Binder in Flexible Pavements," *Transportation Research Circular,* no. E-C165, pp. 23-36, 2012.

[15]   J. Peralta, R. C. Williams, H. M. Silva, and A. V. A. Machado, "Recombination of Asphalt with Bio-Asphalt: Binder Formulation and Asphalt Mixes Application," presented at the 89th Association of Asphalt Paving Technologists' Annual Meeting, 2014.

[16]   X. Yang, J. Mills-Beale, and Z. You, "Chemical Characterization and Oxidative Aging of Bio-Asphalt and Its Compatibility with Petroleum Asphalt," *Journal of Cleaner Production,* vol. 142, pp. 1837-1847, 2017.

[17]   X. Yang, Z. You, and J. Mills-Beale, "Asphalt Binders Blended with a High Percentage of Biobinders: Aging Mechanism using FTIR and Rheology," *Journal of Materials in Civil Engineering,* vol. 27, no. 4, p. 04014157, 2015.

[18]   A. Hemida and M. Abdelrahman, "Component Analysis of Bio-Asphalt Binder Using Crumb Rubber Modifier and Guayule Resin as an Innovative Asphalt Replacer," *Resources, Conservation & Recycling,* vol. 169, p. 105486, 2021.

[19]   L. P. Ingrassia, X. Lu, G. Ferrotti, and F. Canestrari, "Renewable Materials in Bituminous Binders and Mixtures: Speculative Pretext or Reliable Opportunity?," *Resources, Conservation & Recycling,* vol. 144, pp. 209-222, 2019.

[20]   F. Nakayama, "Guayule Future Development," *Industrial Crops and Products,* vol. 22, no. 1, pp. 3-13, 2005.

[21]   Bridgestone. (Dec 06, 2020). *"Plant to Produce Rubber" Grown in Arid Zones - Guayule*. Available: https://www.bridgestone.com/technology_innovation/natural_rubber/guayule/

[22]   S. M. Lusher, "Guayule Plant Extracts as Binder Modifiers in Flexible (Asphalt) Pavement Mixtures," Missouri University of Science and Technology, Rolla, MO, 2018.

[23]   D. Rasutis, K. Soratana, C. McMahan, and A. E. Landis, "A Sustainability Review of Domestic Rubber from the Guayule Plant," *Industrial Crops and Products,* vol. 70, pp. 383-394, 2015.

[24]   W. W. Schloman Jr, D. J. Garrot Jr, D. T. Ray, and D. J. Bennett, "Seasonal Effects on Guayule Resin Composition," *Journal of Agricultural and Food Chemistry,* vol. 34, no. 2, pp. 177-179, 1986.

[25]   F. Cheng, M. Dehghanizadeh, M. A. Audu, J. M. Jarvis, F. O. Holguin, and C. E. Brewer, "Characterization and Evaluation of Guayule Processing Residues as Potential Feedstock for Biofuel and Chemical Production," *Industrial Crops and Products,* vol. 150, p. 112311, 2020.

[26]   A. Hemida and M. Abdelrahman, "Influence of Guayule Resin as a Bio-Based Additive on Asphalt–Rubber Binder at Elevated Temperatures," *Recycling,* vol. 4, no. 3, p. 38, 2019.

[27]   A. Hemida and M. Abdelrahman, "Monitoring Separation Tendency of Partial Asphalt Replacement by Crumb Rubber Modifier and Guayule Resin," *Construction and Building Materials,* vol. 251, p. 118967, 2020.

[28]   A. Hemida and M. Abdelrahman, "A Threshold to Utilize Guayule Resin as a New Binder in Flexible Pavement Industry," *International Journal of Engineering Research and Applications (IJERA),* vol. 8, no. 12, pp. 83-94, 2018 2018.

[29]   A. Hemida and M. Abdelrahman, "Effect of Guayule Resin as a Bio-Based Additive on Storage Stability and Liquid Phase Separation of Asphalt-Rubber Binder," in *Proceedings of the 99th Annual Meeting of the Transportation Research Board*, Washington, DC, 2020.

[30]   A. Hemida and M. Abdelrahman, "Rheological and Component Characterization of an Innovative Bio-Binder Using Guayule Resin in Partial and Entire Asphalt Replacement," in *Proceedings of the 100th Annual Meeting of the Transportation Research Board*, Washington, D.C., 2021.

[31]   Pavement-Interactive. (Dec 06, 2020). *Superpave Performance Grading*. Available: https://pavementinteractive.org/reference-desk/materials/asphalt/superpave-performance-grading/

[32]   M. M. A. Aziz, M. T. Rahman, M. R. Hainin, and W. A. W. A. Bakar, "Alternative Binders for Flexible Pavement," *Carbon (C),* vol. 72, pp. 81-86, 2006.

[33]   J. Gao, H. Wang, Z. You, and M. R. M. Hasan, "Research on Properties of Bio-Asphalt Binders Based on Time and Frequency Sweep Test," *Construction and Building Materials,* vol. 160, pp. 786-793, 2018.

[34]   A. Riddell, S. Ronson, G. Counts, and K. Spenser, "Towards Sustainable Energy: the Current Fossil Fuel Problem and the Prospects of Geothermal and Nuclear Power," *Journal on Trade & Environment-Stanford University, California, USA,* 2004.

[35]   S. Shafiee and E. Topal, "When Will Fossil Fuel Reserves Be Diminished?," *Energy Policy,* vol. 37, no. 1, pp. 181-189, 2009.

[36]   M. Metwally and C. R. Williams, "General Rheological Properties of Fractionated Switchgrass Bio-Oil as a Pavement Material," *Road Materials and Pavement Design,* vol. 11, no. sup1, pp. 325-353, 2010.

[37]   X. Yang, Z. You, Q. Dai, and J. Mills-Beale, "Mechanical Performance of Asphalt Mixtures Modified by Bio-Oils Derived from Waste Wood Resources," *Construction and Building Materials,* vol. 51, pp. 424-431, 2014.

[38]   N. A. A. Raman, M. R. Hainin, N. A. Hassan, and F. N. Ani, "A Review on the Application of Bio-Oil as an Additive for Asphalt," *Jurnal Teknologi,* vol. 72, no. 5, 2015.

[39]   R. C. Williams, J. Satrio, M. Rover, R. C. Brown, and S. Teng, "Utilization of Fractionated Bio oil in Asphalt," in *88th Transportation Research Board (TRB) Annual Meeting*, 2009.

[40]   H. Wen, S. Bhusal, and B. Wen, "Laboratory Evaluation of Waste Cooking Oil-Based Bioasphalt as an Alternative Binder for Hot Mix Asphalt," *Journal of Materials in Civil Engineering,* vol. 25, no. 10, pp. 1432-1437, 2013.

[41]   Z. Sun, J. Yi, Y. Huang, D. Feng, and C. Guo, "Properties of Asphalt Binder Modified by Bio-Oil Derived from Waste Cooking Oil," *Construction and Building Materials,* vol. 102, pp. 496-504, 2016.

[42]   X. Yang, "The laboratory Evaluation of Bio Oil Derived from Waste Resources as Extender for Asphalt Binder," Michigan Technological University, 2013.

[43]   S. M. Lusher and D. N. Richardson, "Guayule Plant Extracts as Recycling Agents in Hot Mix Asphalt with High Reclaimed Binder Content," *Journal of Materials in Civil Engineering,* vol. 27, no. 10, p. 04014269, 2015.

[44]   A. H. Tullo, "Guayule Gets Ready to Hit the Road," *Chemical & Engineering News,* vol. 93, no. 16, pp. 18-19, 2015.

[45]   D. N. Richardson and S. M. Lusher, "The Guayule Plant: a Renewable, Domestic Source of Binder Materials for Flexible Pavement Mixtures," in "New Ideas for Highway Systems, NCHRP-IDEA Project 143," Transp. Res. Board2013.

[46]   W. Schloman Jr, "Processing Guayule for Latex and Bulk Rubber," *Industrial Crops and Products,* vol. 22, no. 1, pp. 41-47, 2005.

[47]   M. E. Salvucci, T. A. Coffelt, and K. Cornish, "Improved Methods for Extraction and Quantification of Resin and Rubber from Guayule," *Industrial Crops and Products,* vol. 30, no. 1, pp. 9-16, 2009.

[48]   W. Schloman Jr, D. McIntyre, A. Hilton, and R. Beinor, "Effects of Environment and Composition on Degradation of Guayule Rubber," *Journal of Applied Polymer Science,* vol. 60, no. 7, pp. 1015-1023, 1996.

[49]   E. P. Jones, "Recovery of Rubber Latex from Guayule Shrub," *Industrial & Engineering Chemistry,* vol. 40, no. 5, pp. 864-874, 1948.

[50]   K. Cornish and J. L. Brichta, "Some Rheological Properties of Latex from Parthenium Argentatum Gray Compared with Latex from Hevea Brasiliensis and Ficus Elastica," *Journal of Polymers and the Environment,* vol. 10, no. 1, pp. 13-18, 2002.

[51]   E. Costa, J. Aguado, G. Ovejero, and P. Cañizares, "Conversion of Guayule Resin to C1・-C10 Hydrocarbons on Zeolite Based Catalysts," *Fuel,* vol. 71, no. 1, pp. 109-113, 1992.

[52]   R. W. Gumbs, "Guayule Resin Multipolymer," 2009.

[53]   W. W. Schloman Jr, R. A. Hively, A. Krishen, and A. M. Andrews, "Guayule Byproduct Evaluation: Extract Characterization," *Journal of Agricultural and Food Chemistry,* vol. 31, no. 4, pp. 873-876, 1983.

[54]   NLM. (Sep 13, 2019). *PubChem*. Available: https://pubchem.ncbi.nlm.nih.gov/

[55]   M. Dehghanizadeh and C. E. Brewer, "Guayule Resin: Chemistry, Extraction, and Applications," in *2020 ASABE Annual International Virtual Meeting*, 2020, p. 1: American Society of Agricultural and Biological Engineers.

[56]   M. Nivitha, E. Prasad, and J. Krishnan, "Ageing in Modified Bitumen Using FTIR Spectroscopy," *International Journal of Pavement Engineering,* vol. 17, no. 7, pp. 565-577, 2016.

[57]   M. Ragab, "Enhancing the Performance of Crumb Rubber Modified Asphalt through Controlling the Internal Network Structure Developed," Ph.D., North Dakota State University, 2016.

[58]   G. Socrates, *Infrared and Raman Characteristic Group Frequencies: Tables and Charts*. John Wiley & Sons, 2004.

[59]   B. Zhang, M. Xi, D. Zhang, H. Zhang, and B. Zhang, "The Effect of Styrene–Butadiene–Rubber/Montmorillonite Modification on the Characteristics and Properties of Asphalt," *Construction and Building Materials,* vol. 23, no. 10, pp. 3112-3117, 2009.

[60]   H. Yao *et al.*, "Rheological Properties and Chemical Analysis of Nanoclay and Carbon Microfiber Modified Asphalt with Fourier Transform Infrared Spectroscopy," *Construction and Building Materials,* vol. 38, pp. 327-337, 2013.

[61]   F. Zhang, J. Yu, and J. Han, "Effects of Thermal Oxidative Ageing on Dynamic Viscosity, TG/DTG, DTA and FTIR of SBS-and SBS/Sulfur-Modified Asphalts," *Construction and Building Materials,* vol. 25, no. 1, pp. 129-137, 2011.

[62]   G. C. Bassler, *Spectrometric Identification of Organic Compounds*. 1981.

[63]   B. C. Smith, *Infrared Spectral Interpretation: a Systematic Approach*. CRC press, 1998.

[64]   J. F. Masson, L. Pelletier, and P. Collins, "Rapid FTIR Method for Quantification of Styrene-Butadiene Type Copolymers in Bitumen," *Journal of Applied Polymer Science,* vol. 79, no. 6, pp. 1034-1041, 2001.

[65]   G. B. Way, K. E. Kaloush, and K. P. Biligiri, "Asphalt-Rubber Standard Practice Guide," *Rubber Pavements Association, Tempe,* 2012.

[66] Clatrans, "2015 Crumb Rubber Report: Cost Differential Analysis between Asphalt Containing Crumb Rubber and Conventional Asphalt," California Department of Transportation, California State Transportation Agency, Sacramento, California.2017, Available: https://dot.ca.gov/-/media/dot-media/programs/maintenance/documents/2015-crumb-rubber-report-a11y.pdf.

[67] USTMA. (Oct 14, 2019). *2017 U.S. Scrap Tire Management Summary*. Available: https://www.ustires.org/system/files/USTMA_scraptire_summ_2017_072018.pdf

[68] B. Williams, A. Copeland, and T. Ross, "Asphalt Pavement Industry Survey on Recycled Materials and Warm-Mix Asphalt Usage: 2017," National Asphalt Pavement Association (NAPA), Lanham, MD, USAIS 138(8e), 2018.

[69] D. Lo Presti, "Recycled Tyre Rubber Modified Bitumens for Road Asphalt Mixtures: A Literature Review," *Construction and Building Materials,* vol. 49, pp. 863-881, 2013.

[70] C. Thodesen, K. Shatanawi, and S. Amirkhanian, "Effect of Crumb Rubber Characteristics on Crumb Rubber Modified (CRM) Binder Viscosity," *Construction and Building Materials,* vol. 23, no. 1, pp. 295-303, 2009.

[71] L. Zanzotto and G. J. Kennepohl, "Development of Rubber and Asphalt Binders by Depolymerization and Devulcanization of Scrap Tires in Asphalt," *Transportation Research Record,* vol. 1530, no. 1, pp. 51-58, 1996.

[72] T. Billiter, J. Chun, R. Davison, C. Glover, and J. Bullin, "Investigation of the Curing Variables of Asphalt-Rubber Binder," *Petroleum Science and Technology,* vol. 15, no. 5-6, pp. 445-469, 1997.

[73] J. F. Chipps, R. R. Davison, and C. J. Glover, "A Model for Oxidative Aging of Rubber-Modified Asphalts and Implications to Performance Analysis," *Energy & Fuels,* vol. 15, no. 3, pp. 637-647, 2001.

[74] A. Ghavibazoo and M. Abdelrahman, "Composition Analysis of Crumb Rubber during Interaction with Asphalt and Effect on Properties of Binder," *International Journal of Pavement Engineering,* vol. 14, no. 5, pp. 517-530, 2013.

[75]   B. J. Putman and S. N. Amirkhanian, "Characterization of the Interaction Effect of Crumb Rubber Modified Binders Using HP-GPC," *Journal of Materials in Civil Engineering,* Article vol. 22, no. 2, pp. 153-159, 2010, Art. no. 006002qmt.

[76]   A. Ghavibazoo, M. Abdelrahman, and M. Ragab, "Mechanism of Crumb Rubber Modifier Dissolution into Asphalt Matrix and Its Effect on Final Physical Properties of Crumb Rubber–Modified Binder," *Transportation Research Record,* vol. 2370, no. 1, pp. 92-101, 2013.

[77]   M. Ragab, M. Abdelrahman, and A. Ghavibazoo, "New Approach for Selecting Crumb-Rubber-Modified Asphalts for Rutting and Permanent Deformation Resistance," *Advances in Civil Engineering Materials,* vol. 2, no. 1, pp. 360-378, 2013.

[78]   M. Ragab, M. Abdelrahman, and A. Ghavibazoo, "Performance Enhancement of Crumb Rubber–Modified Asphalts through Control of the Developed Internal Network Structure," *Transportation Research Record,* vol. 2371, no. 1, pp. 96-104, 2013.

[79]   M. Heitzman, "Design and Construction of Asphalt Paving Materials with Crumb Rubber Modifier," *Transportation Research Record,* vol. 1339, 1992.

[80]   H. B. Takal, "Advances in Technology of Asphalt Paving Materials Containing Used Tire Rubber," *Tire Rubber in Asphalt Pavements,* vol. 1339, p. 23, 1991.

[81]   A. Ghavibazoo, M. Abdelrahman, and M. Ragab, "Effect of Crumb Rubber Modifier Dissolution on Storage Stability of Crumb Rubber–Modified Asphalt," *Transportation Research Record,* vol. 2370, no. 1, pp. 109-115, 2013.

[82]   J. Yu *et al.*, "Modification of Asphalt Rubber with Nanoclay towards Enhanced Storage Stability," *Materials,* vol. 11, no. 11, p. 2093, 2018.

[83]   Y. Lei *et al.*, "Evaluation of the Effect of Bio-Oil on the High-Temperature Performance of Rubber Modified Asphalt," *Construction and Building Materials,* vol. 191, pp. 692-701, 2018.

[84] M. Ragab and M. Abdelrahman, "Enhancing the Crumb Rubber Modified Asphalt's Storage Stability through the Control of its Internal Network Structure," *International Journal of Pavement Research and Technology,* vol. 11, no. 1, pp. 13-27, 2018.

[85] I. Androjić and Z. D. Alduk, "Analysis of Energy Consumption in the Production of Hot Mix Asphalt (Batch Mix Plant)," *Canadian Journal of Civil Engineering,* vol. 43, no. 12, pp. 1044-1051, 2016.

[86] Pavement-Interactive. (Sep 09, 2021). *Energy and Road Construction-What's the Mileage of Roadway?cit*. Available: https://pavementinteractive.org/energy-and-road-construction-whats-the-mileage-of-roadway/

[87] Pavement-Interactive. (Sep 09, 2021). *Warm Mix – A Hot Topic*. Available: https://pavementinteractive.org/warm-mix-a-hot-topic/

[88] J. Bražiūnas and H. Sivilevičius, "Heat transfer and Energy Loss in Bitumen Batching System of Asphalt Mixing Plant," in *9th International Conference on Environmental Engineering. Vilnius, Lithuania*, 2014, vol. 20406080, pp. 100-120.

[89] I. Gillespie, "Quantifying the Energy Used in an Asphalt Coating Plant," *University of Strachclyde: Glasgow, Scotland,* p. 164, 2012.

[90] A. Hemida and M. Abdelrahman, "Performance Assessment of Bio-Asphalt Mixtures ContainingGuayule Resin as an Innovative Bio-Based Asphalt Alternative," *Journal of Materials in Civil Engineering,* 2022. Pre-production version, with permission from ASCE (https://ascelibrary.org/page/ascetermsandconditionsforpermissionsrequests).

[91] K. R. Hansen and D. E. Newcomb, "Asphalt Pavement Mix Production Survey on Reclaimed Asphalt Pavement, Reclaimed Asphalt Shingles, and Warm-Mix Asphalt Usage: 2009-2010," *Information Series,* vol. 138, p. 21, 2011.

[92] G. A. Harder, Y. LeGoff, A. Loustau, Y. Martineau, B. Heritier, and A. Romier, "Energy and environmental gains of warm and half-warm asphalt mix: quantitative approach," 2008.

[93]   M. Abdelrahman, D. R. Katti, A. Ghavibazoo, H. B. Upadhyay, and K. S. Katti, "Engineering Physical Properties of Asphalt Binders through Nanoclay–Asphalt Interactions," *Journal of Materials in Civil Engineering,* vol. 26, no. 12, p. 04014099, 2014.

[94]   A. Ghavibazoo and M. Abdelrahman, "Effect of Crumb Rubber Dissolution on Low-Temperature Performance and Aging of Asphalt–Rubber Binder," *Transportation Research Record,* vol. 2445, no. 1, pp. 47-55, 2014.

[95]   A. Ghavibazoo, M. Abdelrahman, and M. Ragab, "Changes in Composition and Molecular Structure of Asphalt in Mixing with Crumb Rubber Modifier," *Road Materials and Pavement Design,* vol. 17, no. 4, pp. 906-919, 2016.

[96]   *ASTM E178-16a, Standard Practice for Dealing With Outlying Observations*, 2016.

[97]   AASHTO, "AASHTO T 315-12, Standard Method of Test for Determining the Rheological Properties of Asphalt Binder Using a Dynamic Shear Rheometer (DSR)," ed. Washington, D.C.: American Association of State Highway Transportation Officials (AASHTO), 2013.

[98]   *ASTM C670-15, Standard Practice for Preparing Precision and Bias Statements for Test Methods for Construction Materials*, 2015.

[99]   M. Jasso, D. Bakos, J. Stastna, and L. Zanzotto, "Conventional Asphalt Modified by Physical Mixtures of Linear SBS and Montmorillonite," *Applied Clay Science,* vol. 70, pp. 37-44, 2012.

[100]   C. Wekumbura, J. Stastna, and L. Zanzotto, "Destruction and Recovery of Internal Structure in Polymer-Modified Asphalts," *Journal of Materials in Civil Engineering,* vol. 19, no. 3, pp. 227-232, 2007.

[101]   G. Baumgardner and C. Daranga, "Southeast Producer and Contractor Perspective on Asphalt Binder Acceptance and Characterization," in *101st Transportation Research Board (TRB) Annual Meeting*, Washington, D.C., 2022.

[102]   M. Attia and M. Abdelrahman, "Enhancing the Performance of Crumb Rubber-Modified Binders through Varying the Interaction Conditions," *International Journal of Pavement Engineering,* vol. 10, no. 6, pp. 423-434, 2009.

[103]   M. Zaumanis, R. B. Mallick, and R. Frank, "100% Recycled Hot Mix Asphalt: a Review and Analysis," *Resources, Conservation and Recycling,* vol. 92, pp. 230-245, 2014.

[104]   ASTM, "ASTM D92-18 Standard Test Method for Flash and Fire Points by Cleveland Open Cup Tester ", ed. West Conshohocken, PA: ASTM International, 2018.

[105]   ASTM, "ASTM D70-18a Standard Test Method for Density of Semi-Solid Asphalt Binder (Pycnometer Method)," ed. West Conshohocken, PA: ASTM International, 2018.

[106]   ASTM, "ASTM D5/D5M-20 Standard Test Method for Penetration of Bituminous Materials," ed. West Conshohocken, PA: ASTM International, 2020.

[107]   ASTM, "ASTM D4402/D4402M-15 Standard Test Method for Viscosity Determination of Asphalt at Elevated Temperatures Using a Rotational Viscometer," ed. West Conshohocken, PA: ASTM International, 2015.

[108]   ASTM, "ASTM D36/D36M-14(2020) Standard Test Method for Softening Point of Bitumen (Ring-and-Ball Apparatus)," ed. West Conshohocken, PA: ASTM International, 2020.

[109]   ASTM, "ASTM D7173-14, Standard Practice for Determining the Separation Tendency of Polymer from Polymer Modified Asphalt," ed. West Conshohocken, PA: ASTM International, 2014.

[110]   W. H. Daly, I. Negulescu, and I. Glover, "A Comparative Analysis of Modified Binders: Original Asphalts and Materials Extracted from Existing Pavements," Louisiana Transportation Research Center2010.

[111]   AASHTO, "AASHTO T 44-13, Standard Method of Test for Solubility of Bituminous Material," ed. Washington, D.C.: American Association of State Highway Transportation Officials (AASHTO), 2013.

[112]   ASTM, "ASTM D2042-15, Standard Test Method for Solubility of Asphalt Materials in Trichloroethylene," ed. West Conshohocken, PA: ASTM International, 2015.

[113]   D. T. Duong *et al.*, "Molecular Solubility and Hansen Solubility Parameters for the Analysis of Phase Separation in Bulk Heterojunctions," *Journal of Polymer Science Part B: Polymer Physics,* vol. 50, no. 20, pp. 1405-1413, 2012.

[114]   C. M. Hansen, "50 Years with Solubility Parameters—Past and Future," *Progress in Organic Coatings,* vol. 51, no. 1, pp. 77-84, 2004.

[115]   C. M. Hansen, *Solubility Parameters: A User's Handbook*. CRC Press Boca Raton, 2007.

[116]   C. Zhang and M. R. Kessler, "Bio-Based Polyurethane Foam Made from Compatible Blends of Vegetable-Oil-Based Polyol and Petroleum-Based Polyol," *ACS Sustainable Chemistry & Engineering,* vol. 3, no. 4, pp. 743-749, 2015.

[117]   G. Zhao, H. Ni, S. Ren, and G. Fang, "Correlation between Solubility Parameters and Properties of Alkali Lignin/PVA Composites," *Polymers,* vol. 10, no. 3, p. 290, 2018.

[118]   AASHTO, "AASHTO T 316-13, Standard Method of Test for Viscosity Determination of Asphalt Binder Using Rotational Viscometer," ed. Washington, D.C: American Association of State Highway and Transportation Officials (AASHTO), 2017.

[119]   Y. Yildirim, M. Solaimanian, and T. W. Kennedy, "Mixing and Compaction Temperatures for Hot Mix Asphalt Concrete," University of Texas at Austin. Center for Transportation Research2000.

[120]   A. Diab and Z. You, "Small and Large Strain Rheological Characterizations of Polymer and Crumb Rubber-Modified Asphalt Binders," *Construction and Building Materials,* vol. 144, pp. 168-177, 2017.

[121] S.-J. Lee, S. N. Amirkhanian, K. Shatanawi, and K. W. Kim, "Short-Term Aging Characterization of Asphalt Binders Using Gel Permeation Chromatography and Selected Superpave Binder Tests," *Construction and Building Materials,* vol. 22, no. 11, pp. 2220-2227, 2008.

[122] J. Shen and S. Amirkhanian, "The Influence of Crumb Rubber Modifier (CRM) Microstructures on the High Temperature Properties of CRM Binders," *International Journal of Pavement Engineering,* vol. 6, no. 4, pp. 265-271, 2005.

[123] B. J. Putman and S. N. Amirkhanian, "Crumb Rubber Modification of Binders: Interaction and Particle Effects," in *Proceedings of the Asphalt Rubber 2006 Conference*, 2006, vol. 3, pp. 655-677.

[124] AASHTO, "AASHTO T 313-12, Standard Method of Test for Determining the Flexural Creep Stiffness of Asphalt Binder Using the Bending Beam Rheometer (BBR)," ed. Washington, D.C: American Association of State Highway and Transportation Officials (AASHTO), 2016.

[125] M. S. Mamlouk and J. P. Zaniewski, *Materials for Civil and Construction Engineers*. Pearson Prentice Hall Upper Saddle River, NJ, 2006.

[126] F. Roberts, P. Kandhal, E. Brown, D. Lee, and T. Kennedy, "Hot Mix Asphalt Materials, Mixture Design and Construction," 1996.

[127] S. Komaragiri, A. Filonzi, E. Guevara, D. Hazlett, E. Mahmoud, and A. Bhasin, "Examining Different Alternatives to Delta Tc (ΔTc) as a Parameter to Screen Asphalt Binders," *Journal of Testing and Evaluation,* vol. 50, no. 1, 2021.

[128] ASTM, "ASTM D2872-19 Standard Test Method for Effect of Heat and Air on a Moving Film of Asphalt (Rolling Thin-Film Oven Test)," ed. West Conshohocken, PA: ASTM International, 2019.

[129] ASTM, "ASTM D6521-19a Standard Practice for Accelerated Aging of Asphalt Binder Using a Pressurized Aging Vessel (PAV)," ed. West Conshohocken, PA: ASTM International, 2019.

[130]   A. Ghavibazoo, "Characterization of Activities of Crumb Rubber in Interaction with Asphalt and Its Effect on Final Properties," North Dakota State University, 2015.

[131]   E. Deef-Allah, M. Abdelrahman, and A. Hemida, "Improving Asphalt Binder's Elasticity through Controlling the Interaction Parameters between CRM and Asphalt Binder," *Advances in Civil Engineering Materials,* vol. 9, no. 1, pp. 262-282, 2020.

[132]   R. Karlsson and U. Isacsson, "Application of FTIR-ATR to Characterization of Bitumen Rejuvenator Diffusion," *Journal of Materials in Civil Engineering,* vol. 15, no. 2, pp. 157-165, 2003.

[133]   B. Hofko *et al.*, "FTIR Spectral Analysis of Bituminous Binders: Reproducibility and Impact of Ageing Temperature," *Materials and Structures,* vol. 51, no. 2, p. 45, 2018.

[134]   H. Yao, Q. Dai, Z. You, M. Ye, and Y. K. Yap, "Rheological Properties, Low-Temperature Cracking Resistance, and Optical Performance of Exfoliated Graphite Nanoplatelets Modified Asphalt Binder," *Construction and Building Materials,* vol. 113, pp. 988-996, 2016.

[135]   T. Hatakeyama and L. Zhenhai, *Handbook of Thermal Analysis.* Chichester: John Wiley & sons, 2000.

[136]   Y. S. Lee, W.-K. Lee, S.-G. Cho, I. Kim, and C.-S. Ha, "Quantitative Analysis of Unknown Compositions in Ternary Polymer Blends: A Model Study on NR/SBR/BR System," *Journal of Analytical and Applied Pyrolysis,* vol. 78, no. 1, pp. 85-94, 2007.

[137]   S. Seidelt, M. Müller-Hagedorn, and H. Bockhorn, "Description of Tire Pyrolysis by Thermal Degradation Behaviour of Main Components," *Journal of Analytical and Applied Pyrolysis,* vol. 75, no. 1, pp. 11-18, 2006.

[138]   A. Ghavibazoo and M. Abdelrahman, "Monitoring Changes in Composition of Crumb Rubber Modifier During Interaction with Asphalt and Its Effect on Final Modified Asphalt Performance," in *91st Transportation Research Board (TRB) Annual Meeting*, Washington, D.C., 2012.

[139] G. Parkes, P. Barnes, and E. Charsley, "New Concepts in Sample Controlled Thermal Analysis: Resolution in the Time and Temperature Domains," *Analytical Chemistry,* vol. 71, no. 13, pp. 2482-2487, 1999.

[140] A. Hemida and M. Abdelrahman, "Evaluation of Guayule Resin as an Innovative Bio-Based Asphalt Alternative in Mix Performance," in *101st Transportation Research Board (TRB) Annual Meeting*, Washington, D.C., 2022: Transportation Research Board.

[141] AASHTO, "AASHTO M 323-17, Standard Specification for Superpave Volumetric Mix Design," ed. Washington, D.C: American Association of State Highway and Transportation Officials (AASHTO), 2017.

[142] AASHTO, "AASHTO T 340-10, Standard Method of Test for Determining Rutting Susceptibility of Hot Mix Asphalt (HMA) Using the Asphalt Pavement Analyzer (APA)," ed. Washington, D.C: American Association of State Highway and Transportation Officials (AASHTO), 2019.

[143] AASHTO, "AASHTO T 209-20, Standard Method of Test for Theoretical Maximum Specific Gravity (G mm) and Density of Asphalt Mixtures," ed. Washington, D.C: American Association of State Highway and Transportation Officials (AASHTO), 2020.

[144] AASHTO, "AASHTO T 166-16, Standard Method of Test for Bulk Specific Gravity (G mb) of Compacted Asphalt Mixtures Using Saturated Surface-Dry Specimens," ed. Washington, D.C: American Association of State Highway and Transportation Officials (AASHTO), 2020.

[145] AASHTO, "AASHTO R 30-02, Standard Practice for Mixture Conditioning of Hot Mix Asphalt (HMA)," ed. Washington, D.C: American Association of State Highway and Transportation Officials (AASHTO), 2019.

[146] AASHTO, "AASHTO T 312-19, Standard Method of Test for Preparing and Determining the Density of Asphalt Mixture Specimens by Means of the Superpave Gyratory Compactor," ed. Washington, D.C: American Association of State Highway and Transportation Officials (AASHTO), 2019.

[147] W. Rafiq *et al.*, "Investigation on Hamburg Wheel-Tracking Device Stripping Performance Properties of Recycled Hot-Mix Asphalt Mixtures," *Materials,* vol. 13, no. 21, p. 4704, 2020.

[148] H. Radeef *et al.*, "Determining Fracture Energy in Asphalt Mixture: A Review," in *IOP Conference Series: Earth and Environmental Science*, 2021, vol. 682, no. 1, p. 012069: IOP Publishing.

[149] ASTM, "ASTM D7313-20, Standard Test Method for Determining Fracture Energy of Asphalt Mixtures Using the Disk-Shaped Compact Tension Geometry," ed. West Conshohocken, PA: ASTM International, 2020.

[150] AASHTO, "AASHTO T 283-14, Standard Method of Test for Resistance of Compacted Asphalt Mixtures to Moisture-Induced Damage," ed. Washington, D.C: American Association of State Highway and Transportation Officials (AASHTO), 2018.

[151] AASHTO, "AASHTO T 324-19, Hamburg Wheel-Track Testing of Compacted Hot Mix Asphalt (HMA)," ed. Washington, D.C: American Association of State Highway and Transportation Officials (AASHTO), 2019.

[152] G. L. Fitts. (Jul 27, 2021). *Hamburg Wheel Tracking (HWT) Test*. Available: https://www.ltrc.lsu.edu/asphalt/pdf/Hamburg%20Wheel%20Tracking%20Test.pdf

[153] CDOT, "CPL 5112-20, Standard Method of Test for Hamburg Wheel-Track Testing of Compacted Bituminous Mixtures," ed. Colorado: Colorado Department of Transportation (CDOT), 2020.

[154] TXDOT, "Tex-242-F, Test Procedure for Hamburg Wheel-Tracking Test," ed. Texas: Texas Department of Transportation (TxDOT), 2019.

[155] M. Mull, K. Stuart, and A. Yehia, "Fracture Resistance Characterization of Chemically Modified Crumb Rubber Asphalt Pavement," *Journal of Materials Science,* vol. 37, no. 3, pp. 557-566, 2002.

[156] M. Kim, L. N. Mohammad, and M. A. Elseifi, "Characterization of Fracture Properties of Asphalt Mixtures as Measured by Semicircular Bend Test and Indirect Tension Test," *Transportation research record,* vol. 2296, no. 1, pp. 115-124, 2012.

[157] N. Moore, "Evaluation of Laboratory Cracking Tests Related to Top-Down Cracking in Asphalt Pavements," 2016.

[158] S. B. Cooper, W. King, and S. Kabir, "Testing and Analysis of LWT and SCB Properties of Asphalt Concrete Mixtures," 2016.

[159] K. VanFrank, M. VanMilligen, and T. Biel, "Intermediate Temperature Cracking in HMA: Phase 1 Semi-Circular Bending (SCB) Practicality Evaluation," Utah. Dept. of Transportation. Research Division2017.

[160] ASTM, "ASTM D8044-16, Standard Test Method for Evaluation of Asphalt Mixture Cracking Resistance using the Semi-Circular Bend Test (SCB) at Intermediate Temperatures," ed. West Conshohocken, PA: ASTM International, 2016.

[161] S. B. Cooper III and L. N. Mohammad, "Implementation of Balanced Mixture Criteria During Asphalt Mixture Design: Louisiana's Experience," *Transportation Research Circular,* no. E-C251, 2019.

[162] C. Bell, "Relationship between Laboratory Aging Tests and Field Performance of Asphalt-Concrete Mixtures," in *Serviceability and Durability of Construction Materials*, 1990, pp. 745-754: ASCE.

[163] W. Buttlar, P. Rath, H. Majidifard, E. V. Dave, and H. Wang, "Relating DC (T) Fracture Energy to Field Cracking Observations and Recommended Specification Thresholds for Performance-Engineered Mix Design," *Asphalt Mixtures,* vol. 51, 2018.

[164] E. T. Zegeye, K. H. Moon, M. Turos, T. R. Clyne, and M. O. Marasteanu, "Low Temperature Fracture Properties of Polyphosphoric Acid Modified Asphalt Mixtures," *Journal of Materials in Civil Engineering,* vol. 24, no. 8, pp. 1089-1096, 2012.

[165] L. Johanneck, J. Geib, D. Van Deusen, J. Garrity, C. Hanson, and E. V. Dave, "DCT Low Temperature Fracture Testing Pilot Project," 2015.

[166] D. Meier, B. Van De Beld, A. V. Bridgwater, D. C. Elliott, A. Oasmaa, and F. Preto, "State-of-the-Art of Fast Pyrolysis in IEA Bioenergy Member Countries," *Renewable and Sustainable Energy Reviews,* vol. 20, pp. 619-641, 2013.

[167] AASHTO, "AASHTO T 240-13, Standard Method of Test for Effect of Heat and Air on a Moving Film of Asphalt Binder (Rolling Thin-Film Oven Test)," ed. Washington, D.C: American Association of State Highway and Transportation Officials (AASHTO), 2013.

[168] F. Xiao, V. Punith, S. N. Amirkhanian, and B. J. Putman, "Rheological and Chemical Characteristics of Warm Mix Asphalt Binders at Intermediate and Low Performance Temperatures," *Canadian Journal of Civil Engineering,* vol. 40, no. 9, pp. 861-868, 2013.

[169] F. Lionetto, R. Del Sole, D. Cannoletta, G. Vasapollo, and A. Maffezzoli, "Monitoring Wood Degradation during Weathering by Cellulose Crystallinity," *Materials,* vol. 5, no. 10, pp. 1910-1922, 2012.

[170] C. M. Cepeda-Jiménez, M. M. Pastor-Blas, T. Ferrandiz-Gomez, and J. Martín-Martínez, "Influence of the Styrene Content of Thermoplastic Styrene–Butadiene Rubbers in the Effectiveness of the Treatment with Sulfuric Acid," *International Journal of Adhesion and Adhesives,* vol. 21, no. 2, pp. 161-172, 2001.

[171] M. D. Romero-Sánchez, M. M. Pastor-Blas, J. M. Martín-Martínez, and M. Walzak, "Addition of Ozone in the UV Radiation Treatment of a Synthetic Styrene-Butadiene-Styrene (SBS) Rubber," *International Journal of Adhesion and Adhesives,* vol. 25, no. 4, pp. 358-370, 2005.

[172] M. M. Hassan, N. A. Badway, M. Y. Elnaggar, and E.-S. A. Hegazy, "Thermo-Mechanical Properties of Devulcanized Rubber/High Crystalline Polypropylene Blends Modified by Ionizing Radiation," *Journal of Industrial and Engineering Chemistry,* vol. 19, no. 4, pp. 1241-1250, 2013.

[173] K. Kaloush and K. Biligiri, "Asphalt-Rubber Standard Practice Guide," *Links,* 2011.

[174]   F. Navarro, P. Partal, F. Martinez-Boza, and C. Gallegos, "Influence of Crumb Rubber Concentration on the Rheological Behavior of a Crumb Rubber Modified Bitumen," *Energy & Fuels,* vol. 19, no. 5, pp. 1984-1990, 2005.

[175]   I. Gawel, R. Stepkowski, and F. Czechowski, "Molecular Interactions between Rubber and Asphalt," *Industrial & Engineering Chemistry Research,* vol. 45, no. 9, pp. 3044-3049, 2006.

[176]   T. Fwa, H. Pasindu, and G. Ong, "Critical Rut Depth for Pavement Maintenance Based on Vehicle Skidding and Hydroplaning Consideration," *Journal of Transportation Engineering,* vol. 138, no. 4, pp. 423-429, 2012.

VITA

Ahmed Maher Abdeldaim Hemida received his bachelor's degree (Spring 2009) and master's degree (Spring 2014) in Construction and Building Engineering from Arab Academy for Science, Technology and Maritime Transport (AASTMT). Hemida started his Ph.D. in Civil Engineering at North Dakota State University (NDSU) for one semester in Spring 2017. He transferred his Ph.D. program to Missouri University of Science and Technology (Missouri S&T) in Fall 2017. In May 2022, he received his Ph.D. degree in Civil Engineering from Missouri S&T. He received the Missouri Asphalt Pavement Association (MAPA) scholarship award during his Ph.D. program in 2018-2019 and 2021-2022. Hemida also worked as a graduate teaching assistant from 2009 to 2014 at AASTMT, an assistant lecturer from 2014 to 2016 at AASTMT, and a graduate research/teaching assistant from 2017 to 2020 at NDSU and Missouri S&T. It was his honor to deliver a lecture in the Advanced Materials Lecture Series, International Association of Advanced Materials (IAAM), Sweden, and receive the IAAM Young Scientist Medal accordingly.

Hemida had research interests in bio-binders, particularly guayule resin, as an innovative approach for sustainable flexible pavement industry. Guayule resin represented one of the guayule byproducts extracted with the main product (guayule natural rubber). The scope was investigating and enhancing the behavior of guayule resin in partial and entire asphalt cement replacement. Hemida's research got attention of several international journals and conferences. Hemida also made peer-review activities for reputable journals such as Journal of Materials in Civil Engineering, American Society of Civil Engineers (ASCE), and Journal of Renewable Materials, Tech Science Press.